IAEA TECDOC SERIES

IAEA TECDOC 1724

TECDOC No. 1724

Applications of Research Reactors towards Research on Materials for Nuclear Fusion Technology

IAEA
International Atomic Energy Agency

APPLICATIONS OF RESEARCH REACTORS TOWARDS RESEARCH ON MATERIALS FOR NUCLEAR FUSION TECHNOLOGY

The following States are Members of the International Atomic Energy Agency:

AFGHANISTAN
ALBANIA
ALGERIA
ANGOLA
ARGENTINA
ARMENIA
AUSTRALIA
AUSTRIA
AZERBAIJAN
BAHRAIN
BANGLADESH
BELARUS
BELGIUM
BELIZE
BENIN
BOLIVIA
BOSNIA AND HERZEGOVINA
BOTSWANA
BRAZIL
BULGARIA
BURKINA FASO
BURUNDI
CAMBODIA
CAMEROON
CANADA
CENTRAL AFRICAN REPUBLIC
CHAD
CHILE
CHINA
COLOMBIA
CONGO
COSTA RICA
CÔTE D'IVOIRE
CROATIA
CUBA
CYPRUS
CZECH REPUBLIC
DEMOCRATIC REPUBLIC OF THE CONGO
DENMARK
DOMINICA
DOMINICAN REPUBLIC
ECUADOR
EGYPT
EL SALVADOR
ERITREA
ESTONIA
ETHIOPIA
FIJI
FINLAND
FRANCE
GABON
GEORGIA
GERMANY
GHANA
GREECE
GUATEMALA
HAITI
HOLY SEE
HONDURAS
HUNGARY
ICELAND
INDIA
INDONESIA
IRAN, ISLAMIC REPUBLIC OF
IRAQ
IRELAND
ISRAEL
ITALY
JAMAICA
JAPAN
JORDAN
KAZAKHSTAN
KENYA
KOREA, REPUBLIC OF
KUWAIT
KYRGYZSTAN
LAO PEOPLE'S DEMOCRATIC REPUBLIC
LATVIA
LEBANON
LESOTHO
LIBERIA
LIBYA
LIECHTENSTEIN
LITHUANIA
LUXEMBOURG
MADAGASCAR
MALAWI
MALAYSIA
MALI
MALTA
MARSHALL ISLANDS
MAURITANIA
MAURITIUS
MEXICO
MONACO
MONGOLIA
MONTENEGRO
MOROCCO
MOZAMBIQUE
MYANMAR
NAMIBIA
NEPAL
NETHERLANDS
NEW ZEALAND
NICARAGUA
NIGER
NIGERIA
NORWAY
OMAN
PAKISTAN
PALAU
PANAMA
PAPUA NEW GUINEA
PARAGUAY
PERU
PHILIPPINES
POLAND
PORTUGAL
QATAR
REPUBLIC OF MOLDOVA
ROMANIA
RUSSIAN FEDERATION
RWANDA
SAUDI ARABIA
SENEGAL
SERBIA
SEYCHELLES
SIERRA LEONE
SINGAPORE
SLOVAKIA
SLOVENIA
SOUTH AFRICA
SPAIN
SRI LANKA
SUDAN
SWAZILAND
SWEDEN
SWITZERLAND
SYRIAN ARAB REPUBLIC
TAJIKISTAN
THAILAND
THE FORMER YUGOSLAV REPUBLIC OF MACEDONIA
TOGO
TRINIDAD AND TOBAGO
TUNISIA
TURKEY
UGANDA
UKRAINE
UNITED ARAB EMIRATES
UNITED KINGDOM OF GREAT BRITAIN AND NORTHERN IRELAND
UNITED REPUBLIC OF TANZANIA
UNITED STATES OF AMERICA
URUGUAY
UZBEKISTAN
VENEZUELA
VIETNAM
YEMEN
ZAMBIA
ZIMBABWE

The Agency's Statute was approved on 23 October 1956 by the Conference on the Statute of the IAEA held at United Nations Headquarters, New York; it entered into force on 29 July 1957. The Headquarters of the Agency are situated in Vienna. Its principal objective is "to accelerate and enlarge the contribution of atomic energy to peace, health and prosperity throughout the world''.

IAEA-TECDOC-1724

APPLICATIONS OF RESEARCH REACTORS TOWARDS RESEARCH ON MATERIALS FOR NUCLEAR FUSION TECHNOLOGY

PROCEEDINGS OF A TECHNICAL MEETING HELD IN VIENNA, 27–29 JUNE 2011

INTERNATIONAL ATOMIC ENERGY AGENCY
VIENNA, 2013

COPYRIGHT NOTICE

For further information on this publication, please contact:

Physics Section
International Atomic Energy Agency
Vienna International Centre
PO Box 100
1400 Vienna, Austria
Email: Official.Mail@iaea.org

Printed by the IAEA in Austria
November 2013

IAEA Library Cataloguing in Publication Data

Applications of research reactors towards research on materials for nuclear fusion technology. – Vienna : International Atomic Energy Agency, 2013.
p. ; 30 cm. – (IAEA-TECDOC series, ISSN 1011-4289 ; no. 1724)
ISBN 978-92-0-113713-5
Includes bibliographical references.

1. Fusion reactors – Materials. 2. Fusion reactors – Research. 3. Materials – Testing. 4. Controlled fusion. I. International Atomic Energy Agency. II. Series.

IAEAL 13-00854

FOREWORD

Controlled nuclear fusion is widely considered to represent a nearly unlimited source of energy. Recent progress in the quest for fusion energy includes the design and current construction of the International Thermonuclear Experimental Reactor (ITER), for which a licence has recently been obtained as a first of its kind fusion nuclear installation. ITER is designed to demonstrate the scientific and technological feasibility of fusion energy production in excess of 500 MW for several consecutive minutes. ITER, however, will not be able to address all the nuclear fusion technology issues associated with the design, construction and operation of a commercial fusion power plant. The demonstration of an adequate tritium or fuel breeding ratio, as well as the development, characterization and testing of structural and functional materials in an integrated nuclear fusion environment, are examples of issues for which ITER is unable to deliver complete answers. To fill this knowledge gap, several facilities are being discussed, such as the International Fusion Materials Irradiation Facility and, eventually, a fusion demonstration power plant (DEMO). However, for these facilities, a vast body of preliminary research remains to be performed, for instance, concerning the preselection and testing of suitable materials able to withstand the high temperature and pressure, and intense radiation environment of a fusion reactor. Given their capacity for material testing in terms of available intense neutron fluxes, dedicated irradiation facilities and post-irradiation examination laboratories, high flux research reactors or material test reactors (MTRs) will play an indispensable role in the development of fusion technology. Moreover, research reactors have already achieved an esteemed legacy in the understanding of material properties and behaviour, and the knowledge gained from experiments in fission materials in certain cases can be applied to fusion systems, particularly those of materials under development for Generation IV concepts.

International collaboration among MTRs and specialized facilities has been identified as integral to progress in fusion development as well as enhancing reactor utilization. This publication specifies which areas of research remain in the qualification of structural materials and components, and has detailed the characteristics of many research reactors and devices that can accomplish an important portion of these necessary studies. This publication is the outcome of two recent IAEA sponsored meetings under its programme to enhance the utilization and collaboration of research reactor and material test facilities:

- Consultancy meeting on Role of Research Reactors in Materials Research for Nuclear Fusion Technology, 13–15 December 2010, IAEA, Vienna;
- Technical meeting on Materials under High Energy and High Intensity Neutron Fluxes for Nuclear Fusion Technology, 27–29 June 2011, IAEA, Vienna.

These meetings brought together representatives from MTRs, spallation neutron sources, multiple beam irradiation facilities, material scientists as well as fusion community representatives to discuss the current state of fusion research and to plot necessary studies and modes of research collaboration. The IAEA wishes to thank the 29 participants from their respective 20 Member States for their contributions to this publication. The IAEA officers responsible for this publication were D. Ridikas and R. Kamendje of the Division of Physical and Chemical Sciences, and N.D. Peld of the Division of Nuclear Fuel Cycle and Waste Technology.

EDITORIAL NOTE

This publication has been prepared from the original material as submitted by the authors. The views expressed do not necessarily reflect those of the IAEA, the governments of the nominating Member States or the nominating organizations.

This publication has not been edited by the editorial staff of the IAEA. It does not address questions of responsibility, legal or otherwise, for acts or omissions on the part of any person.

The use of particular designations of countries or territories does not imply any judgement by the publisher, the IAEA, as to the legal status of such countries or territories, of their authorities and institutions or of the delimitation of their boundaries.

The mention of names of specific companies or products (whether or not indicated as registered) does not imply any intention to infringe proprietary rights, nor should it be construed as an endorsement or recommendation on the part of the IAEA.

The authors are responsible for having obtained the necessary permission for the IAEA to reproduce, translate or use material from sources already protected by copyrights.

The IAEA has no responsibility for the persistence or accuracy of URLs for external or third party Internet web sites referred to in this book and does not guarantee that any content on such web sites is, or will remain, accurate or appropriate.

CONTENTS

SUMMARY……1

Developing fusion radiation resistant materials: the contribution of the presently available irradiation facilities 19
J.L. Boutard

Role of fission reactors and IFMIF in the fusion materials programme..... 34
S.M. González de Vicente

LVR-15 reactor and fusion related activities in material research and technology at CV Rez.... 41
M. Koleska, J. Kysela, M. Marek, R. Vsolak, O. Zlamal

Some experience and characteristics of Maria RR for material testing irradiation 52
G. Krzystoszek

The Jules Horowitz Reactor: a new research reactor devoted to fuel and material testing for the nuclear industry 59
P. Roux, C. Gonnier, G. Bignan, X. Bravo

Evaluation of microstructural stability of RAFM ODS-EUROFER steel..... 71
H.R.Z. Sandim, R.A. Renzetti, K.D. Zilnyk, A.F. Padilha, R. Lindau, A. Möslang

Radiation effects in functional materials for nuclear fusion application 78
T. Shikama, H. Katsui, S. Nagata, A. Hasegawa, A. Nishimura, T. Muroga, H. Kawamura, B. Tsuchiya, Y. Katoh

Non-destructive evaluation of perspective steels for fusion technologies 86
V. Slugeň, J. Veterníková, M. Petriska, S. Sojak, R. Hinca, P. Ballo, J. Degmová, M. Stracho, S. Kilpeläinen, F. Tuomisto, J. Räisänen, V. Krsjak

Tritium generation and migration in Li based materials for a fusion solid blanket..... 97
I. Tazhibayeva, T. Kulsartov, E. Kenzhin

Feasibility study and installation of thermal neutron driven 14 MeV neutron converter into the TRIGA research reactor..... 109
A. Trkov, L. Snoj, G. Žerovnik

Irradiation damage in China low activation martensitic (CLAM) steel 115
F. Wan, Y. Long

Efforts towards the neutron irradiation behavior study of RAFM steel at SWIP 121
P. Wang, J. Chen, Z. Xu

ABBREVIATIONS 127
CONTRIBUTORS TO DRAFTING AND REVIEW 130

SUMMARY

In light of the initial stages of operation of ITER and the planning of IFMIF and DEMO, as illustrated in Figure 1, the campaign towards the realization of commercial fusion power plants has been launched. With only ITER as a current base for the exploration of fusion core physics and containment, however, vast research and development is necessary in the areas of modelling and neutron science, functional and structural material testing and selection, blanket design and simulation of a fusion environment. As the heat and energy conditions necessary for the exploitation of fusion substantially exceed those of fission reactors, one critical factor is the development of functional, armour and structural materials of high heat and radiation resistant and their associated technologies, similar to the pioneering work of various mock-ups, critical assemblies and MTRs in relation to nuclear power plant development. Building on its contributions in neutronics and material testing for the validation of the design of ITER and its components, the international research reactor community can support further achievement towards the first wave of fusion facilities by conducting irradiation experiments, testing and simulations, and, furthermore, intensifying its collaboration to accomplish complimentary research and joint programmes.

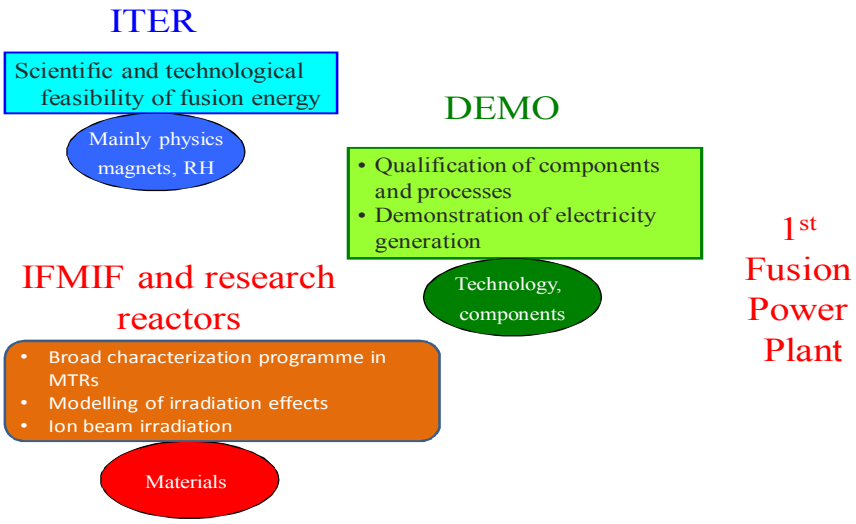

FIG. 1. A simplified scheme depicting fusion technology development.

Some limitations of research reactors in the pursuit of fusion research have been acknowledged. For instance, most research reactors produce neutron fluxes a few orders of magnitude below those of envisioned fusion devices and their operating temperatures are significantly below the projected range of 350–1000°C. The fission neutron spectrum, moreover, does not contain the 14 MeV neutrons of the deuterium–tritium fusion reaction. With low fluxes and less energetic neutrons, research reactors generally fail to produce the expected 30–80 dpa damage rate regarding the materials of DEMO, but also many research reactors were designed for a specific on-going mission or have administrative operational restrictions that limit the availability of the reactor to achieve significant damage rates. Also, only a few MTRs of pertinent flux range exist, although several are expected to become operational in the proceeding decade. Further constraining the ability of research reactors to simulate fusion conditions is the lack of considerable production of hydrogen and helium transmutation products and capacity for magnetic field testing.

Nevertheless, dedicated research reactors of all power ratings and designs can perform services valuable to fusion material research, namely:

- High flux reactors for mechanical property research and functional material testing;
- Medium flux reactors for specific knowledge such as instrumentation development;
- Low flux reactors in support of modelling, nuclear data measurements, etc.;
- Various flux facilities for testing of components and mock-ups as well as integrated tests with bulky objects.

With several high power and high flux MTRs due to come online in the present decade, this variety of research reactor can make possible a sizable body of fusion research. As a result these reactors will assume a function as important as the initial experimental non-nuclear fusion test devices. The expected considerable damage and degradation processes of structural and functional materials in a fusion nuclear environment oblige researchers to conduct a rigorous materials characterization and selection programme that will constitute the most critical phase in fusion technology development. The experimental data and relevant information gathered by this programme constitutes the link between the design and validation of fusion devices and their components.

Much valuable data in these areas can be discovered with a neutron flux of at least 5×10^{14} $cm^{-2}s^{-1}$, and both the mixed spectrum of MTRs and unitary flux of fast research reactors provide unique benefits for materials research, particularly microstructural studies. Figure 2, which demonstrates the disparity in operating conditions between fusion reactors and both current and future Generation IV fission reactors, signifies nevertheless that an advanced level of materials testing of benefit to all potential nuclear power applications must be achieved. A few reactors are attempting to overcome the limitations of fission reactors concerning fusion research, such as the use of Ni coated materials for enhanced helium production and the installation of thermal neutron converters to produce 14 MeV neutrons, e.g. in Slovenia [1] and Poland [2]. Aside from specialized capabilities, nearly all research reactors have some capacity for specific component testing and neutron activation studies. Perhaps the most promising feature of research reactors is that many already claim some level of ties to one or more academic technical faculties, and complimentary research is facilitated by similarly designed reactors such as MTR, TRIGA and WWR.

Furthermore, research reactors will provide the experimental results to support the design of reliable candidate materials to be used in fusion reactors. Also, knowledge gained through MTR experiments will be a key input to select and plan experiments to be performed in IFMIF, in which the available volume for specimens is limited. Although IFMIF is still in a planning stage, it is foreseen that research reactors nevertheless will possess several advantages in research and development to the fully operational accelerator facility in terms of ease and space for testing of engineering application standards, irradiation condition control, availability, costs and time scale.

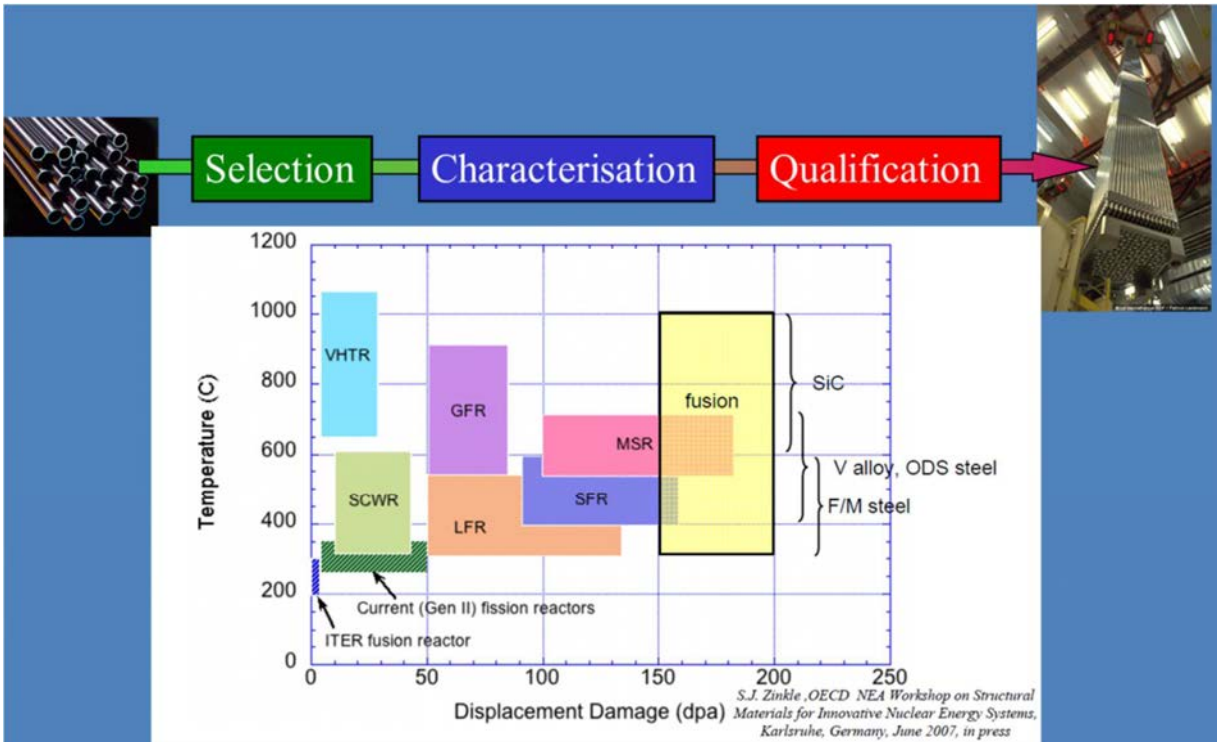

FIG. 2. Schematic representation of operational conditions of structural materials as a function of temperature and irradiation damage rates; VHTR: very high temperature reactor; SCWR: supercritical water reactor; GFR: gas cooled fast reactor; LFR: lead cooled fast reactor; SFR: sodium cooled fast reactor; MSR: molten salt reactor.

This document elaborates on the potential role research reactors can assume regarding fusion materials research and development. In general, the main tasks can be organized into seven areas:

- Generation of a major portion of material properties data for engineering design;
- Optimisation of experiments to be carried out in IFMIF;
- Evaluation and confirmation of performance limits;
- Validation of materials and component behaviour models on a macroscopic scale;
- Reduction of risks of component malfunction during operation in DEMO;
- Identification and insight into critical operational conditions;
- Exploration of unknown failure mode consequences for plant reliability.

1. GUIDELINES FOR FUSION MATERIALS STUDIES

Considering the various techniques available at research reactor facilities, among which are transmission electron microscopy (TEM), X ray and neutron diffraction, small angle neutron scattering (SANS), positron annihilation spectroscopy (PAS), and imaging and tomography, a sizable body of material testing in pursuit of suitable fusion materials can be attained, granting researchers as complete information as possible concerning the processes taking place during irradiation. In the process of validation and modelling, four levels, in which all types of nuclear research devices may contribute, can be distinguished:

1. Environmental control and instrumentation;
2. Mechanical testing;
3. Multi-effects testing; and
4. Verification and validation of modelling.

In these areas one essential observation is that material properties must be studied in isolated, rather than optimized, test environments. One should also keep in mind that for the structures envisaged for DEMO, thousands of tonnes of high quality materials must be manufactured within a single narrow specification window. In this regard, both design and manufacturing practices might have an irreversible influence, e.g. possible deterioration of carefully conditioned bulk materials due to manufacturing or heat input from welding, that must not be neglected. Close cooperation with materials manufacturing and materials processing industrial practice must be established at the earliest development stage. In particular, this implies that resources, irradiation campaigns and testing will not only be concentrated on the base materials but also on material systems such as similar or dissimilar welds and coatings.

1.1. Descriptions of the levels of testing

1.1.1. Environmental control and instrumentation

These experiments involve examples such as studies of radiation effects upon optical fiber degradation, thermal conductivity behaviour of various materials, and bolometer and magnetic sensor changes due to radiation damage as in the US–Japan fusion material programme JUPITER from 1995–2000. Such experiments necessitate a high degree of control in experimental temperature and precise monitoring capabilities of material parameters like stress, load and strain. The outcomes of these experiments are critical for diagnostics instrumentation used in the control of plasma in fusion devices.

1.1.2. Mechanical testing

This genre of testing consists of static in-pile experiments or dynamic testing to examine material fatigue constraints under various loads, including axial and cyclical loading, hold times and relaxation. One facility particularly suited for experiments in load history is the Joint Accelerators for Nano-Science and Nuclear Simulation (JANNuS) triple ion beam facility at the Saclay Centre of the French Atomic Energy and Alternative Energies Commission (CEA). This device arrangement is highly useful for the modelling verification of co-generation of radiation damage with charged ion particles (H and He), the effects of which can then be observed during beam operation by TEM. Research reactor centres possessing capabilities with a particle beam in the MeV range and TEM may also conduct similar research.

1.1.3. Multi-effects testing

The focus of these experiments is the testing of components and materials under mechanical and environmental stress, such as corrosion and microstructural processes during irradiation. The interaction of solid, gaseous and liquid materials in realistic contact during operation of a fusion device is one potentially valuable research area for both core physics and structural components. Additionally, studies of material interaction and corrosion do not necessarily require a very high flux, although specific knowledge and experience in the relevant processes are required.

1.1.4. Verification and validation of modelling

Finally, modelling and testing for selection of fusion materials can be a robust activity of research reactors that involves many processes beyond irradiation alone. For example, the study of extraction and permeation of tritium is vital for blanket research and the understanding of the behaviour of surrounding materials. The modelling of fusion materials goes through four stages:

- Screening of candidate materials;
- Demonstration of material performance limits;
- Qualification through demonstrations and evaluations of performance; and
- Material performance and component specific loading.

Similarly, the focus of such research should comprise four sequential areas, which may correlate to increasing testing device power or experimental capacity:

- Basic science for improved understanding and accelerated development cycles;
- Modelling from micro to macro scale;
- Modelling interpretation and transferability of measurements into design data and guidelines; and
- Macroscopic phenomena related to operation.

1.2. Facility requirements for fusion materials testing

The value of research reactors for fusion materials characterization is defined by, in addition to the availability of neutron flux, specific needs driven objectives like the irradiation of structural or functional materials and the scope of generated data, which differs among, for example, generic development, licensing and model verification. For a given objective some requirements such as precise temperature control and online measurements of tritium release might be considered essential or advantageous. Without being complete, the list of requirements includes:

1. For in-pile tests:
    - A materials palette;
    - Various types of in-pile static and dynamic testing devices such as flux detectors, instrumentation and means for the control of parameters like temperature and stress;

2. For characterization of structural materials:
    - Devices for microscopy, spectroscopy and tomography for characterization during the entire operational temperature window of the test materials;

3. For characterization of functional materials:
    - Breeder blanket;
    - Coatings;
    - Insulators;
    - Windows;

4. For post-irradiation examination:
    - Access to hot cells and devices for advanced test capabilities like elemental analysis, hardness testing and spectroscopy;
    - Specific knowledge in such areas as corrosion, handling of beryllium and behaviour of ceramics.

Other requirements may involve software for modelling and analysis, tools for very precise control of parameters and a certain level of flux, as many useful experiments can only be conducted in the large fluxes of high power reactors and MTRs.

1.3. Requirements for fusion structural materials

End of life service conditions for fusion structural materials are defined by the neutron fluence and operational temperature range, such as, for reduced activation ferritic–martensitic (RAFM) steels, the accumulation fluence of 10–20 MW/m^2 in a range of 300–550°C. The following two tables provide a summary of present fusion structural materials developments, and as a rule of thumb, the neutron loading on a diverter target plate is close to one third of that experienced upon the first wall, or 10–30 dpa in steel.

TABLE 1. SERVICE CONDITIONS FOR A DEMO TARGET OF BREEDER BLANKET RAFM STEEL

Temperature (°C)	285–550 (Maximum temperature for oxide dispersion strengthened RAFM is 650/750°C)
Neutron fluence (MW/m^2)	3–5 (First DEMO blanket), 10 (Final goal)
Damage level (dpa)	30–100 (steel)
Coolant	Water or helium

TABLE 2. SERVICE CONDITIONS OF MATERIALS FOR ADVANCED CONCEPT BLANKETS AND DIVERTERS

Material	Vanadium alloys	SiC/SiC composites
Maximum temperature (°C)	<700	<1100
Coolant	Liquid metal	He gas or liquid metal

The application of small specimen test techniques, in particular the high flux test module of IFMIF, is favourable for several reasons:

- To make best use of available irradiation volume;
- To keep temperature gradients in the specimen as low as possible, for example, step gradients for changes of material properties within 20–50°C; and
- These techniques are already used for tensile, creep and fatigue specimens in irradiation campaigns utilizing fission research reactors in the EU, Japan, USA and Russian Federation. In these areas the fundamentals of IFMIF type small sample test techniques have been already widely established.

However, small specimen test techniques for fracture toughness and fatigue crack growth tests are still under development. Moreover, the gap between these techniques and the design methodology for high temperature structures irradiated to high damage levels by high energy

neutrons still remains. Finally, small sample test techniques may become a broader requirement from the fusion community in order to harmonize databases.

2. CURRENT FUSION MATERIAL RESEARCH AND DEVELOPMENT

Fusion materials research, as indicated by the presentations of the two IAEA meetings, can be grouped into three general areas. The meeting participants described various activities relating to structural material investigation, test blanket development and multi-purpose studies that have advanced through the use of an array of experimental techniques afforded by research reactor facilities. The following summaries confirm the important role played by today's research reactors in the support of ITER operation and preparations for IFMIF and DEMO. The submitted papers attached as an annex to this document provide greater detail on many of these projects.

2.1. Structural material characterization at research reactors

In Japan, both the Japan Atomic Energy Agency (JAEA) and Institute for Material Research at Tohoku University intend to use reactor of high, medium and small flux for studying and testing materials performance under simulated fusion conditions (See Figure 3), although many activities have been suspended following the Fukushima Daiichi NPP Disaster. High flux reactors such as JOYO, with its large experimental volume, are expected to facilitate studies of material behaviour under high irradiation damage rates, particularly RAFM steels as a primary structural material, prior to final verification in IFMIF. In situ studies of functional material properties can be accomplished in more accessible medium flux reactors, which tend to offer more controllable environments with lower nuclear heating rates, like the Japan Material Test Reactor (JMTR). Finally, considering smaller neutron fluences, e.g., $<10^{23}$ m^{-2}, small research reactors can provide a platform for cryogenic testing of candidate material tensile properties. Much international collaboration in joint projects with facilities of a similar scale, such as the JAEA partnership with Oak Ridge National Laboratory for high flux reactor experiments, is also expected [3].

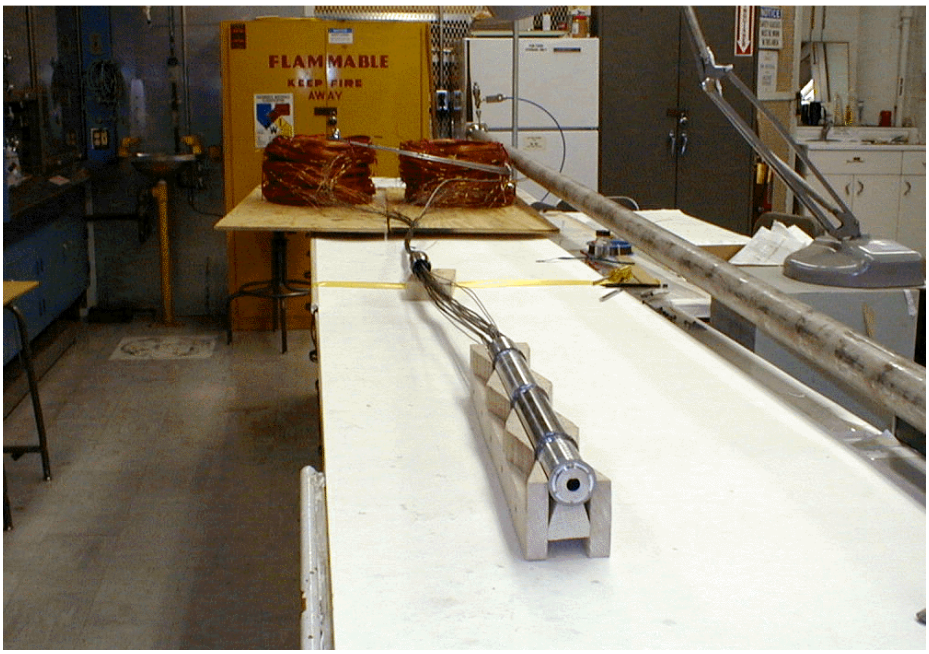

FIG. 3. Apparatus for thermal conductivity measurements of SiC composites at JAEA.

The University of São Paulo, Brazil, is carrying out a programme to evaluate the microstructural stability during recrystallization of RAFM ODS EUROFER steels in collaboration with the Karlsruhe Institute of Technology in Germany. A number of characterization techniques such as SEM, TEM, electron back scattering diffraction (EBSD), Vickers micro-hardness and magnetization have been used, with research now being planned for collaborative recrystallization studies under neutron irradiation [4].

The characterization of many low activation materials useful as structural materials is on-going at the A.A. Bochvar Institute of Inorganic Materials in Moscow, Russian Federation in order to assist in the design of DEMO and imminent tokomak construction projects. High power fast and thermal research reactors are used to study defect formation and evolution, mechanisms of radiation phenomena and properties, the effects of alloy composition and micro-structure formation and evolution on irradiation properties, and the resulting data will complete a structural materials database over a wide range of neutron fluences and temperatures. Consequently, design guidelines for these materials and ageing and degradation programmes for fusion devices can be more easily formulated [5].

The cascade accelerator arrangement at the Slovak University of Technology (See Figure 4) and the positron beam facility at the Technical University of Munich have been utilized for PAS techniques involving helium implanted in Fe–Cr alloys. The differences between the damage created by ion irradiations of H and He with respect to neutron damage were thus able to be analyzed. In H and He ion implantations by cascade accelerator in particular, PAS techniques based on moderated slow positron beams provided valuable data about vacancy type defects caused by ion bombardment. Complimentary techniques such as SEM, TEM, Mössbauer spectroscopy and X ray diffraction were used to confirm several results [6].

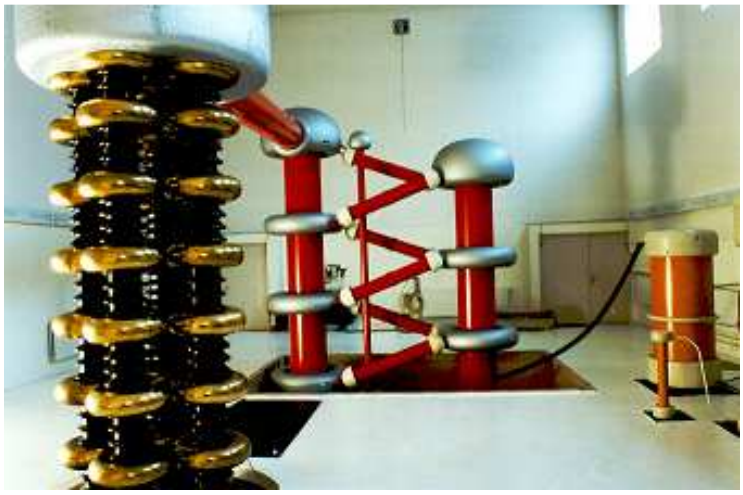

FIG. 4. Cascade accelerator at Slovak University of Technology.

Because of the complex effects of transmutation and radiation induced defects in fusion materials, the EFDA Close Support Unit in Garching, Germany, has divided its materials research into four areas. First is the modelling of steel and iron based alloy behaviour and development of a framework for experimental validation. Development of a versatile nano-structured ODS ferritic steel and SiC composite are also interests. Finally, EFDA is concerned with the use of tungsten and its alloys as a structural and armour material in DEMO [7].

The possibilities of the Polish research reactor Maria, a multipurpose high flux reactor of 30 MW, for material testing irradiations is dependent on the acquisition of hot cells with appropriate shielding, but the staff of the Institute of Atomic Energy (IAE POLATOM) have partnered with CEA to utilize the Laboratory for Studies on Irradiated Fuel (LECI) hot laboratory for post-irradiation examination. The IAE POLATOM facility contains three thermostatic gaseous rigs reserved for material testing, and the reactor itself features movable core and reflector elements for excellent flexibility [8]. The HANARO reactor of the Korean Atomic Energy Research Institute is also an interesting platform for fusion materials studies, considering its fuel test loop and hydraulic rabbit systems. Furthermore, advanced rabbit capsules capable of high temperature irradiation technology up to 1000°C are under development for analysis of high temperature radiation damage phenomena [9].

In the Australia National Science and Technology Organisation (ANSTO), research teams possess multiple material examination capabilities following irradiation in the OPAL research reactor (See Figure 5), and researchers have shifted the focus of their materials research toward nuclear applications. Neutron scattering techniques such as neutron diffraction, small angle neutron scattering and reflectometry are highly advantageous in that no special metallurgical preparation is generally required, and sample manipulation can be minimized when compared to other techniques. ANSTO is also equipped with a fabrication bay, hot cells and a new TEM facility, and the staff claims experience in multi-scale modelling for effective fusion structural materials research [10].

FIG. 5. OPAL research reactor at ANSTO.

2.2. Test blanket research at research reactors

Research in China has centered on two groups developing RAFM steels for fusion breeder blankets, resulting in two variants, China low activation ferritic (CLF-1) and China low activation martensitic (CLAM) steel that have been tested at the Southwestern Institute for Physics in Chengdu and University of Science and Technology in Beijing. In both cases material fabrication is done at an industrial level of 1–2 tonnes prior to irradiation and post-irradiation examination. These irradiation campaigns have included multiple techniques such as Charpy tests and heavy ion irradiation, while small sample test techniques are under research. CLF–1 presents some issues due to a lack of control regarding impurities, and in the case of CLAM, the impact of additions of Si is being studied. Electron irradiations by a high voltage electron accelerator have

been carried out in Japan to analyse the consequences of adding a higher amounts, and no delta phase has been found to date in the samples, such as in Figure 6. China's two newest high power research reactors, the China Advanced Research Reactor (CARR) and China Experimental Fast Reactor (CEFR), are expected to contribute to fusion research as well [11, 12].

In India the main efforts are concentrated upon fast breeder reactors, but support programmes for ITER encompass test blanket module and diverter assemblies. In this context, RAFM steels are being developed for the Indian Test Blanket at an industrial scale of two tonnes. The work of the Indira Ghandi Centre for Atomic Research (IGCAR) in cooperation with the Institute for Plasma Research involves mainly refining the chemical composition, most recently, the effects of tungsten and tantalum for the improvement of stability and toughness, respectively. The main conclusion is that India has developed a RAFM steel suitable for test blankets comparable to EUROFER or F82H with a grain size of 15–20 microns but with variable content of Ta. ODS RAFM steels are also being developed to improve high temperature creep resistance in test blanket materials [13].

The Institute for Nuclear Physics in Kazakhstan is working closely with JAEA to study the retention, diffusion and release of tritium in different compounds useful for the test blanket module. Breeder material enriched in Li was provided by JAEA for the performance of experiments in the Institute's WWR-K reactor. In-pile studies of lithium ceramic Li_2TiO_3 for relatively high Li burn-up and temperature were conducted to assess possible long term effective generation of tritium. Crucial parameters to characterize tritium release and kinetics such as activity, concentration in residual gas spectra and diffusion mechanisms (See Figure 7) were analysed according to burn-up percentage and temperature. Concerning the tritium breeding ratio, the validation of cross-sections and computational methods for accurate predictions was also found to be very important [14].

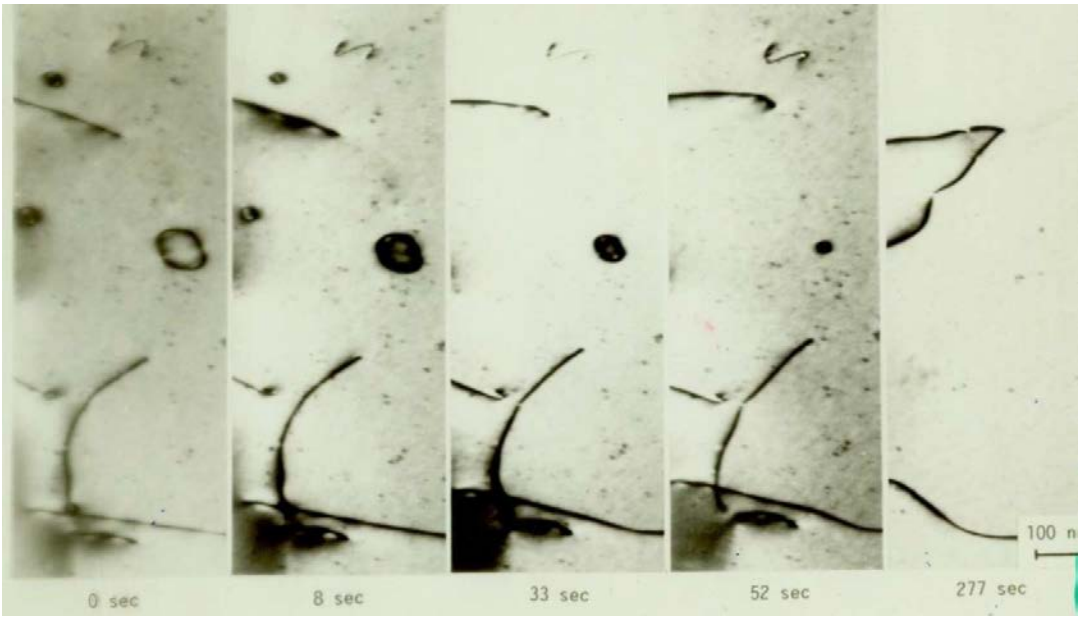

FIG. 6. Change of loops during electron irradiation after H^+ implantation in pure iron.

FIG. 7. Experimental device VIKA for tritium collection and spectroscopy.

2.3. Multipurpose testing at research reactors

Lithium also serves as the basis for an extensive research programme at the Institute of Physics and Power Engineering in Obninsk, Russian Federation, which devised a Li test loop for testing hydrodynamics in a circulating coolant loop and the behaviour of Li neutron targets. Both of these aspects are pertinent for the design of IFMIF, but further investigations have continued into corrosion and compatibility with fusion structural materials composed of vanadium and ferritic-martensitic steels. To this end, a test facility was constructed for the analysis of disk shaped samples in high temperature environments, and the Institute possesses additional reactor loops for the monitoring of various impurities [15].

Coordinated by the Nuclear Research Consultancy Group (NRG), irradiations at the High Flux Reactor (HFR) in Petten, Netherlands, have resulted in much data on irradiation behaviour of ITER candidate materials now contained in the ITER Material Properties Handbook, including parameters for 316L(N) plates, electron beam and tungsten inert gas welds, hot isostatic pressing bonds and products and explosive forming and cladding. Microstructural characterization for ceramic breeder development, as opposed to steel based, is one current focus. A broad programme for qualification of EUROFER steel in fusion operation conditions as well as tritium release by lithium ceramic pebbles will assist in the design of the ITER test blanket module and the DEMO device [16].

Finally, with a number of tightly controlled loops and rigs, the LVR-15 reactor of the Research Centre Řež in the Czech Republic has participated in the European Fusion Development Agreement (EFDA) and the European Union's Fusion for Energy (F4E) programmes. The former has concerned determination of material properties of EUROFER97 steel in the reactor's Pb–Li loop, while in-pile tests with beryllium clad first wall mock-ups (See Figure 8) and tritium extraction tests in the Pb–Li loop have been conducted under F4E [17].

FIG. 8. Loop sample holder with in-pile thermal testing device for primary first wall mock-ups.

In collaboration with the University of Science and Technology in Beijing, fabrication and microstructural characterization of oxide dispersion strengthened (ODS) steels has been examined with the dry irradiation rig and hot cells of the Budapest Research Reactor at the Centre for Energy Research in Hungary. The spark plasma sintering method has been utilized so that the densification of ODS samples without considerable grain growth process can be achieved within a few minutes Tungsten rods, nanocarbon fiber reinforced ceramics and EUROFER97 ageing processes have also been studied. JAEA is planning to irradiate superconductors in this reactor as well [18].

Given the excellent thermo-physical and nuclear properties of many liquid metals, the National Academy of Science of Ukraine has launched a study devoted to corrosion mechanisms at the point of contact of liquid metals and structural materials. These experiments aspire to describe the corrosive effects of non-metal impurities like oxygen, nitrogen and carbon in particular, as well as the adsorption property of heavy liquid metals such as lead and bismuth for the potential of these materials as a fusion reactor coolant [19].

Jožef Stefan Institute in Slovenia is planning to develop and install a 14 MeV converter in the existing TRIGA Mark II reactor to extend their capabilities in the area of reactor physics, mainly the validation and improvement of nuclear data at energies above 10 MeV and the irradiation of low activation materials. Notably, the thermal to 14 MeV neutron converter is a passive device easy to maintain and operate at a low cost [1].

Two new high flux research reactors, the Jules Horowitz Reactor presently under construction at CEA Cadarache in France and the PALLAS reactor intended to replace HFR in Netherlands, will soon be operational in Europe for fusion candidate material research. The Jules Horowitz Reactor will be mainly devoted to testing Generation IV materials, but the facility is also open to work with the fusion community as one segment of service as an international multi-user facility. High flux neutron irradiations and post-irradiation examination will be two prominent activities of relevance to fusion research at these facilities [20, 21].

3. THE ROLE OF RESEARCH REACTORS IN FUTURE FUSION MATERIALS STUDIES

Currently nearly half of the operational RRs are under-utilized, whereas some countries are planning to build new ones [22]. Given the range of material irradiation and examination programmes described in the previous section, fusion materials development can serve as a major

catalyst for enhanced utilization and component in strategic planning toward progress along the fusion facility road map. Many data have already been obtained to validate the design of ITER components and in support of the conceptual designs of subsystems towards DEMO and beyond. With ITER in its initial operation stage and IFMIF and DEMO years off, the fusion community depends on research reactors of various power levels and experimental capabilities to perform various irradiations and tests.

The present available facilities to study fusion materials are threefold, namely, accelerators, spallation neutron sources and fission research reactors, and capable of combining a sizable portfolio of techniques for material characterization like TEM, X ray, neutron radiography and neutron diffraction, SANS and PAS, and others. Each of these must be explored to obtain as complete information as possible regarding the processes taking place in materials during irradiation, although none can provide the full information required for the final qualification and validation of candidate materials for future fusion devices, necessitating complimentary studies with IFMIF, in which key measures like fusion radiation damage, He/dpa and H/dpa ratios and He and H production rates can be mapped.

3.1. Defining the role of research reactors

3.1.1. Status of R&D related to fusion materials

Conclusions of fusion materials studies to date not only delineate how much progress has been accomplished, but also highlight crucial studies yet to be undertaken. The participants of the two IAEA sponsored meetings identified several aspects that may serve as guidelines for future research.

Considering structural and functional materials, only RAFM steels are ready for qualification for DEMO, while ODS ferritic–martensitic and ferritic steels are still under development, partially due to a lack of industrial manufacturers in Europe and US. Vanadium alloys for Li cooled tritium breeding blankets are still under development in the Russian Federation and Japan, along with SiC/SiC composites, which may or may not be suitable for many applications, in many states. Tungsten alloys for fusion are at the initial stages of development.

Furthermore, various joining techniques still must be developed and selected. Radiation effects in functional materials such as Be and tritium breeding materials are in many cases glaringly unexplained. Radiation effects in insulators of DEMO windows, diagnostics and heating devices remain unexplored. Other issues to be addressed are, but not limited to: tritium behaviour in irradiated materials, a vacuum vessel for DEMO, activation of various materials, waste generation and management, shielding of superconducting magnets, and many more.

3.1.2. Role of fast high flux reactors in the area of materials development for fusion

Fast neutron or very high flux reactors like BOR-60 (Russian Federation) and High Flux Isotope Reactor (HFIR) (USA) provide a representative dpa rate and are therefore suitable for issues linked with material phase stability. Point defects produced by fission neutrons and 14 MeV neutrons seem to be identical in Fe and most probably in all transition metals. However, He/dpa and H/dpa ratios are too low as compared with fusion neutrons at least by one order of magnitude as shown in Figure 9. The suitable ranges of He production and damage rates, of which only

DEMO, IFMIF and the experimental accelerator driven system (XADS) qualify, are indicated by the pink circle.

Dedicated particle beam experiments must provide qualitative data to validate theory and modelling in order to complement the lack of co-generation of gas and displacement damage before IFMIF is able to deliver the required irradiation conditions, in particular for structural materials. One critical issue remaining is the availability of sufficient number of fast high-flux research reactors, although new reactors in planning or under construction are MYRRHA in Belgium, Multipurpose Fast Neutron Research Reactor (MBIR) in the Russian Federation, Advanced Sodium Technical Reactor for Industrial Demonstration (ASTRID) in France and Prototype Fast Breeder Reactor (PFBR) in India.

3.1.3. Role of other research reactors in the area of materials development for fusion

MTRs are generally limited to a dose rate of ~7 dpa/year, with ~15 dpa/yr expected in the future Jules Horowitz Reactor and up to ~12 dpa/yr in PALLAS. For all research reactors, low production rates of He and H can be partially compensated through combined methods such as Ni coated specimens, boron enrichment and direct implantation of He and H prior to irradiation with neutrons. Many research reactors can contribute through neutron beam science, on-site post-irradiation examination, development of corrosion or coolant compatibility loops, nuclear data measurements, characterization of activation and waste generation, documenting experience and good practices in nuclear infrastructure development, nuclear engineering and human resource development, among a number of additional activities.

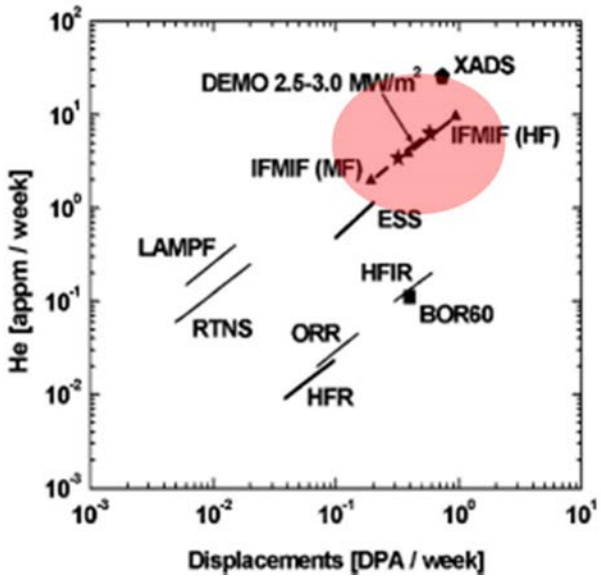

FIG. 9. Accessible conditions for materials testing and operation by various facilities are represented as a function of He production (y axis) and dpa rates (x axis) [23].

3.2. Synergy of fission and fusion materials development

A significant overlap remains between the application spectra in the fission and fusion technology domains, most importantly considering shared roots in materials science and engineering, not to mention manufacturing technology. The environments differ principally in the

neutron spectrum from the first wall of a fusion reactor to half a meter inside the blankets. There the co-generation of H and He and radiation damage from neutron interactions with matter differ strongly from fission reactor core conditions. The remaining structures, however, undergo neutron interactions comparable to materials in a fission reactor core, except for effects from the presence of magnetic fields.

Indeed, fission and fusion domains can both benefit from a coherent programme for basic material science and modelling from the micro- to macro-scale. The nature of the fusion nuclear environment has led to fusion specific activities addressing the co-generation of H, He and solid transmutation products, as well as radiation damage. It should be noted that adverse transmutation effects resulted in the late 1970s and early 1980s in the complete abandonment of applications based on nickel bearing steels and, consequently, the development of low activation steels. For the same reasons high temperature alloys of niobium and molybdenum were abandoned, and advocacy of vanadium alloys began. In the context of advanced fission reactors the fission community has also developed a prominent interest in the use of low activation alloys. Due to joint interest, collaborative research between the fusion and fission communities certainly exists and will become more intense from necessary input regarding manufacturing practices and nuclear materials use and recycling. The fusion domain can substantially gain from fission design and licensing procedures within the nuclear industry.

Similar experiences exist in the technological transition from thermal neutron based power reactors to fast spectrum power reactors, although notably, several differences between them are not as pronounced as between fission and fusion. Aspects of the development of fast reactor technology, e.g., the development of austenitic steels, can serve as an example of the lasting impact from basic insight originally gained in thermal neutron power generation. Basic science and material behaviour modelling, of course, also form a foundation for fusion research. The knowledge and applications in ceramic fuels and blanket component technology have attractive similarities with which to stimulate the development of synergy mechanisms.

Paramount for synergy is also the attendant services provided by irradiation experts and auxiliary facilities connected to the research reactors. Ties with hot laboratories and universities specialized in radiation damage studies in solid materials are essential for the successful initiation and completion of irradiation programmes. Last but not least, although fusion and fission address similar materials, the development goals are different on account of different uses. For example, fusion breading blanket materials are subjected to high thermal loads at moderate primary stresses, requiring the exchange therefore of breading blankets and diverters every 3–5 years. Creep resistance is hence not the key issue. On the contrary, in fission technology many critical components are designed and licensed to remain in service for at least 40–50 years.

4. CONCLUSIONS

Citing numerous pathways for improved cooperation among research organizations for advanced fusion materials research, the participants generated a series of recommendations to all stakeholders. For the two groups of experts themselves, a template recording the characteristics of irradiation devices and post-irradiation examination facilities most valuable for material irradiation and research could be prepared and distributed. This data could then be collected and disseminated through an online database or publication. The template could also be enhanced by describing all research reactor capabilities with respect to specific requirements of the fusion

community. Also, the international fusion community, as in the case of ITER, was recommended to develop reference documents on DEMO requirements and candidate materials to facilitate cooperation and publicize fusion materials science and engineering related irradiations and research.

Within fusion materials research, the shared benefits to fusion and fission research should be promoted in support of expanded ion and neutron irradiation studies as well as modelling exercises. The use of neutron beams for the characterization of highly irradiated materials should also be explored. Joint materials development could also be organized through platforms such as the IAEA's International Project on Innovative Nuclear Reactors and Fuel Cycles (INPRO) and Accelerator Simulation and Theoretical Modelling of Radiation Effects (SMoRE) programme, and research reactor managers and related academicians should consider the creation of dedicated reactor coalitions and networks for materials studies.

With a view toward future international meetings, finally, a dedicated Consultancy Meeting on international efforts for tritium generation, transport and breeding based on evaluated needs by the fusion community could be organized. Additional meetings and workshops to bring together the fusion and fission communities, as in the 2011 Technical Meeting "Materials under High Energy and High Intensity Neutron Fluxes for Nuclear Fusion Technology," will provide a constructive space for the sharing of experiences and good practices, which can only benefit each of the parties.

REFERENCES

[1] TRKOV, A., SNOJ, L., "Feasibility study and installation of thermal neutron driven 14 MeV neutron converter into the TRIGA research reactor", Materials under High Energy and High Intensity Neutron Fluxes for Nuclear Fusion Technology, IAEA Proceedings Series, IAEA, Vienna (2013).

[2] PROKOPOWICZ, R., PYTEL, K., DOROSZ, M., MARCINKOWSKA, Z., WIERZCHNICKA, M., "The thermal to 14 MeV neutron converter design in Maria reactor", National Centre for Nuclear Research Annual Report 2011, National Centre for Nuclear Research, Otwock-Świerk (2012).

[3] SHIKAMA, T., et al., "Radiation effects in functional materials for nuclear fusion application", Materials under High Energy and High Intensity Neutron Fluxes for Nuclear Fusion Technology, IAEA Proceedings Series, IAEA, Vienna (2013).

[4] SANDIM, H.R.Z., et al., "Evaluation of microstructural stability of RAFM ODS-Eurofer steel", Materials under High Energy and High Intensity Neutron Fluxes for Nuclear Fusion Technology, IAEA Proceedings Series, IAEA, Vienna (2013).

[5] CHERNOV, V., "Energy related material research in Russia", presented at IAEA Consultancy Meeting on Role of Research Reactors in Materials Research for Nuclear Fusion Technology, Vienna, 2010.

[6] SLUGEŇ, V., "Non-destructive evaluation of perspective steels for fusion technologies", Materials under High Energy and High Intensity Neutron Fluxes for Nuclear Fusion Technology, IAEA Proceedings Series, IAEA, Vienna (2013).

[7] GONZÁLEZ DE VICENTE, S.M., "Current irradiation experiments for fusion materials: status and prospects", presented at IAEA Consultancy Meeting on Role of Research Reactors in Materials Research for Nuclear Fusion Technology, Vienna, 2010.

[8] KRZYSZTOSZEK, G., "Some experience and characteristics of Maria RR for material testing irradiation", Materials under High Energy and High Intensity Neutron Fluxes for Nuclear Fusion Technology, IAEA Proceedings Series, IAEA, Vienna (2013).
[9] SHIN, C., "Current status and perspectives of materials irradiation tests in HANARO", presented at IAEA Consultancy Meeting on Role of Research Reactors in Materials Research for Nuclear Fusion Technology, Vienna, 2010.
[10] DI PIETRO, P., "ANSTO Institute of Materials Engineering", presented at IAEA Technical Meeting on Materials under High-Energy and High-Intensity Neutron Fluxes for Nuclear Fusion Technology, Vienna, 2011.
[11] WANG, P., CHEN, J., XU, Z., "Efforts towards the neutron irradiation behavior study of RAFM steel at SWIP", Materials under High Energy and High Intensity Neutron Fluxes for Nuclear Fusion Technology, IAEA Proceedings Series, IAEA, Vienna (2013).
[12] WAN, F., LONG, Y., "Irradiation damage in China low activation martensitic (CLAM) steel", Materials under High Energy and High Intensity Neutron Fluxes for Nuclear Fusion Technology, IAEA Proceedings Series, IAEA, Vienna (2013).
[13] SAROJA, S., "Materials research at IGCAR for Indian nuclear energy and fusion programmes", presented at IAEA Consultancy Meeting on Role of Research Reactors in Materials Research for Nuclear Fusion Technology, Vienna, 2010.
[14] TAZHIBAYEVA, I., KULSARTOV, T., KENZHIN, E., "Tritium generation and migration in Li-based materials for a fusion solid blanket", Materials under High Energy and High Intensity Neutron Fluxes for Nuclear Fusion Technology, IAEA Proceedings Series, IAEA, Vienna (2013).
[15] LOGNIOV, N., "Some issues of coolant technology and corrosion of structure materials for fission and fusion reactors", presented at IAEA Consultancy Meeting on Role of Research Reactors in Materials Research for Nuclear Fusion Technology, Vienna, 2010.
[16] VAN DER LAAN, J.G., "Fusion nuclear technology activities at NRG Petten", presented at IAEA Consultancy Meeting on Role of Research Reactors in Materials Research for Nuclear Fusion Technology, Vienna, 2010.
[17] KOLESKA, M., KYSELA, J., MAREK, M., VSOLAK, R., ZLAMAL, O., "LVR-15 reactor and fusion related activities in material research and technology at CV Rez", Materials under High Energy and High Intensity Neutron Fluxes for Nuclear Fusion Technology, IAEA Proceedings Series, IAEA, Vienna (2013).
[18] HORVÁTH, Á., GILLEMOT, F., BALÁZSI, C., TÖRÖK, G., "Contribution of Budapest Neutron Centre to the fusion materials program", presented at IAEA Technical Meeting on Materials under High-Energy and High-Intensity Neutron Fluxes for Nuclear Fusion Technology, Vienna, 2011.
[19] YELISEYEVA, O.,"Compatibility of structural materials with liquid metal breeders/coolants", presented at IAEA Consultancy Meeting on Role of Research Reactors in Materials Research for Nuclear Fusion Technology, Vienna, 2010.
[20] ROUX, P., GONNIER, C., BIGNAN, J., BRAVO, X., "The Jules Horowitz Reactor: a new research reactor devoted to fuel and material testing for the nuclear industry", Materials under High Energy and High Intensity Neutron Fluxes for Nuclear Fusion Technology, IAEA Proceedings Series, IAEA, Vienna (2013).
[21] VAN DER SCHAAF, B., "PALLAS for fusion", presented at IAEA Consultancy Meeting on Role of Research Reactors in Materials Research for Nuclear Fusion Technology, Vienna, 2010.

[23] INTERNATIONAL ATOMIC ENERGY AGENCY, IAEA Research Reactor Data Base (RRDB), available at http://nucleus.iaea.org/RRDB/, last accessed in March 2013.
[23] VLADIMIROV, P., MOESLANG, A., Comparison of material irradiation conditions for fusion, spallation, stripping and fission neutron sources, Journal of Nuclear Materials **329–333** (2004) 233–237.

DEVELOPING FUSION RADIATION RESISTANT MATERIALS
The contributions of the presently available irradiation facilities

J.-L. BOUTARD
CEA Saclay Nuclear Research Centre,
Atomic Energy and Alternative Energies Commission (CEA),
Gif sur Yvette, France
jean-louis.boutard@cea.fr

Abstract

Radiation effects under a fusion environment are reviewed. Phase stability can be simulated using fission neutrons or ion irradiation. He and H point defect accumulation can be easily simulated using multiple ion beam irradiation. Effects of He and H on mechanical properties requires additional techniques. Examples presented show that only materials with deliberately tailored chemical composition and microstructure will be able to withstand fusion reactor conditions. The systematic and complementary use of presently available neutrons and ion beams facilities have the capability of developing a first set of reference materials to be validated in IFMIF and used in the safely and economically building and operation of a fusion demonstration device. Finally the paper underlines the need for modelling to interpolate data obtained under various spectra, optimise the IFMIF program and extrapolate its data to the broad operating conditions of an actual reactor.

1. INTRODUCTION

Following ITER's successful operation, the European strategy foresees constructing a first demonstration thermonuclear device, DEMO, with the objective of safe and economical production of electricity using the deuterium–tritium fusion reaction.

Tritium, with a half-life of 12.32 years, must be produced within DEMO for self-sustained operation, i.e., each time a tritium atom is consumed, another must be produced in the tritium breeding blanket (TBB). In addition, electricity production requires TBB operation at high temperatures. Two helium cooled concepts have been selected within the European Union. In the He cooled lithium lead (HCLL) blanket, the eutectic liquid metal $Li_{17}Pb_{83}$ provides lithium atoms. In the He cooled ceramics pebble bed (HCPB) concept, solid orthosilicate ceramic Li_4SiO_4 is foreseen as the breeding material. To compensate the unavoidable loss of neutrons, neutron multipliers capable of (n,xn) reactions with x>1 must be introduced:

- Pb nuclei within the Pb–Li eutectic for the HCLL concept;
- Solid Be metal or berylites for the HCPB concept [1].

The DEMO TBB structures are foreseen to be made of reduced activation ferritic–martensitic (RAFM) steels. RAFM steels have a maximum operating temperature ~550°C given by their thermal creep resistance. Oxide dispersion strengthened (ODS) martensitic or ferritic steels with maximum expected operating temperatures up to ~650°C and ~750°C, respectively, are being developed to be used for the hottest parts [2].

The α particles and impurities exhausted from the plasma, essential for the very long pulse of DEMO or steady state operation of a reactor, will be ensured via the divertor, which is expected to withstand high heat fluxes between 10 and 20 MW/m^2. Structure and armour materials must withstand a maximum temperature significantly above 1000°C. Tungsten alloys have been selected on the basis on their high melting points.

Beryllium used in ITER as armour material for the first wall is discarded for DEMO because of its too low melting temperature. Tungsten is foreseen as armour material for the first wall and divertor because of its high melting point, 3422°C, and very low sputtering rate.

Table 1 summarizes the data concerning structural and armour materials with their operating conditions for the DEMO reference concepts of in-vessel components.

TABLE 1. STRUCTURAL AND ARMOUR MATERIALS FORESEEN FOR THE TRITIUM BREEDING BLANKET AND THE DIVERTOR OF DEMO

Components	Materials and conditions	HCLL blanket	HCPB blanket
Tritium breeding blankets	Structural material	EUROFER	
	Armour material	W	
	Coolant	He	
	T: inlet/outlet (°C)	300/500	
	Tritium breeding material	Eutectic $Li_{17}Pb_{83}$	Li_4SO_4
	Maximum dose (dpa)	50–80	
	Helium deposition in EUROFER (ppm/dpa)	12	
	Thermal flux (MW/mw^2)	0.1–1	
Diverter	Structural material	W alloys	
	Armour material	W	
	Coolant	He	
	T: inlet/outlet (°C)	~540/720	
	Helium deposition in tungsten (ppm/dpa)	~0.4	
	Thermal flux (MW/mw^2)	10–20	

Developing and qualifying structural, armour and functional materials to withstand high temperatures and doses under a fusion environment are among the main challenges for DEMO. Among all the materials quoted above, only EUROFER has reached maturity with a good understanding of its in-service properties as a function of its chemical composition and thermal mechanical treatment. All others require innovative scientific and technological development, implying metallurgical studies, neutron and ion irradiation, chemical–physical characterisation and modelling to come to a proper mastering of their in-service properties.

The second section describes the main mechanisms of interaction between fast neutrons and materials, which will strain the crystalline structure, the chemical composition and the microstructure, i.e., the three characteristics determining in-service properties. In the third section main features about long term point defects and helium accumulation as well as phase stability under irradiation will be described. Phase stability under a fusion environment may be simulated by ion and fission neutron irradiation; conversely accumulation of point defects and He requires additional techniques. In the fourth section experimental data on phase stability of ferritic–martensitic steels and tungsten alloys under irradiation will be given. The fifth section will briefly discuss simulation methods used to simulate He and H production specific to 14 MeV neutrons. In the sixth section experimental data will be analysed concerning the swelling resistance and He

embrittlement of RAFM steels under a fusion environment. In the seventh section, elements of strategy for developing high heat and resistant materials for DEMO will be sketched, especially the need for using neutron and ion sources and modelling to prepare the IFMIF validation programme and extrapolate expected data to the wide range of operating conditions in a DEMO device.

2. INTERACTION OF FAST NEUTRONS WITH MATERIALS

Fast neutrons promote inelastic and elastic interactions. The former induce transmutations, and the latter displace atoms from their crystalline sites, creating primary knock-on atoms (PKA). Once created, PKAs lose their energy via inelastic interactions with electrons and elastic shocks with nuclei. The profiles of electronic and nuclear stopping power for PKAs in pure Fe are given as function of their kinetic energy in Figure 1a. In Figure 1, vacancies are in yellow, self-interstitial atom (SIAs) in red and substituted atoms in blue. Simulation was carried out via molecular dynamics using classical mechanics with inter-atomic forces derived from an empirical potential.

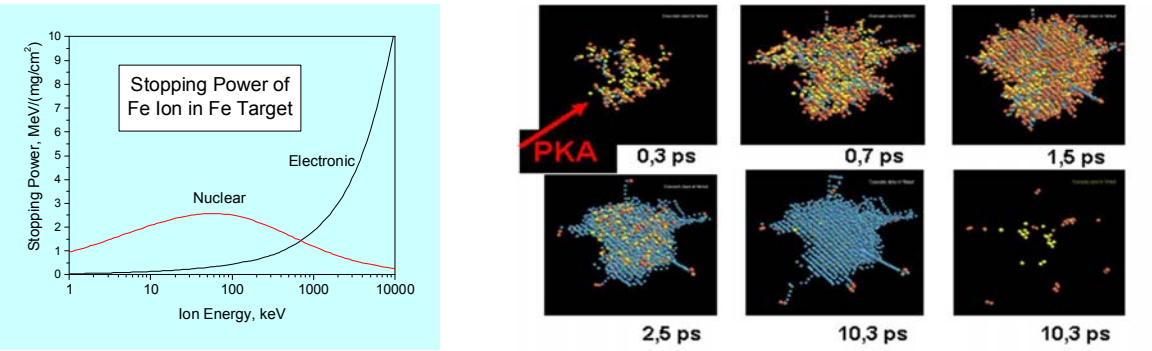

a) b)

FIG. 1. (a) PKA electronic and nuclear stopping power versus kinetic energy in pure Fe [3] and (b) Time evolution of an atomic displacement cascade due to a 7 keV PKA in Ni. (Source: Nguyen Doan, CEA Saclay).

In insulators or semiconductors, the electronic excitations could result in charged defects or donor and acceptor electronic states in the gap of the electronic band structure. In polymers, electronic excitations may produce chemically active radicals and considerably change compatibility with their environment. In metals, the time scale of the electronic excitations, triggered by the plasma frequency of the conduction electrons, is typically ~10^{-15} s. This is short compared to the lattice time scale, ~10^{-13} s, given by the Debye frequency. Therefore electronic excitations are usually neglected in metals for all properties concerning the energetic of atoms.

2.1. Atomic displacement cascades

By the end of their trajectories, PKAs induce cascades of displacements, a molecular dynamics simulation that is presented in Figure 1b. An atomic displacement is formed by a vacancy, the empty site left by an ejected atom, and this ejected atom comes to rest in an interstitial lattice position, creating a SIA. Vacancies and SIAs are at both ends of a replacement sequence. Replacement events do not create point defects but induce athermal jumps of atoms that

contribute to diffusion and ballistic disorder. Both are particularly important for the phase under irradiation, as shown hereafter.

One displacement cascade is thus an event localised in space and time, which strongly strains the crystalline structure. During the ballistic phase, which lasts up to ~1 ps, a significant number of defects are created. Most of them recover during the following 10 ps, which typically corresponds to ~100 lattice vibrations for usual metals. The remaining defects after the recovery phase are vacancies, SIAS and their clusters. Therefore there will be a significant super-saturation under irradiation, which enhances vacancy controlled diffusion mechanisms and introduces SIAs controlled ones. The latter are irradiation specific.

When the energy of the PKA increases, the size and energy of cascades may not steadily increase. Molecular dynamics simulations show that for PKAs above 20 keV, cascades break down into sub-cascades, the energy of which is ~10–20 keV [4]. 14 MeV fusion neutrons will create PKAs with higher kinetic energy than fast fission neutrons, the energy of which is ~1–2 MeV. The expected result is therefore not larger and more energetic cascades but a larger number of sub-cascades of energy in the range 10–20 keV, similar in terms of size and energy to those obtained under a fission spectrum. Therefore ballistic disorder is expected to be similar under fission and fusion spectra.

The received dose is measured in displacement per atom (dpa). The dose on the first wall of DEMO is expected in the range 50–80 dpa, i.e., of the same order of magnitude as for the cladding materials within fast neutron reactors, on which doses up to ~150 dpa are foreseen.

2.2. Nature of point defects under a fusion neutron spectrum

The recovery stages of electronic resistivity during isochronal annealing of pure α-Fe irradiated at cryogenic temperature with fission or 14 MeV neutrons occur at the same temperatures [5]. Therefore, as far as the nature of mobile point defects and their clusters are concerned, they should be similar under both spectra. Since mobile point defects control the diffusion of chemical species, recovery mechanisms of the ballistic disorder and radiation induced segregation may be similar under fission and 14 MeV neutrons.

2.3. Transmutation: helium and hydrogen production

Transmutation reactions strain the chemical composition. (n,γ) and (n,p) reactions are particularly important as they produce chemical elements such as He and H, which can embrittle materials and induce swelling. In a fusion neutron spectrum, because of 14 MeV neutrons, ~12 ppm(He)/dpa and ~45 ppm(H)/dpa are produced in steels. (n,γ) and (n,p) cross sections tend to decrease as a function of the atomic weight. Helium production in tungsten is only ~0.3 ppm/dpa, whereas in materials made of light elements such as silicon carbide, ~110 ppm/dpa can be produced [6]. Because neutrons are less energetic, He production is a few ppm/dpa within steels of fast neutron reactor cores.

2.4. Transmutation: nuclear activation and low activation materials

Due to the decay of transmuted nuclei, a conventional 9%Cr1%MoVNb ferritic–martensitic steel as the first wall in DEMO irradiated up to ~100 dpa must be considered as a high level waste for

~10^5 years. RAFM 9%Cr steels have been fabricated that replace molybdenum and niobium with tungsten, which also forms carbides that improve mechanical strength and thermal stability. Impurities such as Nb, Mo, Ni, Cu, Al and Co were also strictly limited. These reduced activation steels can be considered as low level waste after a few hundred years of decay. Stricter analytical requirements that may allow for low activation ferritic–martensitic (LAFM) steels to be fabricated are accessible within present steel manufacturing technology. Activation calculations show that these LAFM steels could be reintroduced in a normal hands-on fabrication process after a few hundreds of years of decay following an irradiation up to ~100 dpa as a DEMO first wall [2].

Low nuclear activation is a key requirement for safe and economical operation of future fusion reactors. As a consequence an accurate knowledge of transmutation cross-sections up to 14 MeV is essential for the development of fusion relevant materials.

3. RADIATION INDUCED MICROSTRUCTURE AND MACROSCOPIC CONSEQUENCES.

During operation within a fusion reactor, the initial microstructure of materials will be affected by two main mechanisms, accumulation of point defects and transmuted species as well as phase stability, both of which will significantly modify in-service properties.

3.1. Accumulation of point defects and transmutation species

During their migration controlled by diffusion, surviving point defects will recombine, eliminate to various sinks (dislocations, grain boundaries, semi-coherent or incoherent interfaces between matrix and precipitates) or agglomerate.

SIAs and vacancies can form dislocation loops. At low temperatures up to ~$0.3T_m$, dislocation loops undergo limited growth, forming a dense population that contributes to hardening and loss of ductility of materials. At higher temperature, above ~$0.45T_m$, they will grow and interact among each other and with the pre-existing dislocation network to form a new network.

Agglomeration of vacancies promotes void nucleation. Voids can grow further by absorbing an excess of vacancies, provided that SIA biased sinks can preferentially absorb a net flux of SIAs. As swelling is a nucleation growth process, it has a maximum located typically in the range 0.3–$0.45T_m$. In cubic metallic alloys swelling is usually isotropic.

Beryllium, a hexagonal close packed metal, is foreseen to be used as the neutron multiplier in HCPB blankets. Radiation effects data in Be are extremely scarce. By analogy with hexagonal close packed Zr alloys, extensively used in light water reactors, SIAs are expected to agglomerate in the form of dislocation loops parallel to the base plane [7]. Due to the crystalline texture introduced by the fabrication process during extrusion and rolling, the base planes might not be randomly oriented; growth is therefore expected to occur in the direction normal to the base plane.

Under a fusion neutron spectrum the production of helium favours agglomeration of vacancies due to the significant binding energies of He with vacancies or with vacancy–helium clusters as shown in Figure 2 [8], which shows dissociative energy is the opposite of binding energy. Especially at low temperatures rather dense populations of He–vacancy clusters that will harden materials are expected. Due to its high solution energy in α-Fe, 4.08 eV, in ground configuration,

which is substitutional [9], a significant effect of He on the cohesion of ferritic–martensitic steel is to be expected. As a consequence fission neutron simulation of damage accumulation under fusion conditions will be poor, if not misleading.

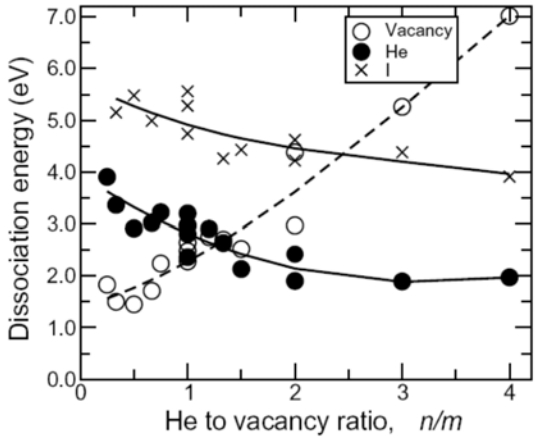

FIG. 2. Dissociative energies of a vacancy (V), a self-interstitial atom (I) from a He_nV_m cluster as a function of the He to vacancy ratio.

3.2. Phase stability under irradiation

Adequate in-service properties are usually obtained by tailoring an initial microstructure over several different phases. Phase stability must be mastered, as it will trigger stability of in-service properties. It is a complex field. Irradiation could dissolve or amorphize phases. Thermal precipitation of phases can also simply accelerate, whereas radiation induced precipitation might also take place.

As shown in Figure 3, phase stability and kinetic pathways under irradiation are controlled by the balance between ballistic or chemical disorder induced by the replacement sequences, and recovery controlled by enhanced diffusion due to point defect super-saturation. Preferential coupling to sinks by some chemical species with point defect fluxes will result with local depletion or enrichment of these species, in addition to possible radiation induced precipitation if the solubility limit is locally exceeded. At low temperatures or high flux, ballistic disorder overwhelms recovery. Radiation specific phenomena such as dissolution or amorphisation might occur. At high temperatures or low flux, ageing under irradiation will be similar to thermal ageing with quicker kinetics due to point defect super-saturation. In addition, radiation induced segregation can take place at sinks where point defects are eliminated. For instance slowly diffusing species via the vacancy mechanism or species diffusing via mixed self-interstitial dumbbell enrich at point defect sinks. As a consequence precipitation may occur when the solubility limit is locally exceeded [10].

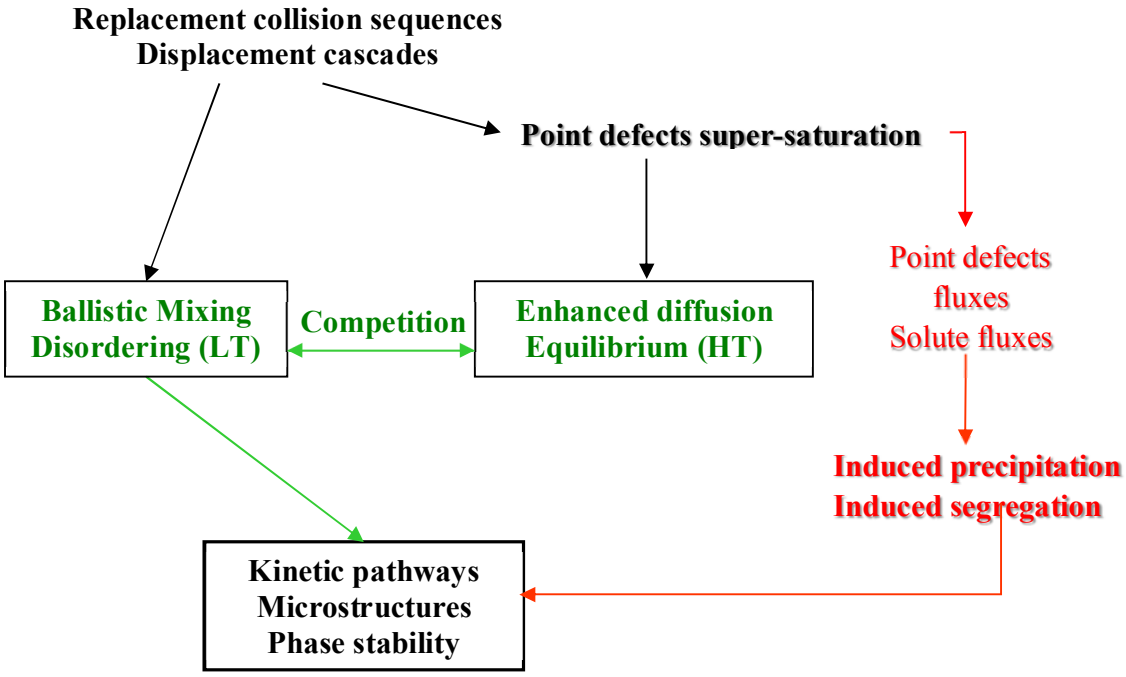

FIG. 3. Phase stability is kinetically triggered by the balance between ballistic disorder and diffusion controlled recovery processes. (Source: F. Soisson, CEA Saclay).

It should be noted that these various mechanisms are directly triggered by replacement sequences within sub-cascades and the nature of point defects. Phase stability under fusion relevant conditions should therefore be satisfactorily simulated using fission neutrons.

4. FERRITIC AND FERRITIC/MARTENSITIC STEELS: PHASE STABILITY, HARDENING AND EMBRITTLEMENT

Following irradiation, the so called 475°C embrittlement of high chromium ferritic–martensitic steels is very well documented and associated with γ/γ' unmixing, in which Cr content and temperature are such that the steel lies in the miscibility gap of the Fe–Cr phase diagram [11].

Under fast neutron irradiation, embrittlement of ferritic and ferritic–martensitic steels strongly depends on irradiation temperature and Cr content, as shown in Figure 4. For specimens irradiated in the Phénix reactor from 400–550°C to doses in the range 70–110 dpa, 9%Cr ferritic–martensitic steels hardly embrittle and no γ/γ' unmixing is reported. Conversely, 17%Cr ferritic steel highly embrittles and undergoes an intense precipitation of the Cr rich γ' phase. The limited radiation hardening of 9%Cr is in agreement with transmission electron microscopy (TEM) observation [12]. In addition to the absence of γ/γ' unmixing, the dislocation density is hardly affected by irradiation, as shown in Figure 5. After 75 dpa at 398°C dislocation loops have grown and are large enough to interact with the pre-existing dislocation network, and at higher temperatures dislocation density exhibits a tendency to decrease as temperature increases. The overall martensitic lath microstructure is hardly affected by irradiation.

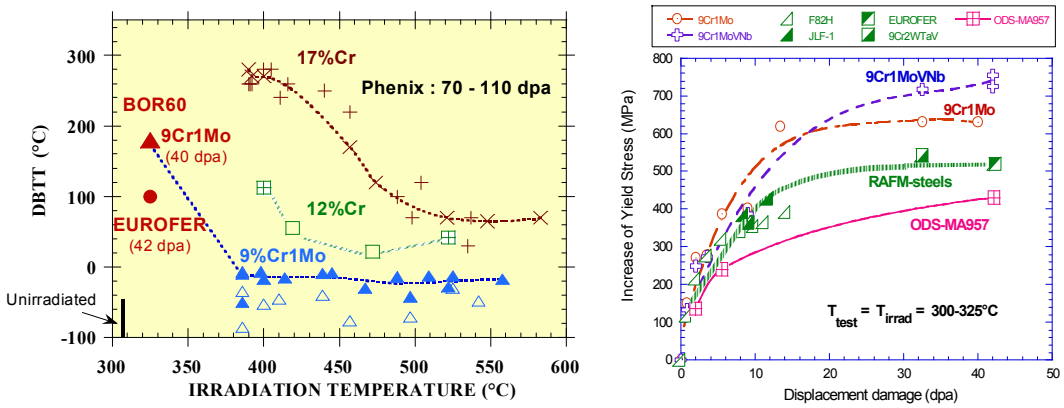

FIG. 4. (a) DBTT of ferritic and ferritic–martensitic steels after irradiation in the Phénix reactor up to doses of 70–110 dpa and in BOR60 up to ~40 dpa. (b) Hardening of conventional (9%Cr1%Mo) and RAFM steels (EUROFER) and ODS ferritic steel (MA957).

When irradiated at 325°C in the BOR60 reactor up to 40 dpa, conventional 9%Cr1%Mo ferritic–martensitic steels exhibit significant hardening and embrittlement with a ductile to brittle transition temperature (DBTT) up to 200°C. The embrittlement of low activation EUROFER is less than for conventional 9%Cr1%Mo. It is nevertheless significant with a DBTT amounting to ~100°C after irradiation compared to ~-100°C in its initial metallurgical condition. TEM examinations are being carried out to quantify point defect accumulation and phase stability. A contribution of γ/γ' unmixing cannot be excluded, since after irradiation at 325°C up to 0.7 dpa, a significant volume fraction of the γ' phase is detected in ferritic–martensitic with Cr content above 8.5% [13]. It should be noted that the occurrence of γ/γ' unmixing observed in the above experimental data is in qualitative agreement with the prediction of the Fe–Cr phase diagram. Therefore the high temperature conditions for the phase stability under irradiation prevail.

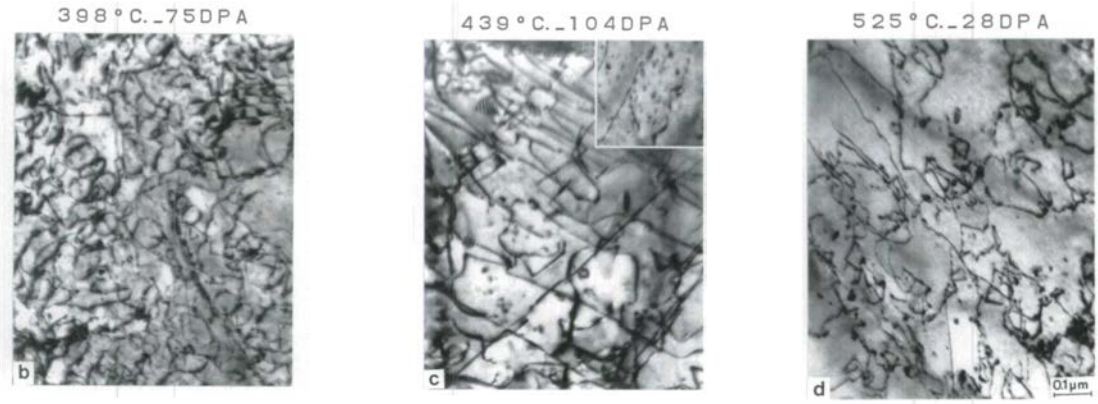

FIG. 5. TEM of dislocation microstructure in 9%Cr1%Mo conventional steels after irradiation in Phénix at indicated temperatures and doses (Source: D. Gilbon, CEA Saclay).

Taking into account the similarity between fusion and fission spectra as far as ballistic disorder and nature of point defects are concerned, this sensitivity to γ/γ' unmixing under fission irradiation should hold under fusion spectrum, making fission reactors relevant tools for this kind of simulation.

5. TUNGSTEN–RHENIUM ALLOYS: INITIAL SOFTENING AND PHASE STABILITY UNDER IRRADIATION

Tungsten and tungsten alloys have among the highest DBTTs of all the metallic alloys with body centred cubic crystalline structure. DBTT of W alloys varies with metallurgical condition, but typically amounts to ~500°C compared to approximately –100°C for RAFM steels under the conditions of impact tests. Alloying and refining the microstructure have long been used to improve ductility and decrease DBTT of W alloys. Alloying with rhenium is in fact very effective in softening tungsten [14], and W–Re alloys up to 25% Re have a DBTT low enough to be ductile at room temperature with a rather easy cold workability.

W–Re alloys with Re content equal to 5, 11 and 25% were irradiated in the HFIR reactor at 1100°C. The W25%Re alloy was also irradiated at 675°C. All alloys underwent during irradiation a high density of χ phase WRe_3 precipitates. This precipitation must be attributed to a radiation induced mechanism, although this has not completely clarified yet, since, taking into account composition and irradiation temperature, thermodynamics predicts that either no precipitation or a γ phase should occur as shown in Figure 6 [15].

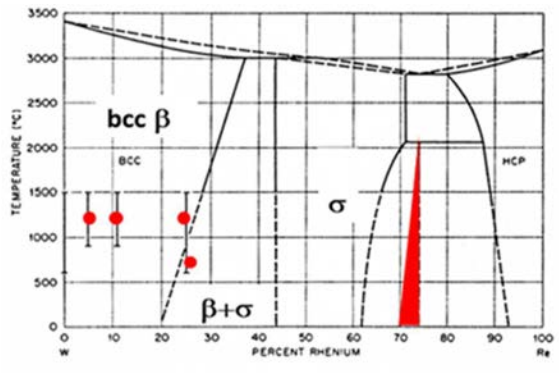

FIG. 6. W–Re alloys irradiated in HFIR. The domain of χ phase is coloured in red.

The fusion relevance of fission irradiation concerning phase stability implies that W–Re alloys are to be discarded at least for structural application within future fusion reactors.

6. FERRITIC AND FERRITIC/MARTENSITIC STEELS: POINT DEFECTS AND HELIUM ACCUMULATION

Helium has a major impact on swelling and mechanical properties of RAFM steels.

6.1. Swelling of ferrtic–martensitic steels

Whatever their Cr content from 9–17%, ferritic and ferritic–martensitic steels have good resistance to swelling, as opposed to austenitic steels, in the temperature range 390–550°C up to 150 dpa, as shown in Figure 7 [16]. It is to be noted that this swelling resistance must be associated with a long incubation dose rather than immunity against swelling, since for example, α–Fe has been reported to swell under fission neutron irradiation [17].

Ion irradiation under a single beam configuration to simulate only point defects production confirmed this good resistance to swelling. Conversely triple beam irradiation with simultaneous

production of point defects, He and H, typical of a fusion neutron spectrum, significantly degrades the swelling resistance of 9%Cr steel with a 3.2% swelling value after irradiation at 470°C up to 50 dpa as shown in Figure 7. Figure 7a compares austenitic steels 316 Ti (18%Cr12%NiTi) and 15/15 Ti (15%Cr15%NiTi); ferritic–martensitic steels with 9–12%Cr DIN1.4970 (12%CrMoVNb), EM10 (9%Cr1%Mo) and EM12 (9%Cr2%Mo); and 17%Cr ferritic steel. Figure 7b displays the swelling of a RAFM steel under a triple ion beam simulating fusion conditions of 50 dpa, 900 ppm (He) and 3500 ppm (H) [18], while Figure 7c indicates little swelling in a Ni coated ODA steel irradiated in the HFIR reactor, USA, at 500°C up to 9 dpa with simultaneous production of 380 ppm (He) in the few micrometers below the Ni coating [19]

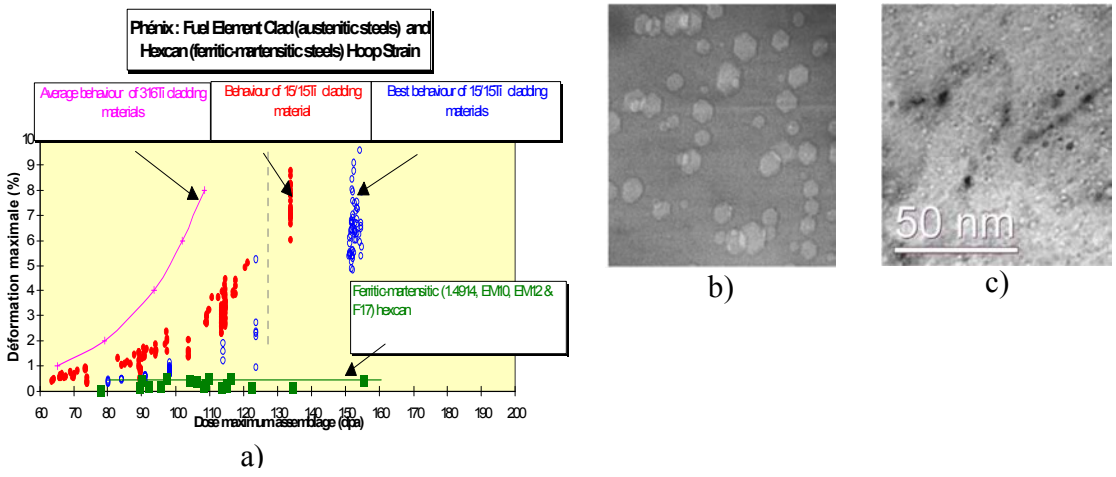

FIG. 7. (a) Swelling maximum deformation versus dose for 3 steels, (b) 3.2% swelling of a RAFM steel with 9% irradiated at 470°C, (c) negligible swelling of a Ni coated ODS 14%Cr ferritic steel.

Consequently RAFM steels will have most probably a lifetime duration significantly lower than one that can be extrapolated from their high swelling resistance under a fission neutron spectrum. In addition these data pointed out that accumulation of point defects, He and H might be a critical issue for RAFM under a fusion environment.

6.2. He embrittlement of ferritic–martensiric steels

TABLE 2. VARIOUS TECHNIQUES AND IRRADIATION DEVICES TO SIMULATE FUSION RELEVANT PRODUCTION OF POINT DEFECTS, HELIUM AND HYDROGEN.

He producing technique	Irradiation device	ppm (He)/dpa
Ferritic–martensitic steels	D–T fusion reactor	~10
Ferritic–martensitic steels	MTR or fast reactor	~0.3
Ni coated steels	MTR	~40
B or Ni doped steels	MTR	Small
^{54}Fe enriched steels	MTR	~2
Mixed spallation neutron spectrum	Spallation target	~100
Energetic (20–100 MeV) alpha particles	Cyclotron	~1000–10 000

In the absence of an intense 14 MeV neutron source, various methods and irradiation devices have been used to simulate the production of dpa and He as shown in Table 2. Some limitations

must be pointed out. Data obtained using Ni doping are doubtful. Adding Ni changes the phase transformation temperatures of RAFM steels. The initial mechanical properties are therefore affected for a given set of thermal mechanical treatments. If some change is observed after irradiation, it is not possible to attribute it to helium production or to the initial Ni content. Boron doping could be also misleading, unless uniform distribution is obtained and verified. Finally irradiation under mixed a spallation neutron spectrum creates, in addition to He and H, many other spallation residues. Although produced in significantly less quantity than He and H [3], possible effects associated with their production at the high doses needed for fusion appear difficult to ignore.

In the following we report data obtained via implantation of α particles of ~25 MeV produced by the cyclotron of Forschungszentrum Jülich, Germany. Due to the energy and a degrader, uniform implantation on a thickness of ~100 μm can be achieved, allowing for post-mortem tensile testing. If this method does not introduce any chemical bias, the ratio ppm(He)/dpa is rather high, ~10 000. Implantations have been conducted up to 0.5%He at 250–550°C, followed by TEM observation and tensile tests at the implantation temperature [20, 21].

As shown in Figure 8, He implantation at 550°C induces limited hardening and embrittlement. Implantation at 250°C induces large hardening, and brittle failure occurs along prior austenitic grain boundaries. The same martensitic steel irradiated in the OSIRIS reactor at 325°C exhibits similar yield strength but fails via a transgranular ductile mechanism. Therefore matrix hardening does not itself explain the brittle intergranular failure of the implanted sample. Although no He bubbles have been observed along grain boundaries by TEM, a reasonable assumption is that He atoms or tiny He bubbles too small to be observed by TEM may embrittle RFM steels along prior austenitic grain boundaries [21].

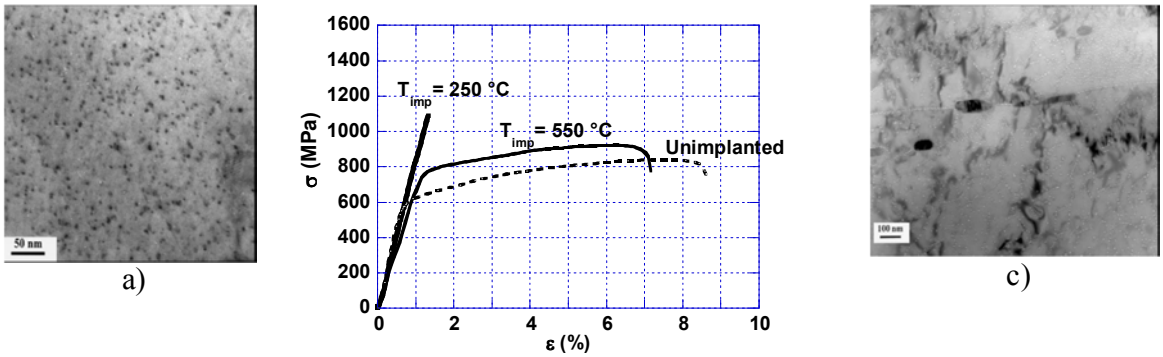

FIG. 8. (a) TEM observation of a dense microstructure of He bubbles after implantation at 250°C, (b) Tensile tests at the implantation temperature after implantation at 250°C (brittle intergranular failure) and at 550°C (transgranular ductile failure), (c) TEM observation of He bubbles preferentially distributed along grain boundaries or dislocations after implantation at 550°C [21].

Finally data analysis of hardening and intergranular failure occurrence after fission neutron and mixed spallation–neutron spectrum bombardment has been carried out. Intergranular failure has been identified in 9%Cr steels for He contents above 500 ppm at constant hardening [22]. Assuming this result could be applied directly to fusion, brittleness could occur in RAFM steels at ~50 dpa under DEMO conditions.

Taking into account the high ratio of ppm(He)/dpa and high He content at the end of implantation, this type of experiment is certainly extreme, but, as shown above, it deserves to be used in conjunction with other fission irradiations in order to identify underlying mechanisms. Additional data and modelling for understanding hardening induced by He bubbles in microstructure and intergranular helium embrittlement are required to select possible improvement.

7. DEVELOPING HEAT AND RADIATION RESISTANT MATERIALS

The few examples described above show that materials with chemical composition and microstructure tailored purposefully will be required to withstand the in-service conditions foreseen regarding internal components of future fusion reactors. Following the experience gained internationally in developing RAFM steels, presently available neutron sources and ion beam facilities used in a combined and systematic manner in association with modern chemical and physical characterisation techniques should provide a relevant simulation of the various aspects of radiation damage under fusion conditions. Subsequent sub-sections will present some important aspects of this required innovative development effort.

7.1. Nanostructuring materials

Nanostructuring a material means introducing a high density, $\sim 10^{23}$–10^{24} m^{-3}, of nanometric precipitates with incoherent or semi-coherent interfaces with the matrix that can act as point defect sinks. The expected consequences are a better resistance to radiation effects. ODS ferritic and ferritic–martensitic steels belong to this class of materials. As shown in Figure 4b, they exhibit after irradiation in fast neutron reactors lower hardening than RAFM steels or conventional 9%Cr ferritic–martensitic steels. A significantly improved resistance to swelling is also expected as shown by TEM examination of Ni coated samples irradiated in HFIR (Figure 7c).

Fabrication of ODS steels requires developing an unconventional fabrication plan based on powder metallurgy and mechanical alloying. An important effort for fusion and fission applications is ongoing [23].

7.2. Ion beam irradiation to simulate fusion radiation efforts

Irradiations under dual or triple beam conditions to simulate point defects and He production or point defects and He and H production have proven to be reliable and versatile techniques in terms of irradiation conditions [24]. An irradiated thickness of a few micrometers makes possible the use of all modern chemical and physical characterisation techniques. These can also be performed in a cold lab, since samples are not activated. Ion beam irradiation allows very rapid feedback as compared to neutron irradiation. Multiple beam ion irradiation is therefore an attractive and fruitful technique for microstructure studies. There are, however limitations, since irradiated thickness restricts, for example, mechanical testing of nano-indentation.

Ion beam irradiations have been used to study swelling of RAFM steels under fusion conditions, as quoted above. First irradiations carried out in dual beam configuration on ODS ferritic steels indicate that interfaces between a nanometric precipitate and a matrix may be effective traps for He [25]. Dispersion might therefore be effective in improving swelling resistance as expected

from Ni coated irradiation in fission reactors and intergranular He embrittlement under fusion relevant conditions.

7.3. Physical modelling

Irradiation conditions in presently available facilities are varied. Interpolating them as well as extrapolating to the actual conditions of a fusion reactor will require physical modelling starting from the scales at which the physics of point defects and radiation damage can be described with definite assumptions for the electronic structure and atomic scale. Boutard and Dudarev [26] give an overview of the effort being performed in the European Union to model fusion relevant radiation effects in FeCrC model steel. Ab initio calculations play a central role in determining, for example, cohesion of the system in the presence of point defects and helium, energy of the point defects controlling diffusion mechanisms and dislocation glide mechanisms as an essential basis of plasticity. The paper underlines also the need for defining a strategy for experimental validation, essential to improve the reliability of predictions.

8. IFMIF: INTENSE SOURCE OF NEUTRONS TO QUALIFY FUSION MATERIALS

Developing structural, armour and functional materials capable of withstanding fusion reactor operating conditions is an immense challenge unlike any the materials community has ever faced. The material developments sketched above based on existing facilities and physical modelling must be carefully discussed and established. In strong association with the design team of the future DEMO, the objective of a fusion materials development programme will be the selection of a first set of reference materials that must be qualified in an intense prototypical neutron source such as IFMIF for safe and economical construction and operation of DEMO [27]. Modelling will be a precious tool to optimise the IFMIF programme and to understand, evaluate and extrapolate its data to the larger range of operating conditions within an actual reactor.

ACKNOWLEDGEMENTS

The author is grateful to colleagues of the European Fusion Development Agreement for fruitful discussions. The views and opinions expressed in this paper do not necessarily reflect those of the European Commission.

REFERENCES

[1] MAISONNIER, D., et al., DEMO and fusion power plant conceptual studies in Europe, Fusion Eng. and Design **81** (2006) 1123–1130.

[2] LINDAU, R., et al. , Present development status of EUROFER and ODS-EUROFER for application in blanket concepts, Fusion Eng. and Design **75–79** (2005) 989–996.

[3] VLADIMIROV, P., et al., Displacement damage and transmutations in metals under neutron and proton irradiation, Comptes Rendus Physique **9** 3–4 (2008) 303–322.

[4] STOLLER, R.E., GREENWOOD, L.R., Subcascade formation in displacement cascade simulations: Implications for fusion reactor materials, J. Nucl. Mater. **271–272** (1999) 57–62.

[5] MATSUI, H., et al., Material responses of ferritic steels by 14 MeV neutron bombardments at 20 and 300 K, J. Nucl. Mater. **155–157**, Part 2, (1988) 1284–1289.

[6] GILBERT, M.R., SUBLET, J.C., Neutron-induced transmutation effects in W and W-alloys in a fusion environment, Nuclear Fusion **51** (2011) 043005.
[7] CHRISTIEN, F., BARBU, A., Cluster dynamics modelling of irradiation growth of zirconium single crystals, J. Nucl. Mater. **39** (2009) 153–161.
[8] FU, C.C., WILLAIME, F., Interaction between helium and self-defects in α-iron from first principles, J. Nucl. Mater. **367–370** (2007) 244–250.
[9] FU, C.C., WILLAIME, F., Ab initio study of helium in alpha-Fe: Dissolution, migration, and clustering with vacancies, Phys. Rev. B, **228** (2005).
[10] NASTAR, M., CLOUET, E., Mean field theories for the description of diffusion and phase transformations controlled by diffusion, Physical Chemistry Chemical Physics **6** (2004) 3611–3619.
[11] PECKNER, D., et al., Handbook of Stainless Steels, Mac Graw-Hill Company, Columbus (1977) 800 pp.
[12] SERAN, J.L., et al., Pre- and post-irradiation mechanical properties of ferritic-martensitic steels for fusion applications: EM10 base metal and EM10/EM10 welds, J. Nucl. Mater. **212–215** (1994) 588–593.
[13] MATHON, M.H., et al., A SANS investigation of the irradiation-enhanced α–α′ phases separation in 7–12 Cr martensitic steels, J. Nucl. Mater. **312** (2003) 236–248.
[14] RAFFO, P.L., Yielding and fracture in tungsten and tungsten-rhenium alloys, J. of Less Common Metals, **17** (1968) 133.
[15] HERSCHITZ, R., SEIDMAN, D.N., Radiation-induced precipitation in fast-neutron irradiated tungsten-rhenium alloys: An atom-probe field-ion microscope study, Nuclear Instr. & Methods in Phys Research B **7–8** (1985) 137–142.
[16] BOUTARD, J.L., et al., Fissile core and tritium-breeding blanket: structural materials and their requirements, Compte Rendus Physique **9** 3–4 (2008) 287–302.
[17] GARNER, F.A., TOLOCZKO, M.B., SENCER, B.H., Comparison of swelling and irradiation creep behavior of fcc-austenitic and bcc-ferritic/martensitic alloys at high neutron exposure, J. Nucl. Mater. **276** (2000) 123–142.
[18] WAKAI, E, et al., Swelling behavior of F82H steel irradiated by triple/dual ion beams, J. Nucl. Mater. **318** (2003) 267–273.
[19] ODETTE, G.R., et al., Helium transport, fate and management in nanostructured ferritic alloys: In situ helium implanter studies, J. Nucl. Mater. **417** (2011) 1001–1004.
[20] JUNG, P., HENRY, J., CHEN, J., BRACHET, J.C., Effect of implanted helium on tensile properties and hardness of 9% Cr martensitic stainless steels, J. Nucl. Mater. **318** (2003) 241–248.
[21] HENRY, J., MATHON, M.H., JUNG, P., Microstructural analysis of 9% Cr martensitic steels containing 0.5 at.% helium, J. Nucl. Mater. **318** (2003) 249–259.
[22] YAMAMOTO, T., et al., On the effects of irradiation and helium on the yield stress changes and hardening and non-hardening embrittlement of ~8Cr tempered martensitic steels: Compilation and analysis of existing data, J. of Nucl. Mater. **356** 1–3 (2006) 27–49.
[23] DE CARLAN, Y., Metallic materials, one of the keys for the fourth generation, Les Clefs CEA **59** (2010) 71–75.
[24] SERRUYS, Y., et al., JANNUS: experimental validation at the scale of atomic modelling, Comptes Rendus Physique **9** (2008) 437–444.
[25] HSIUNG, L.L., et al., Formation mechanism and the role of nanoparticles in Fe-Cr ODS steels developed for radiation tolerance, Phys. Rev. B **82** (2010).

[26] BOUTARD, J.L., DUDAREV, S., Modelling structural and plasma facing materials for fusion power plants: Recent advances and outstanding issues in the EURATOM fusion materials programme, J. Nucl. Mater. **417** (2011) 1042–1049.
[27] IBARRA, A., "IFMIF and its role in the context of DEMO design", presented at IAEA Technical Meeting on "Materials under high-energy and high-intensity neutron fluxes for nuclear fusion technology", Vienna, 2011.

ROLE OF FISSION REACTORS AND IFMIF IN THE FUSION MATERIALS PROGRAMME

S.M. GONZALEZ DE VICENTE
EFDA Close Support Unit.
Garching, Germany

Abstract

In fusion power reactors, the plasma facing (first wall and divertor) and breeding blanket components will suffer irradiation by an intense flux of 14.1 MeV neutrons coming from the plasma. These fusion neutrons will produce nuclear transmutation reactions and atomic displacement cascades causing the presence of impurities and defects. Therefore, the chemical composition and the microstructure of the materials will change after irradiation, affecting its physical and mechanical properties. The study and evaluation of the changes in the material properties under irradiation is a top priority for the design of a fusion reactor. Key irradiation parameters include the accumulated damage, expressed in the number of displacements per atom or dpa, the damage rate in dpa/s, the rates of production of impurities (e.g. ppm(He)/dpa and ppm(H)/dpa ratios) and the temperature of the materials under irradiation. Unfortunately, at the moment, the existing sources of 14 MeV neutrons have very small intensity and do not allow us to get significant damage accumulation in a reasonable time. Therefore, it is necessary to simulate irradiation by fusion neutrons through the use of fission neutrons, high energy protons or heavy ions. Although the irradiation conditions provided by such particles are very different from those expected to occur in a fusion power reactor, especially in terms of damage rate and rates of production of impurities, relevant information can be obtained from present available fission reactors. In the paper a list with relevant experiments suitable for the fusion community is given, and the role of the future International Fusion Materials Irradiation Facility is discussed.

1. INTRODUCTION

In fusion power reactors, the plasma facing (first wall and divertor) and breeding blanket components will suffer irradiation by an intense flux of 14.1 MeV neutrons coming from the plasma. These fusion neutrons will produce nuclear transmutation reactions and atomic displacement cascades inside the various encountered, and therefore irradiated, materials. From the point of view of material science, the nuclear transmutation reactions will produce impurities such as helium and hydrogen gas atoms as well as eventually radioactive metallic impurities, while atomic displacement cascades will produce mainly point structure defects such as vacancies and interstitial atoms in addition to clusters of point structure defects and segregation of alloying elements. The final microstructure of the irradiated materials will result from a balance between the primary radiation damage and thermal annealing. It will be composed of complex secondary defects including small defect clusters, interstitial dislocation loops, vacancy dislocation loops, stacking fault tetrahedra, precipitates, voids and helium bubbles.

This degraded microstructure will have a strong impact on the physical and mechanical properties of the irradiated materials. It may engender local changes in the chemical composition as well as a decrease of electrical conductivity, especially at low temperatures, and possibly a decrease of thermal conductivity, especially in the case of ceramic materials. It may also lead to degradation of the mechanical properties, including hardening and embrittlement effects and a decrease of creep strength. It may also lead to a loss of dimensional stability resulting from the phenomena of swelling, as the helium bubbles may engender a macroscopic increase in the volume of the materials, irradiation creep and irradiation growth. Irradiation assisted stress corrosion cracking may also occur. The materials may also become radioactive due to the formation of radioactive metallic impurities as a result of nuclear transmutation reactions.

The key irradiation parameters include the accumulated damage, expressed in the number of displacements per atom or dpa, the damage rate in dpa/s, the rates of production of impurities

(e.g. ppm(He)/dpa and ppm(H)/dpa ratios) and the temperature of the materials under irradiation. At low temperatures, e.g. <673 K in the case of steels, one observes mainly hardening and embrittlement effects, including a loss of ductility as measured in tensile tests, a loss of fracture toughness and an increase in the ductile to brittle transition temperature (DBTT) in the case of body centred cubic (bcc) materials like OPTIMAX A (main elements, wt%: Fe9.24Cr0.56Mn0.24V0.96W) and D (main elements: Fe9.2Cr0.5Mn0.2V2W) and F82H, as illustrated in Figures 1 and 2. At intermediate temperatures, e.g. 573–873 K in the case of steels, one observes a peak in swelling located at about 723 K for reduced activation ferritic–martensitic (RAFM) steels. At high temperatures, e.g. above 873 K in the case of steels, one observes mainly irradiation enhanced precipitation and creep effects as well as helium embrittlement effects.

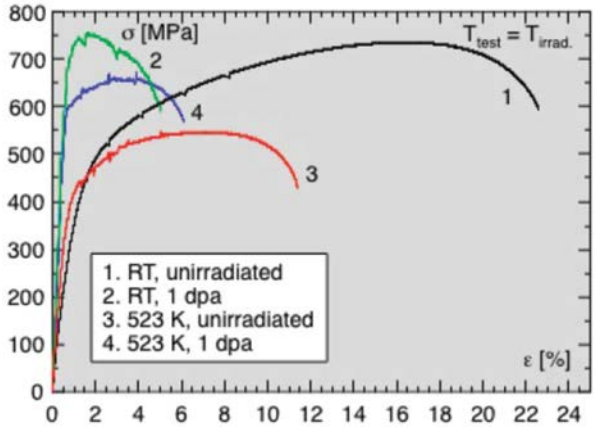

FIG. 1. Tensile engineering stress–strain curves of specimens of the OPTIMAX D RAFM steel before and after irradiation with high energy 590 MeV protons at room temperature and 523 K to about 1 dpa [1].

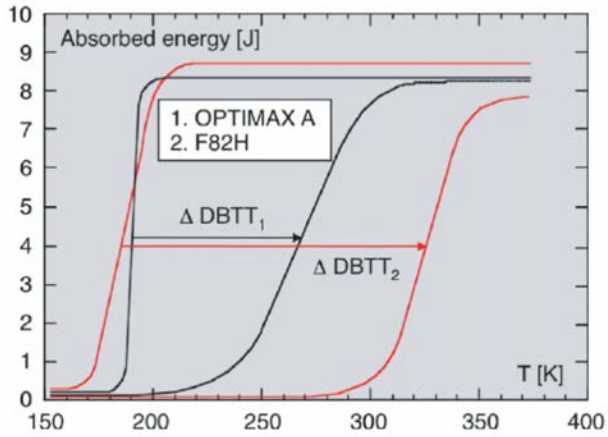

FIG. 2. Schematic of the absorbed energy versus test temperature, measured by means of Charpy impact tests on specimens of OPTIMAX A and F82H steels before and after irradiation with neutrons at 523 K and 573 K, respectively, to about 2.5 dpa. The DBTT increase is equal to 78 K for OPTIMAX A and 141 K for F82H [1].

To investigate in detail the effects of irradiation by fusion neutrons on the properties of candidate materials for fusion power reactors in absence of 14 MeV neutron sources with high intensity, a combination of techniques must be used to obtain complementary information. Therefore, it is necessary to simulate irradiation by fusion neutrons through the use of fission neutrons, high

energy protons or heavy ions. However, the irradiation conditions provided by such particles are very different from those expected to occur in a fusion power reactor, especially in terms of damage rate and rates of production of impurities. For instance, fission neutrons produce much less helium and hydrogen with respect to fusion neutrons, while high energy protons produce too much helium and hydrogen as well too many metallic impurities. Therefore, currently materials are irradiated with fission neutrons and in parallel tests with high energy protons, for instance, and the obtained results are tentatively interpolated for fusion irradiation conditions. However, such an approach is far from being adequate because it is difficult to separate effects of particle type, particle energy, temperature, accumulated damage, damage rate and rates of production of impurities, and in addition, candidate materials must be submitted to actual fusion irradiation conditions in order to be fully qualified by the designers and engineers who will construct fusion power reactors

2. NEUTRON IRRADIATION TOOLS

The neutron spectra of the most typical nuclear facilities: High Flux Reactor (HFR) at Petten, Netherlands; BOR-60 facility, Dimitrovgrad, Russian Federation; the European Spallation Source (ESS), Lund, Sweden; and the experimental accelerator driven system (XADS), are compared with those corresponding to the DEMO helium cooled pebble bed blanket concept (HCPB) and the International Fusion Materials Irradiation Facility (IFMIF) [2] in Figure 3. The spectra shown as bands correspond to the high and medium flux test module in the case of IFMIF, and to the maximum and minimum fluxes at irradiation rigs in the case of ESS. The most important for the comparison is an energy range of neutrons contained in each spectrum. The spectra of spallation (ESS and XADS) and stripping (IFMIF) accelerator driven sources have some fraction of neutrons with energy higher than the characteristic fusion neutron peak of 14.1 MeV. In ESS the neutron flux in the energy range 5–14 MeV is a factor of 4–5 lower than in DEMO, and a neutron tail with energies up to hundreds of MeV is present. The IFMIF spectrum reproduces quite well the shape of the DEMO fusion reactor spectrum near the 14 MeV peak and at intermediate energies, while the ESS and XADS neutron spectra are an order of magnitude smaller in flux.

The data on the displacement damage and gas production rates for each of these facilities are summarized in Table 1. All the data refer to pure iron as a major component of reduced activated ferritic–martensitic steels presently considered as prime candidate for fusion structural materials.

Fission reactors cannot fulfil all fusion irradiation conditions due to very low gas production rates and low gas to dpa production ratios. The high flux test module (HFTM) of IFMIF provides damage and gas production values exactly in the same range as the fusion DEMO reactor. In spite of the fact that the displacement damage produced at the ESS irradiation rigs is about two times lower than for DEMO and IFMIF, the gas to dpa ratios are still acceptable for fusion material irradiation. However, the lower damage rate in ESS implies about a twice as long irradiation campaign to reach the same irradiation dose. In the IFMIF HFTM the neutron damage ranges from 55–20 dpa/fpy in a volume of 0.5 l.

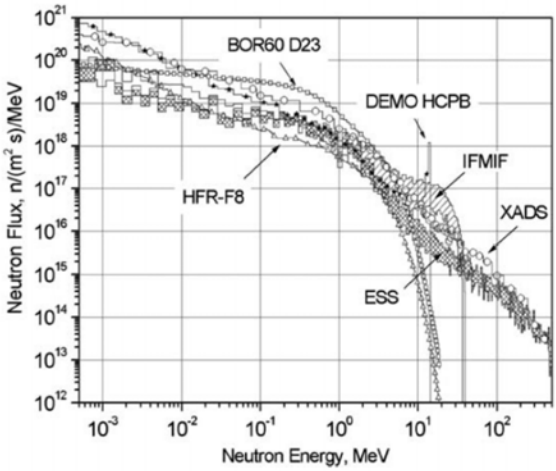

FIG. 3. Neutron spectra of the HCPB blanket of fusion DEMO reactor, the IFMIF high and medium flux test volumes, the spallation sources ESS and XADS as well as of fission reactors HFR and BOR-60 [3]

TABLE 1. DISPLACEMENT DAMAGE AND GAS PRODUCTION IN IRON FOR SEVERAL NEUTRON IRRADIATION ENVIRONMENTS [3]

Irradiation parameter	DEMO first wall 3 W/m^2	IFMIF HFTM	ESS irradiation rigs reflector	XADS 1 MW window	HFR position F8	BOR-60 position D23
Neutron flux (cm^{-2}s^{-1})	1.3×10^{15}	5.7×10^{14}	6.5×10^{14}	1.2×10^{15}	3.8×10^{14}	2.3×10^{15}
Proton flux (cm^{-2}s^{-1})	0	0	2.5×10^{12}	2.7×10^{14}	0	0
Damage (dpa/fpy)	30	20–55	5–10	38	2.5	20
H (ppm/fpy)	1240	1000–2400	160–360	16250	1.9	14
He (ppm/fpy)	320	250–600	25–60	1320	0.8	5.8
ppm(H)/dpa	41	35–54	33–36	430	0.8	0.70
ppm(He)/dpa	11	10–12	5–6	35	0.3	0.29

At the typical ESS irradiation position the total proton flux is about 2.5×10^{12} cm^{-2}s^{-1}, i.e. only 0.4% of the neutron flux, which is about 6.5×10^{14} cm^{-2}s^{-1}. However, most of the protons, ≈97%, have energies far above 15 MeV and thus contribute significantly to the total H and He production. The gas production is increased due to spallation reactions, which produce numerous light elements as debris of the target elements

The He/dpa ratio in Fe based alloys in ESS is between 5 and 6, about a factor of two lower than expected for DEMO, while the H/dpa ratio is about 33–36 which is only a factor of about 1.5 below DEMO. In the IFMIF HFTM the He/dpa and H/dpa are 10–12 and 35–50 respectively and therefore practically identical to the related DEMO values. This is shown in Figure 4, which for comparison also presents the data for several other irradiation facilities: Los Alamos Meson Physics Facility (LAMPF) at Los Alamos National Laboratory; Rotating Target Neutron Source (RTNS) at the University of California, Berkley; Oak Ridge Research Reactor (ORR) and High Flux Isotope Reactor (HFIR) at Oak Ridge National Laboratory [3].

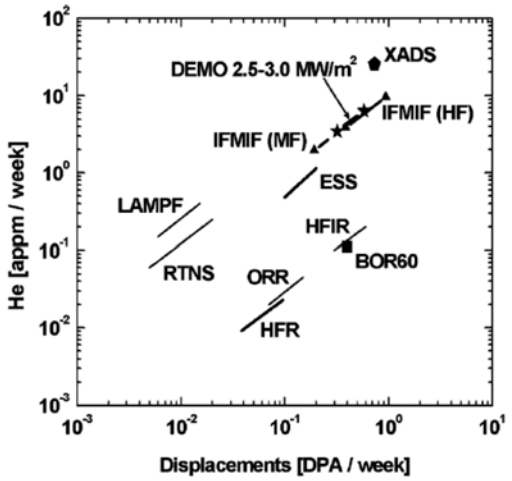

FIG. 4. Ranges of helium and damage production of various neutron sources for fusion studies.

Hard (fast neutron induced) and soft (e.g. electron irradiation induced) primary knock-on atom (PKA) spectra can produce very different damage morphologies. Low energy recoils produce only Frenkel defects, that is, isolated pairs of vacancies and interstitials. A significant fraction of these defects survive recombination and can be involved in further defect kinetics. On the other hand, high energy recoils generate atomic collision cascades in which a high fraction of the defects recombine during collision and cooling phases. For a PKA with energy higher than a critical value, according to different authors in the range of 10–40 keV for Fe [4, 5], the formation of sub-cascades is more probable.

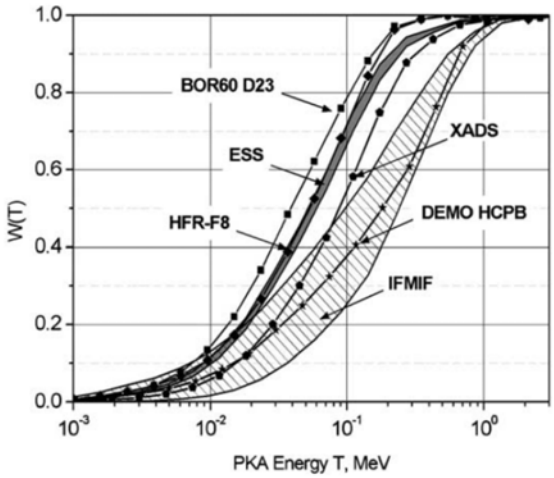

FIG. 5. Damage production function W(T) in iron for the HCPB blanket of the DEMO reactor in comparison with the stripping neutron source IFMIF (hatched); neutron spallation sources ESS and XADS; and fission reactors HFR, Petten and BOR-60 [3].

To characterize the entire PKA spectrum, a cumulative damage production function W(T), which represents the fraction of damage energy released by all PKA recoils with recoil energies less than given recoil energy T, is used. According to the Norgett, Robinson, Torrens (NRT) standard [6], damage energy is the energy spent for displacement production and is defined as initial recoil energy minus energy spent for electron excitation and ionization by the initial and all secondary

recoils produced in atomic collision cascade. The cumulative damage production function thus depends on the neutron spectrum and can show a difference in damage morphology for different irradiation sources.

The W(T) function usually increases smoothly without steps in fusion structural materials with an exception for ^{6}Li based tritium breeder materials [7]. The hatched area in Figure 5 shows that the relevant test volume of IFMIF meets perfectly over the entire PKA energy range the DEMO reactor conditions in iron based alloys because the shape of the W(T) function can be adjusted by using an appropriate combination of W moderator [8]. It is clear that computer simulation techniques need to be further developed to relate more precisely the relationship between neutron spectrum, damage morphology and mechanical properties of irradiated materials.

3. CONCLUSIONS

A comparison among the available neutron sources, the future IFMIF facility and DEMO spectrum has been described. It is clear that an intense neutron source is needed to fill two complimentary roles: scientific investigations of radiation degradation phenomena and microstructural evolution under fusion relevant irradiation conditions, plus engineering database development for design and licensing of DEMO.

TABLE 2. OVERVIEW OF FISSION, SPALLATION, AND ^{2}H–LI NEUTRON SOURCES FOR FUSION MATERIALS R&D [9]

Neutron source	Advantages	Disadvantages
Fission reactors	Well-characterized spectra Allows medium–high damage regimes to be investigated in bulk specimens Operating funds provided by multiple users (non-fusion)	Low He/dpa ratio Limited in situ test capability
Spallation	Allows high He irradiation conditions to be explored	Not designed for materials irradiations (physics/neutron scattering facility) He/dpa,H/dpa ratio too high Pulsed irradiation; requires detailed analysis
^{2}H–Li (IFMIF)	Correct He/dpa ratio, etc. Dedicated materials irradiation facility	Limited high flux volume Operating funds completely provided by fusion

Unfortunately this kind of facility is not available yet. Fission research reactors should play a very relevant role in materials testing; and not only these facilities, but also, ion and electron accelerators and other neutron sources, along with strong support and guidance given by theory and modelling. In summary, Table 2 provides an overview of fission, spallation, and ^{2}H–Li (IFMIF) neutron sources for fusion materials R&D.

DISCLAIMER

The views and opinions expressed herein do not necessarily reflect those of the European Commission.

REFERENCES

[1] BALUC, N., Material degradation under DEMO relevant neutron fluences, N. Baluc, Physica Scripta **T138** (2009).

[2] MÖSLANG, A., HEINZEL, V., MATSUI, H., SUGIMOTO, M., The IFMIF test facilities design, Fusion Engineering and Design **81** (2006) 863–871.

[3] VLADIMIROV, P., MÖSLANG, A., Comparison of material irradiation conditions for fusion, spallation, stripping and fission neutron sources, Journal of Nuclear Materials **329–333** (2004) 233–237.

[4] STOLLER, R.E., The role of cascade energy and temperature in primary defect formation in iron, J. Nucl. Mater. **276** (2000) 22–32.

[5] BACON, D.J., GAO, F., OSTESKY, Y.N., The primary damage state in fcc, bcc and hcp metals as seen in molecular dynamics simulations, J. Nucl. Mater. **276** (2000) 1–12.

[6] NORGETT, M.J., ROBINSON, M.T., TORRENS, I.M., A proposed method of calculating displacement dose rates, Nucl. Eng. Des. **33** (1975) 50.

[7] LIZUNOV, Y., MÖSLANG, A., RYAZANOV, A., VLADIMIROV, P., New evaluation of displacement damage and gas production for breeder ceramics under IFMIF, fusion and fission neutron irradiation, J. Nucl. Mater. **307–311** (2002) 1680–1685.

[8] MÖSLANG, A., VLADIMIROV, P., Neutronics calculations and design for the medium flux test module of IFMIF, Fusion Eng. Des. **63–64** (2002) 121.

[9] ZINKLE, S., MÖSLANG, A., Evaluation of irradiation facility options for fusion materials research and development, Proc. 27th Symposium on Fusion Technology, Liege, 2012, Fusion Eng. Des. (in press).

LVR-15 REACTOR AND FUSION RELATED ACTIVITIES IN MATERIAL RESEARCH AND TECHNOLOGY AT CV REZ

M. KOLESKA, J. KYSELA, M. MAREK, R. VSOLAK, O. ZLAMAL
Research Centre Řež,
Husinec-Řež, Czech Republic
kmi@cvrez.cz

Abstract

The LVR-15 is a light water, tank type reactor operating with a power rating of 10 MW_{th}. The reactor is currently undergoing conversion from IRT-2M fuel of 36 wt% ^{235}U enrichment to IRT-4M fuel of 19.7% enrichment. Due to its power output and achievable neutron flux the LVR-15 reactor is suitable for the study of combined effects of radiation and ambient media on materials. The reactor is equipped with experimental facilities such as irradiation loops and rigs that permit an exposure under simulated conditions corresponding to those in power reactors. Irradiation rigs permit the exposure starting from small samples (ring, tensile) up to very large samples (1T CT, 2T CT). Four loops simulating either pressurized or boiling water reactor conditions in various irradiation channels and Generation IV loops (SCWL, HTHL) are in either active or inactive operation at the reactor. Reactor LVR-15 has been engaged in research of fusion reactor materials and technology under EFDA and F4E/ITER. These projects are oriented toward developing a PbLi ancillary system for the He cooled PbLi test blanket module and on testing of small scale mock-ups of the ITER first wall.

1. INTRODUCTION

The Research Centre Řež (CV Řež) Company was founded in 2002 as a subsidiary of Nuclear Research Institute Řež plc for the purpose of research and development in the area of natural and engineering sciences related particularly to the utilization of ionizing radiation and nuclear energy. The CV Řež is a private non-profit company meeting the definition of a research organization according to European Commission Community Framework 2006/C 323/01. Its research and development activities are focused on three sections: basic and applied research of neutron sources in the industry and health sectors, participation in international project Jules Horowitz Reactor for development and construction of an experimental reactor on the site of the Cadarache Research Centre in France, and completion of a sustainable energy project oriented largely on research into Generation IV reactor concepts as well as support to and optimization of the operation of current power facilities.

In 2010, CV Řež started to operate 2 experimental reactors, LR-0 and LVR-15, formerly operated under Nuclear Research Institute Řež. Along with operating the reactors, CV Řež adopted fusion and fission projects formerly led by the Institute.

2. LVR-15

The LVR-15 is a tank type light water nuclear reactor operated with thermal power of 10 MW.

The reactor was restarted in 1989 following reconstruction of the VVR-S reactor. During the reconstruction a stainless steel reactor vessel was substituted for the original aluminum, and core components and reactor instrumentation were replaced. The core contains 28–32 fuel assemblies surrounded by a beryllium reflector (Figure 1). Since the reconstruction, the reactor had been using highly enrich uranium (HEU) IRT-2M fuel of 36 wt% ^{235}U. Currently, under the Reduced Enrichment for Research and Test Reactors programme with sponsorship by the US Department of Energy, it is undergoing conversion to low enriched uranium (LEU) IRT-4M 19.7% via mixed cores. In September 2011 the conversion will be accelerated to complete the fuel replacement.

The reactor is utilized for basic and extended material research, sample irradiation, isotope production and medical treatment at the boron neutron capture therapy facility. Material research can be performed either through nine horizontal beams or through irradiation loops and flat rigs in specified conditions of pressure, temperature and tensile stress. Sample irradiation and isotope production is suitable in several vertical channels, which include the pneumatic rabbit system and silicon doping facility via a rotational vertical channel. The main isotopes produced in the reactor are ^{99}Mo from HEU targets, ^{153}Sm, ^{192}Ir, ^{177}Lu, ^{203}Hg and ^{127}Xe.

TABLE 1. MAIN PARAMETERS OF THE LVR-15 REACTOR

Reactor type	Tank type
Pressure [MPa]	Atmospheric
Average temperature [^{o}C]	45
Fuel	IRT-2M 36% ^{235}U (HEU)
	IRT-4M 19.7% ^{235}U (LEU)
Nominal power	10 MW
Thermal flux	1.5×10^{18} m^{-2}s^{-1}
Fast flux	2.5×10^{18} m^{-2}s^{-1}

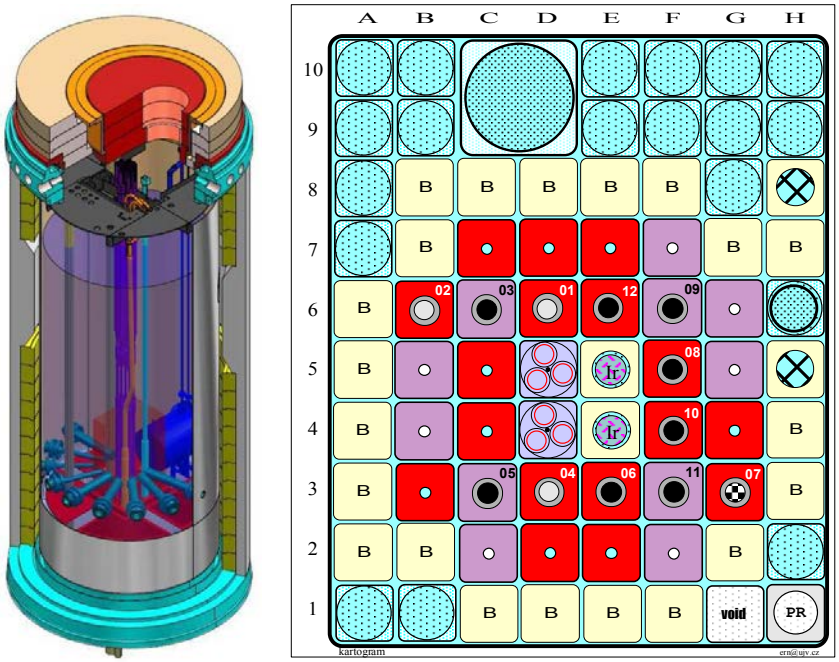

FIG. 1. LVR-15 design and core layout.

3. IN-PILE EXPERIMENTS

Reactor water loops and irradiation rigs are used for irradiation under well defined thermo-hydraulic conditions. Reactor loops are used to study effects of surrounding environment on materials in the core of power reactors. Phenomena under study include corrosion, influence

of physical and radiation stresses, interaction of fuel cladding and coolant, and water chemistry of pressurized water (VVER/PWR) and boiling water reactors (BWR).

The loops are closed stainless steel piping systems with technological auxiliary systems similar to simulated reactors. The loop's irradiation channels are placed in the core's reflector, heated with electrical heating rods and equipped with different sample holders, 1T CT and 2T CT. There are two main BWR types, BWR-1 and BWR-2, and two VVER/PWR types, RVS-3 and RVS-4, water loops with parameters reaching values in Table 2.

TABLE 2. MAIN PARAMETERS OF WATER LOOPS

Loop	Water chemistry	Temperature [°C]	Pressure [MPa]	Flow rate [t/h]
RVS-3	VVER/PWR	345	16.5	3–10
BWR-1	BWR	300	10	2
BWR-2	BWR	300	12	8
RVS-4	VVER	322	15.7	2

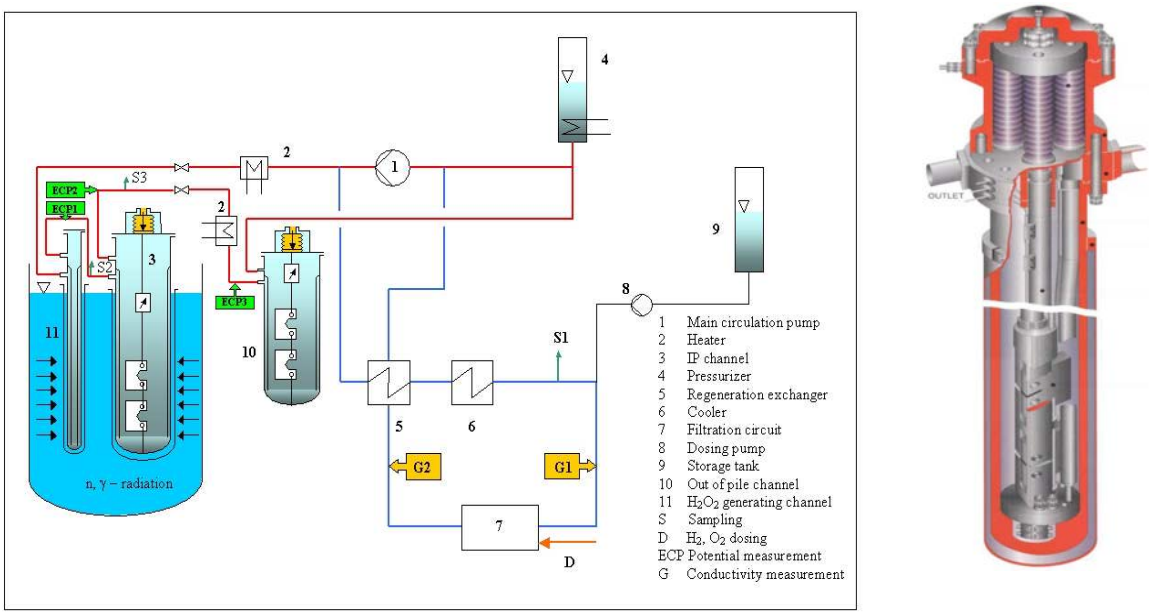

FIG. 2. BWR-2 loop design.

Irradiation rigs are used for irradiation of reactor pressure vessel materials in an inert gas atmosphere. Rigs have 6–8 heating sections that ensure an irradiation temperature range from 200±10°C to 350±10°C in an Ar, He or Ar+He atmosphere. Rig specimen holders allow for irradiation of Charpy V-impact specimens, tensile specimens, slow strain rate test specimens and fracture toughness 0.5 CT, 1T CT, 2T CT specimens (Figure 3). Rigs are dismantled in reactor hot cells, in which specific post irradiation evaluation can be performed. For advanced post irradiation evaluation specimens are transported to semi-hot cells situated near the reactor building.

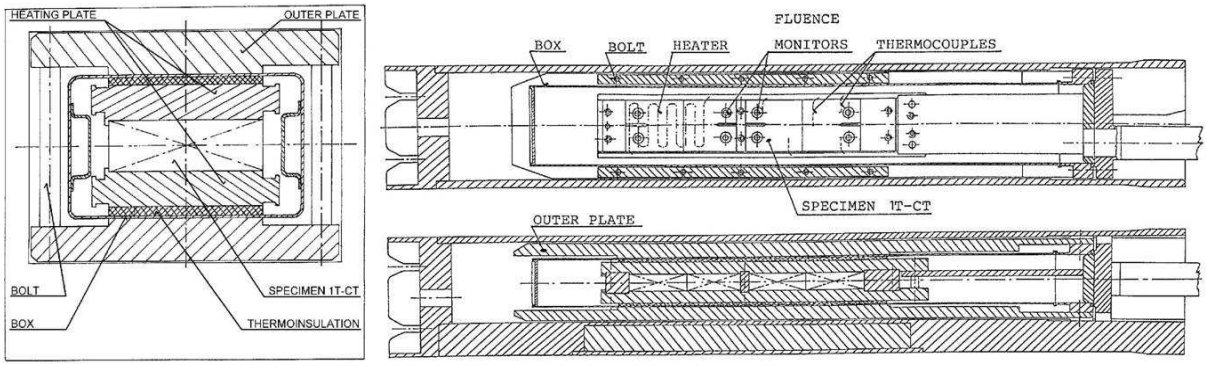

FIG. 3. 1T CT flat rig.

4. ADVANCED EXPERIMENTAL SYSTEMS

In the last few years, research and development activities have started to focus on advanced systems for Generation IV reactors and fusion devices. The main activities for Generation IV are in the fields of corrosion testing, material degradation, water chemistry and radioactivity transport. The supercritical water loop (SCWL) and high temperature helium loop (HTHL) are dedicated to Gen. IV research.

Fusion activities are related to the development of the International Thermonuclear Experimental Reactor. CV Řež actively takes part in two main component deliveries, the test blanket module (TBM) and blanket section. For purpose of TBM, the PbLi loop MeLiLoo was constructed, while the beryllium thermal sample (BESTH) loop and TW3 rig are dedicated to material testing for the blanket section.

All advanced systems have been so far operated in the out-of-pile mode, while the SCWL and HTHL loops together with the TW3 rig are planned for in-pile operation.

4.1. Super critical water loop

The SCWL is designed to be cooled and moderated with supercritical water, i.e., water with parameters above the critical point of 22.15 MPa and 374°C. The main parameters reach values in Table 3.

TABLE 3. MAIN PARAMETERS OF THE SCWL LOOP

Coolant/Medium	High purity supercritical water
Pressure [MPa]	25
Average temperature [^{o}C]	300
Maximum temperature [^{o}C]	600
Average flow rate [kg/h]	200
Chemical compounds analyzed	H_2,0_2
No. of cooling circuits	2

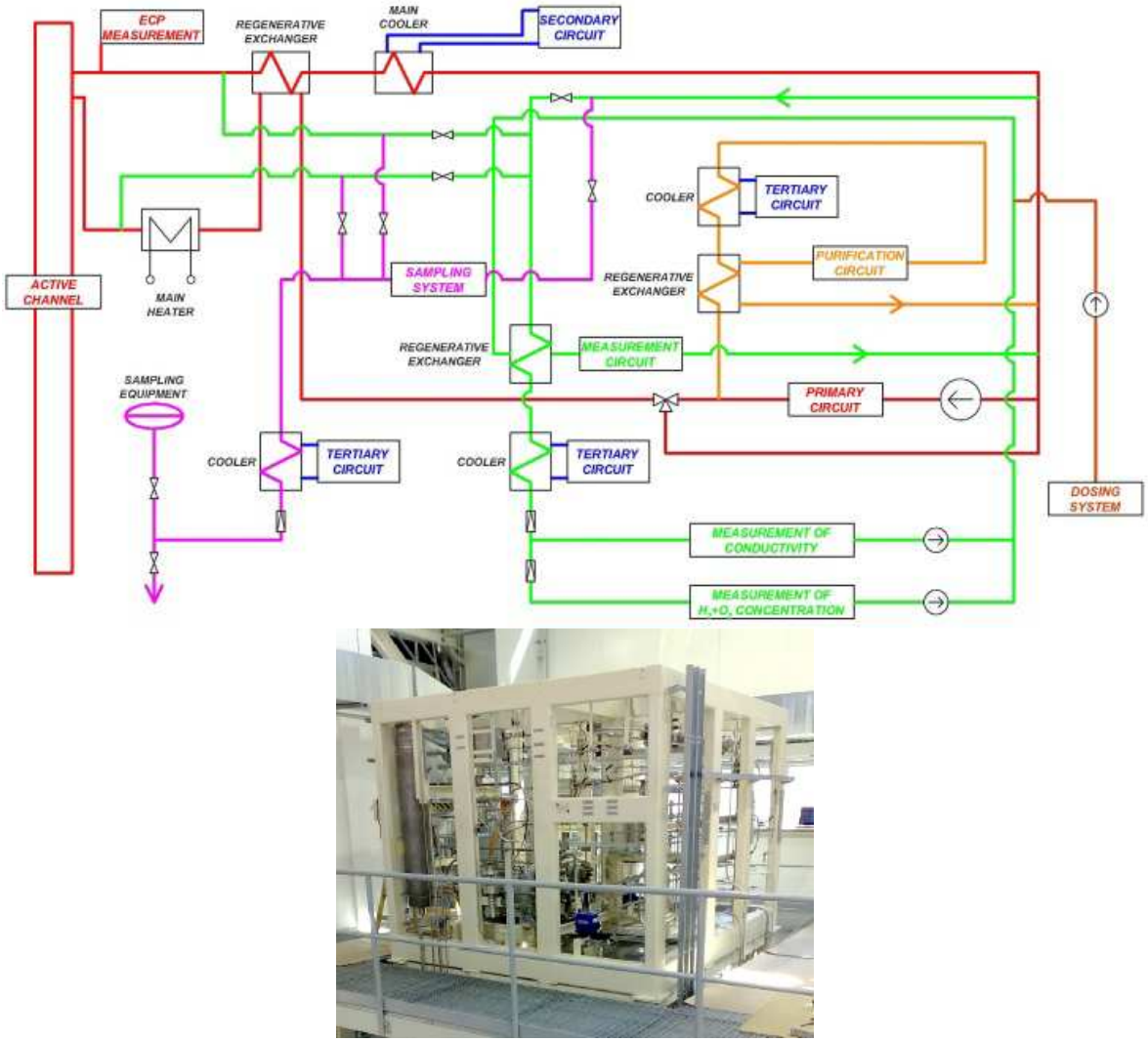

FIG. 4. SCWL loop design and image.

Its main research focuses on the following issues:

- Corrosion testing of candidate materials;
- Water radiolysis at supercritical conditions;
- Testing of water chemistry suitable for operation;
- Testing the corrosion of fuel cladding materials;
- Radioactivity transport.

Testing during 2009 included four days of full power out-of-pile operation, and the loop had reached more than 20 days of out-of-pile by March 2010. In-pile operation is planned in 2012.

4.2. High temperature helium loop

The HTHL is designed for inspection of helium chemical modes under high temperature conditions with neutron and gamma irradiation of a wide range of impurities. The main parameters reach values in Table 4.

TABLE 4: MAIN PARAMETERS OF THE HTHL LOOP

Coolant/medium	High purity helium
Pressure [MPa]	7
Maximum temperature [°C]	900
Average flow rate [kg/h]	38
Chemical compounds analyzed	CO, CO_2, CH_4, H_2O, H_2, O_2
No. of cooling circuits	2

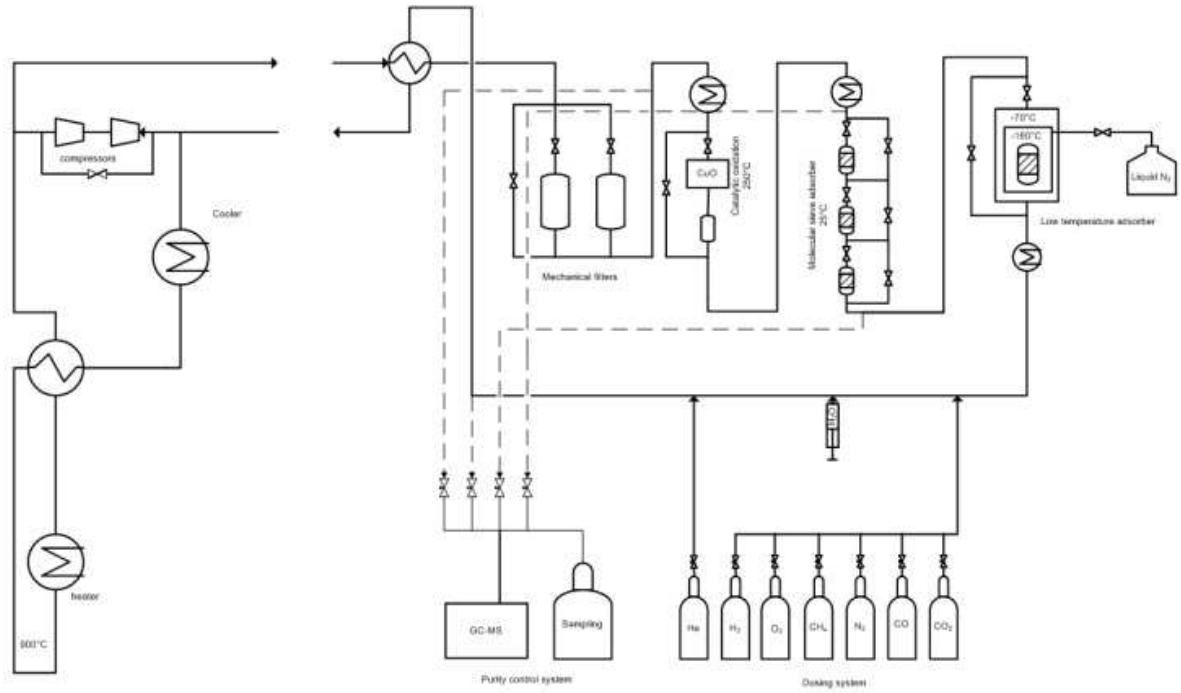

Active channel

Dosing and helium purification system

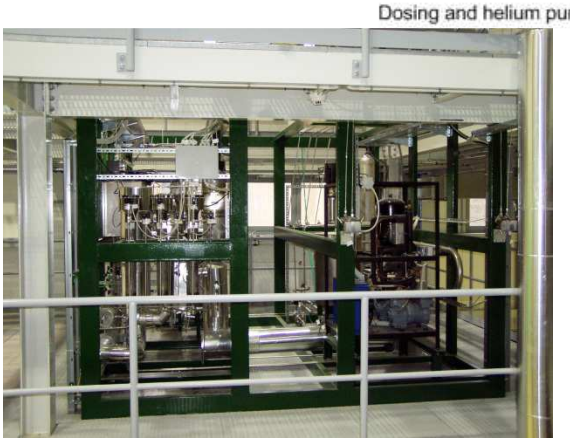

FIG. 5. HTHL loop design and image.

Its main research is focused on following issues:

- He purification system;
- Study of degradation mechanism of metallic materials under high temperature reactor conditions;
- Tests of nuclear graphite.

The loop was widely tested during 2010. In-pile operation is planned in 2012–2013

4.3. Metal liquid loop PbLi

The metal liquid loop PbLi, named MeLiLoo, was designed for development and testing of key components for the PbLi ancillary system proposed as the tritium removal system from the TBM developed under the EU TBM Consortium of Associates. The main components developed and tested in the MeLiLoo were the mechanical pump, cold trap and high temperature flanges. These components were designed and tested for a small MeLiLoo loop. The main parameters are in Table 5.

TABLE 5. THE MAIN PARAMETERS OF THE MELILOO

Circulating medium	Pb-Li (17% lithium) liquid eutectic
Maximum operating temperature [°C]	550
Operating pressure [MPa]	2.5
Cover gas	Ar
Purge gas (for tritium extraction)	He
Pump	
Type	Impeller
Rotation	Variable per minute
Vessel material	EUROFER
Maximum operating temperature [°C]	550
TBM relevant flow rates [cm/s]	1–15
Cold trap	
Operational temperature [°C]	280–330
Vessel material	EUROFER
Other used materials	T91 steel, Austenitic steel

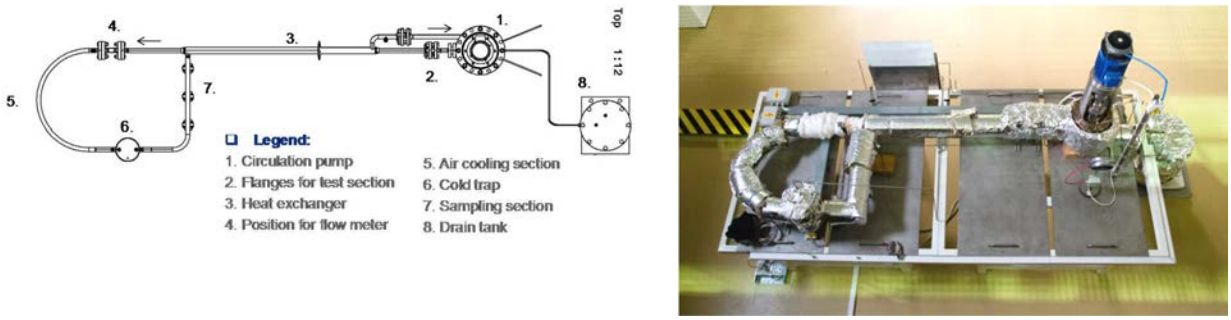

FIG. 6. MeLiLoo loop design.

The loop was successfully operated in 2010 for 2500 h. After the operation and dismounting the pump, no visible damage was found. Evaluation of concentration shows the below reduction of concentrations:

- Fe: about 30%;
- Mn: about 80%;
- Ni: about 70%;
- Cr: no change at all, although on the level of the trap its concentration was higher.

4.4. Beryllium sample thermal device

The BESTH device was designed for out-of-pile testing of the primary first wall (PFW) and first wall qualification mock-ups (FWQMs) from the blanket section. Each tested mock-up consists of three layers, a stainless steel body, a CuCrZr heat sink and beryllium armor joined by a diffusion joint under extreme pressure and temperature to the CuCrZr heat sink. The BESTH device tests the diffusion joint connection by cyclic thermal load with heat flux peak of 0.62 MW/m^2 and cycle duration 5 min (30 s rising power, 180 s full power, 30 s decreasing power, 60 s zero power).

At each testing cycle, two mock-ups facing each other's beryllium side are tested in a helium atmosphere. The thermal load is provided by a graphite heating panel inserted between mock-ups, and the generated heat is removed by a water cooling system consisting of a stainless steel body and CuCrZr heat sink. The result of such design is that all generated heat must pass through the joint between the beryllium and CuCrZr heat sink so that system durability is tested. The main parameters of the BESTH device are in Table 6.

TABLE 6. MAIN PARAMETERS OF THE BESTH LOOP

Thermal load	~0.62 MW/m^2
Number of cycles	12 000
Cooling system	Loop water cooling system
Purge gas	He
No. of mock-ups tested at once	Up to 4
Operation	Out-of-pile

Primary circuit parameters	
Inlet/outlet temperature	~100/110 °C
Pressure	~0.5 MP
Flow-rate	1.6 m^3/h (~1.2 m/s)
Secondary circuit parameters	
Temperature in the heat exchanger	30/110°C
Pressure	~0.2 MPa
Flow-rate	2.7 m^3/h
Two independent air ventilations	Be-lab HEPA filters
	Central ventilation system of the building

FIG. 7. BESTH mock-ups placement.

Since June 2008 when full power operation was commenced, a number of mock-ups have been successfully tested: EU and US FWQM mock-ups with 12000 cycles, French and Korean FWQM mock-ups (12 000 cycles), CN FWQM and EU PROXY mock-ups (12 000 cycles). Also lifetime tests were carried out with two EU mock-ups; the mock-ups lasted 30 000 cycles.

4.5. TW3 rig

Based on the BESTH device, the TW3 rig for in-pile testing was developed. The development of TW3 rig was under EFDA/F4E programme TW3-TVB-INPILE. Two PFW mock-ups are placed in a helium atmosphere one above the other. The cyclic thermal load of 0.5 MW/cm^2 with length of 7 min (30 s rising power, 180 s full power, 30 s decreasing power, 180 s zero power) is provided by a high quality grade graphite heating panel; cooling is established by the reactor cooling system (Table 7).

TABLE 7. MAIN PARAMETERS OF THE TW3 DEVICE

Thermal load	~0.5 MW/m^2
Number of cycles	20 000
Cycle duration	7 min
Cooling system	Reactor cooling system
Purge gas	He

No. of mock-ups tested at once	Up to 2
Operation	In-pile

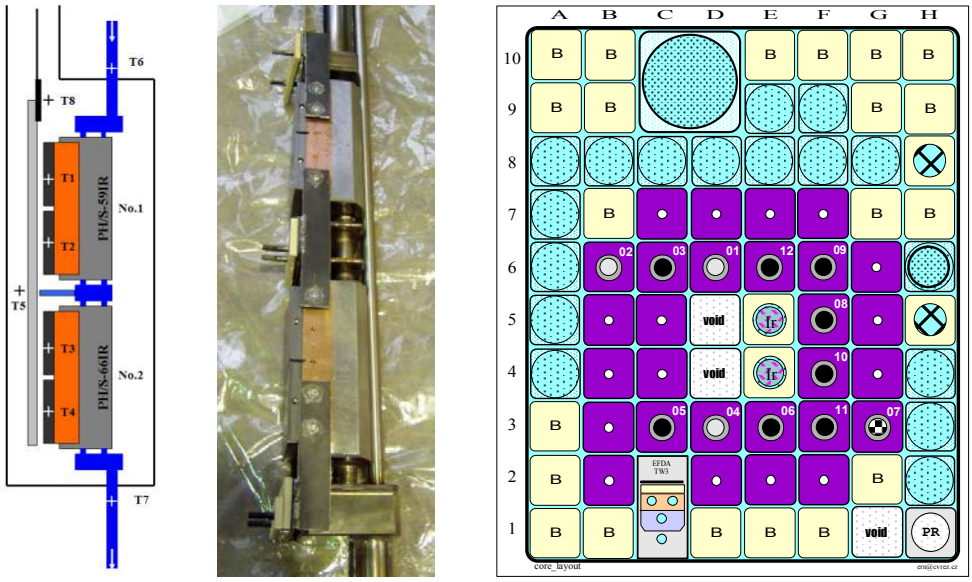

FIG. 8. TW3 rig layout and core position.

The rig had been successfully tested by 2010 for 5000 cycles out-of-pile. For in-pile operation, an application file to the Czech Nuclear Regulatory Authority (SONS) was submitted. After the approval, the rig will be placed in September 2011 to the core in position C1–C2. The in-pile operation will last 20 000 cycles during which the rig should accumulate 0.6 dpa. After the irradiation, the rig will be cut in hot cells during May 2012, and the PFWMs will be sent to Forschungszentrum Jülich, Germany, for evaluation and further testing, which is planned for June–July 2012.

5. CONCLUSION

CV Řež successfully builds on the Nuclear Research Institute's long term experimental programme. The LVR-15 reactor is continuously modernized and equipped with advanced experimental facilities in order to meet current project requirements. The research and development programme has successfully focused on Gen. IV (HTHL, SCWL) and fusion facilities (MeLiLoo, BESTH, TW3) that can be successfully utilized for experimental conditions and know-how.

REFERENCES

[1] MIKLOŠ, M., et al., "Experimental devices for the fusion and Generation IV applications", Proc. Fraunhofer Alliance Numerical Simulation Conference NUSIM, 2010, Fraunhofer Gesellschaft, Munich (2010).

[2] ZLÁMAL, O., KLABÍK, T.,MÜHLBAUER, P., BELLIN, B., TW3-TVB-INPILE: In-pile thermal testing device for Primary First Wall mock-ups with Be cladding, Part II: Out-of-pile 1000 cycles test run, Rep. UJV-Z 2817, Nuclear Research Institute Řež, Řež (2010).

[3] KLABÍK, T., ZLÁMAL, O., HÁJEK, P., ZMÍTKOVÁ, J., TW3-TVB-INPILE: In-pile thermal testing device for Primary First Wall mock-ups with Be cladding, Part I: Preparation of the test rig, Rep. UJV-Z 2678, Nuclear Research Institute Řež, Řež (2009).
[4] KLABÍK, T., ZLÁMAL, O., MASAŘÍK, V., Final Technical Test Report: FWQ-CN-05, Rep. UJV-Z 2588, Nuclear Research Institute Řež, Řež (2009).

EXPERIENCE AND CHARACTERISTICS OF MARIA RR FOR MATERIAL TESTING IRRADIATION

G. KRZYSZTOSZEK
Institute of Atomic Energy POLATOM,
Otwock, Poland
gkrzysz@cyf.gov.pl

Abstract

The research reactor Maria is operated at the Institute of Atomic Energy POLATOM. The multipurpose high flux research reactor Maria is a water and beryllium moderated reactor of pool type with a graphite reflector and pressurized channels containing concentric six tube assemblies of fuel elements. It was designed to provide a high degree of flexibility mainly for materials testing in loops and rigs. Movable core and reflector elements, fuel channels and beryllium and graphite blocks allow for the configuration of the reactor core according to research channels and rigs and ensure these devices are surrounded by nuclear fuel. The equipment cooperating with the channels to be examined can be installed in the experimental hall or in the technological hall of the reactor. Nuclear parameters in the locations for material examinations are as follows: a fast neutron flux of $1.0–1.5\times10^{14}$ $cm^{-2}s^{-1}$, a thermal neutron flux of $1.0–2.0\times10^{14}$ $cm^{-2}s^{-1}$ and gamma thermal heating of 20–50 W/cm^3 (Fe). In Maria reactor were conducted material investigations in thermostatic gaseous rigs KAMA, SR-1, KRS-M.

1. INTRODUCTION

The high flux research reactor Maria is a water and beryllium moderated reactor of pool type with a graphite reflector and pressurised channels containing concentric six tube assemblies of fuel elements. It has been designed to provide a high degree of flexibility.

The fuel channels are situated in a matrix containing beryllium blocks and enclosed by a lateral reflector made of graphite blocks in aluminium cans. The Maria reactor is equipped with vertical channels for irradiation of target materials, a rabbit system for short irradiations and six horizontal neutron beam channels.

The main characteristics and data of Maria reactor are as follows:

- Nominal power: 30 MW_{th};
  - Thermal neutron flux density: 4.0×10^{14} $cm^{-2}s^{-1}$;
- Moderator: H2O, beryllium;
- Cooling system: Channel type;
- Fuel assemblies:
  - Material: UO2–Al alloy;
  - Enrichment: 36%;
  - Cladding: aluminium;
  - Shape: six concentric tubes;
  - Active length: 1000 mm;
- Output thermal neutron flux:
  - At horizontal channels : $3–5\times10^{9}$ $cm^{-2}s^{-1}$.

The Maria reactor reached its first criticality in December 1974. The reactor was in operation until 1985 when it was shut down for modernization. The modernization encompassed refurbishment and upgrading of technological systems. In particular, the efficiency of the ventilation and cooling systems was improved. In 1993 the Maria reactor was put into operation again.

The main areas of reactor application are as follows:

- Production of radioisotopes;
- Testing of fuel and structural materials for nuclear power engineering;
- Neutron radiography;
- Neutron activation analysis;
- Neutron transmutation doping;
- Research in neutron and condensed matter physics.

IAE POLATOM currently has a programme for Maria research reactor operation until 2050.

2. CHARACTERISTICS OF MARIA REACTOR FOR INSTALLATION LOOPS AND RIGS.

The Maria reactor core contains the fuel assemblies, which are installed in pressurized channels embedded in matrix sockets. The matrix is composed of beryllium blocks which are fastened to the support slab in the reactor pool at the level +2.75 m.

The beryllium blocks of the core matrix as well as graphite blocks create a 6×8 radial reflector that is positioned in the sockets of the separator slab on the level -1.4 m (See Figures 1 and 2). The configuration of the core matrix and reflector is also shown in Figure 2.

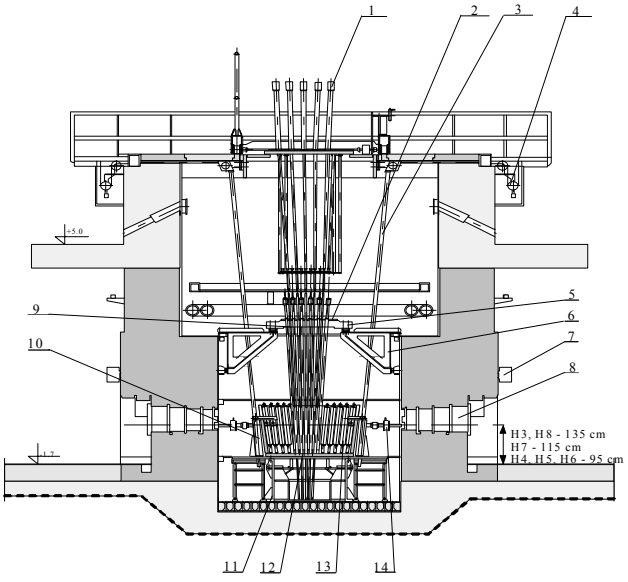

FIG. 1. Cross-section of the reactor block.

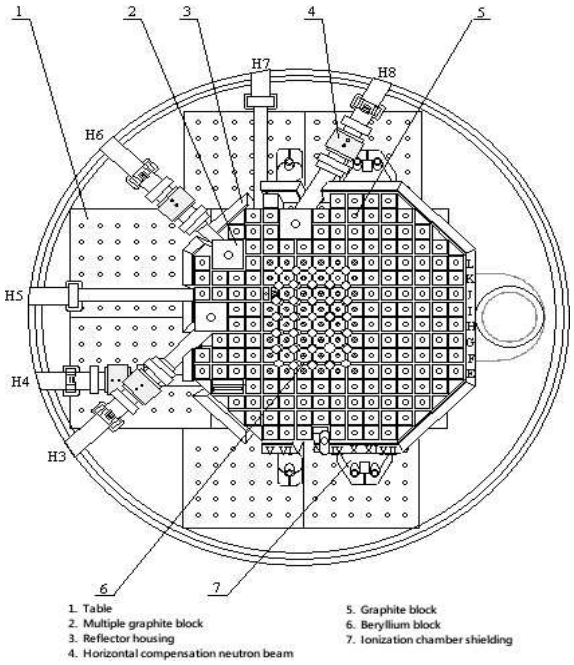

FIG. 2. Top view of the reactor core and reflector.

At the support slab for the fuel and loop channels shown in Figure 3, there are altogether 33 connectors to be used for the fuel channels.

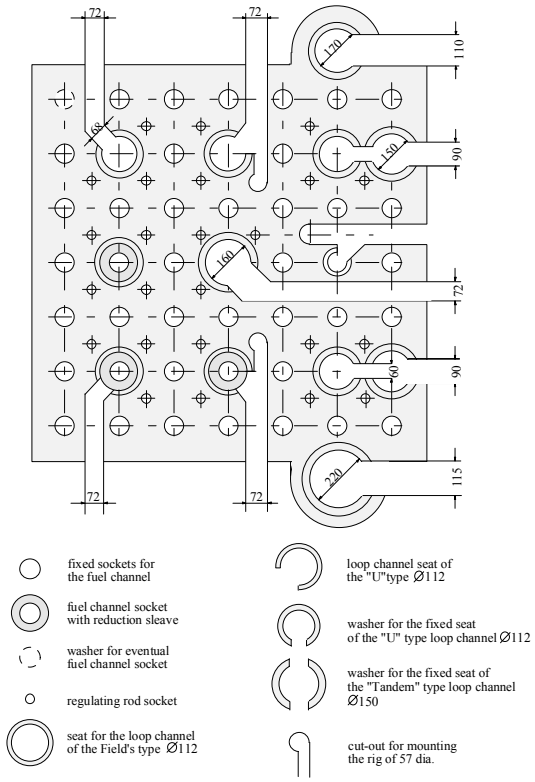

FIG. 3. Layout of the socket in the mounting plate over the reactor core.

The possibilities for placement of experimental channels, i.e., channels, rigs and loops, depend on two factors: the position in the core and arrangement and dimensions of holes in the support slab.

The location within the core can be matched to any experimental device by means of constructing suitable beryllium and graphite blocks.

However, the distribution of openings, i.e., the sockets in the mounting plate, is totally determined by its construction (See Figure 3). Beyond this, tracks have been made in the mounting plate for installing U tube loops. On the mounting plate are located the following sockets:

- 1 of 112 mm diameter for a field type tube;
- 4 of 112 mm diameter for U type channels;
- 1 of 160 mm diameter for a U type channel;
- 1 of 900 mm diameter for a U type channel;
- 2 of 112 mm diameter that are compatible with sockets of 150 mm in diameter;
- 1 of 220 mm diameter; and
- 1 of 170 mm diameter.

Lattice pitch in the core at half of its length is 130 mm. The neutron and thermal characteristics for the research channels are as follows:

- Fast neutron flux Φ_f=1.0–1.5×10^{14} $cm^{-2}s^{-1}$;
- Thermal neutron flux Φ_{th}=1.0–2×10^{14} $cm^{-2}s^{-1}$; and
- Heat generation q(Fe)=3–4 W/g.

The relative axial distribution of gamma generation in steel and the correlation between the quantity of heat generated and power of adjoining fuel channels are shown in Figures 4 and 5.

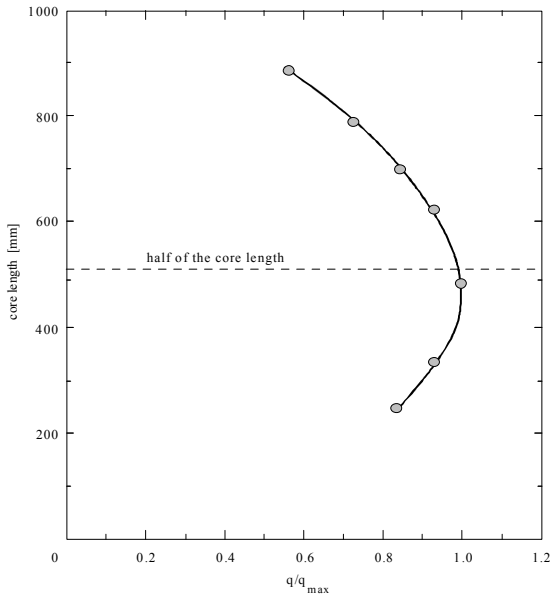

FIG. 4. Relative distribution of gamma heat generation in steel along the vertical axis of the irradiation channel.

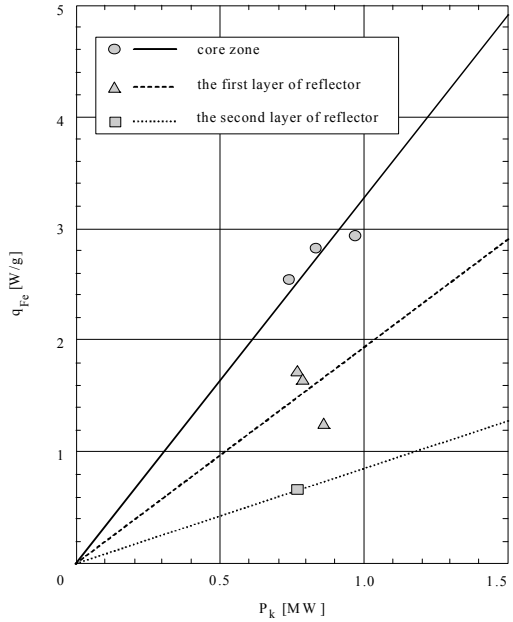

FIG. 5. Correlation between the heat generation in steel and the average power generated in the adjoining channels.

The values of heat generation in steel, expressed in W/g, are representative of all materials with a small atomic number Z; for materials with a large atomic number, e.g., lead and bismuth, the values presented in Figure 5 are double.

The pipelines and instrument leads of experimental installation to be placed inside the reactor core and reflector can be pulled out from the reactor pool by means of the following routes:

- Installation channels running inside the shielding walls of the storage pool and sloping down on the level -1.7 m;
- Culverts for instrument leads in the shielding hall of the reactor pool on the level +5 m.

The heavy and required effective shielding for the equipment and installation of loop circuits is set up in the experimental hall near the storage pool walls. Admissible load of the floors at that location is 6 t/m^2.

Between the experimental hall and reactor hall there are two hatchways of overall dimensions 388×968 cm and 388×628 cm in the region of the loop installations. These hatchways are to be used during the construction of the loop installations and their shielding by using the main overhead crane with a lifting capacity of 16 t.

For the expansion of the loop installations culverts in the building wall have been provided to enable the withdrawal of ancillary devices to the pavilion adjoining the reactor building.

3. SOME EXPERIENCE IN REACTOR LOOPS AND RIGS IRRADIATION

Research reactor loops and rigs make possible the performance of material and technological studies for nuclear power reactors. These types of studies continue to be one of the basic tasks for the Maria reactor, having been also the primary motive for the reactor's design and construction.

By means of rigs mentioned below a number of research programmes in the 1980s were executed. The following are brief descriptions of the equipment only.

3.1. Thermostatic gaseous rigs of KAMA type

In the rigs of this type, SR-1, KAMA-1 and KAMA-2, investigations of samples made of stainless steel and zirconium were conducted. The rigs were equipped with systems that enabled the irradiation of samples at constant temperature in a gaseous atmosphere of helium or nitrogen.

The rig KAMA consisted of a furnace with equalization heaters, a charge with samples, a control and adjustment system as well as a gaseous system.

The purpose of the heating furnace is to maintain a constant stable temperature for a sample pack. The adjustment of temperature can be achieved by changing the composition of gases within the adjustment gap. The separation of the rig into two parts, furnace and charge, enables the repeated usage of the furnace while exchanging only the examined samples in the charge.

Austenitic steel samples of 1H18N9T type and zirconium samples were irradiated. The rig KAMA allowed the application of a wide range of temperatures on the materials tested. The measurements revealed that for a reactor power of 20 MW and with the rig positioned in the reactor reflector such that reactor heating is used exclusively, variations in temperature on samples within a range from 230°C, with the isolation gap filled with helium, up to 570°C, with the isolation gap filled with nitrogen, were possible.

Thermostatic gaseous rig GAPISZON enabled prolonged testing of detectors in the reactor core. In the rig the temperature in a range of 200–450°C was achieved by means of a helium and nitrogen mixture in the slot composing the core part of the rig.

3.2. Rig KRS-M for examining zirconium alloy in a water vapour environment

A Polish–Czech programme aimed at investigating the behaviour of zirconium alloys to be used for cladding of fuel elements in boiling water power reactors. The Department of Nuclear Fuels (ZPJ) in Prague, Czech Republic, constructed the reactor rig KRS-M that was irradiated in the Maria reactor.

The programme established the irradiation of zirconium alloys samples in an atmosphere of superheated steam parameters:

- Pressure: 1–0.2 MPa;
- Temperature: 450–30°C;
- Steam flow rate: 10–30 g/h; and
- Time of irradiation: 3000 h.

This rig operated in Maria reactor from July 1982 until March 1983. In that time the reactor operated at 20 MW power in cycles 120 hours each week. The rig was installed in the reflector in the aluminium block. The investigated samples absorbed a neutron dose of $\Phi \sim 3\times10^{20}$ cm^{-2} during 3118 hours of testing and achieved a maximum temperature of ~530°C.

After termination of irradiation these samples were transported by a special shielded container for material examination in the hot cells in of ZPJ in the Czech Republic.

3.3. The rigs of MAK type

The rigs of MAK type aimed to test structural materials to be used in fast power reactors in an atmosphere of the dissociating gas N_2O_4. They were operated at variable power levels in a range up to 30 MW, which provided the maximum parameters:

- Temperature: 500°C; and
- Pressure: 59 MPa.

4. CONCLUSION

Maria research reactor still possesses good possibilities for material testing in loops and rigs. However for the last 20 years companies interested in material testing at research reactors were difficult to find. IAE POLATOM and the Atomic Energy and Alternative Energies commission (CEA), France, have begun discussions to find an area for material testing cooperation between Maria and the Jules Horowitz Reactor.

THE JULES HOROWITZ REACTOR: A NEW RESEARCH REACTOR DEVOTED TO FUEL AND MATERIAL TESTING FOR THE NUCLEAR INDUSTRY

P. ROUX, C. GONNIER, G. BIGNAN
CEA Cadarache Centre,
Atomic Energy and Alternative Energies Commission (CEA),
St Paul lez Durance, France
patrick.roux@cea.fr

X. BRAVO
CEA Saclay Nuclear Research Centre,
Atomic Energy and Alternative Energies Commission (CEA),
Gif Sur Yvette, France

Abstract

The future Jules Horowitz material testing reactor is a pool tank water reactor under construction in the CEA Cadarache Centre. It will be a major research infrastructure within the European Research Area for the scientific studies of new materials and fuels under irradiation. At present, civil engineering works are in progress, and CEA expects the beginning of operation in 2016. The reactor core of 60 cm in height, 70 cm in diameter, is designed to operate at 100 MW_{th} and provide experimental cavities hosting experimental devices. The 10 experimental locations situated inside the reactor core have a diameter ranging between 30–95 mm and provide high fast neutron flux conditions. The locations situated in the surrounding reflector of the reactor core have a maximum diameter of 200 mm and provide high thermal neutron flux conditions. The design of the facility allows for the operation of 20 experiments simultaneously. For the purpose of testing fission and fusion reactor technology, the design of some experimental devices will allow investigating irradiations under high temperature conditions up to 1000°C. For research on materials for fusion reactors technologies, JHR can offer its central locations in the reactor core, which provide the highest fast neutron flux (up to 10^{15} $cm^{-2}s^{-1}$ of E>0.1MeV), corresponding to material damage of 16 dpa/year.

1. INTRODUCTION

Before using new materials or fuels in power plants, utilities must perform experimental irradiation of the components. Development is generally performed in three steps:

- First is a basic selection experiment that aim at choosing the best products among a new panel;
- Second is a series of highly instrumented characterization tests that aims at precisely measuring the physical properties of the products under neutron flux;
- Third is a set of qualification tests that aims at reproducing the operation of the fuel or material under power plant conditions to demonstrate that the product can be used safely.

This development process requires specific facilities such as the Jules Horowitz Reactor (JHR). It will have all necessary equipment to perform all experimental steps and to reproduce all types of fission reactor technology environments in terms of thermohydraulics, chemistry and neutron flux.

This document will describe in at first the JHR facility and all systems participating in its operation. Next it will describe its experimental capacity with a focus on the material devices under construction. Finally, a discussion is presented on what may interest the fusion community.

2. GENERAL DESCRIPTION OF JHR FACILITY

The JHR design is optimized in order to provide the most modern and efficient equipment and the best conditions in order to perform experimental irradiations for the nuclear industry.

2.1. Organization of the project

JHR is designed, built and will be operated as an international user facility, driven and funded by an international consortium gathering vendors, utilities and public stakeholders. The consortium was set up in March 2007 when construction began. The start of operation is scheduled for 2016.

At the present time, the partners of the consortium are:

- Research laboratories: CIEMAT (Spain), CEA (France), NRJ/UJV (Czech Republic), European Commission, SCK/CEN (Belgium), VTT (Finland), DAE (India), JAEA (Japan);
- Industrial organisation: Areva, EDF, Vattenfall

Discussions to enlarge the JHR consortium are ongoing with research institutes and utilities.

2.2. Nuclear unit

The nuclear unit is comprised of two buildings. The reactor building houses the reactor pool encasing the reactor and the nuclear auxiliary building, which provides the necessary equipment in support of the operation of the reactor and experiments (See Figure 1).

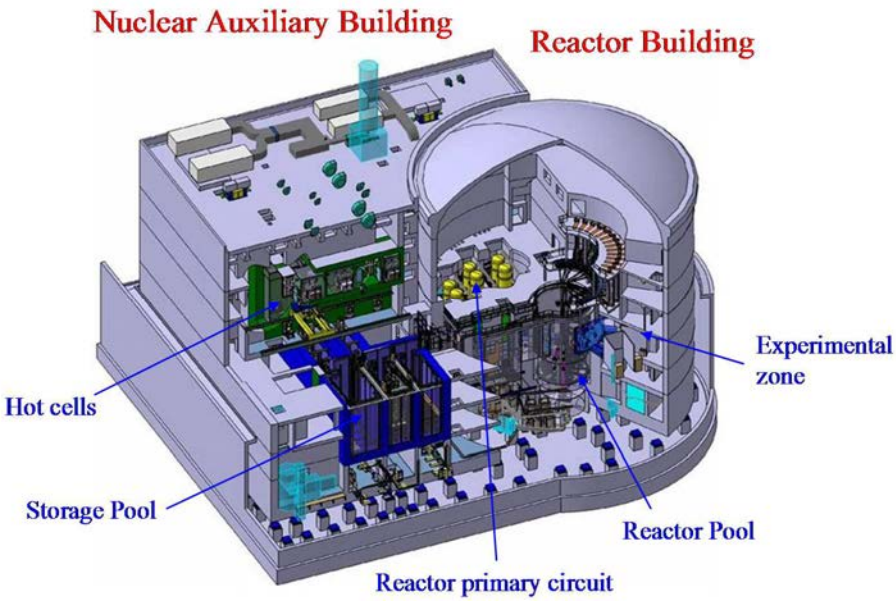

FIG. 1. JHR nuclear unit.

The reactor building is cylindrical with a diameter of 36.6 m and a height of 44.9 m. It contains the reactor pool, 7 m in diameter and 12 m depth, in its centre. The building is separated into two zones:

- One half of the building is dedicated to the operation of the reactor primary circuit. It contains all components of the primary circuit and participates in the exploitation of the reactor;
- The other half is an experimental zone available for exploitation and monitoring of experimental devices.

The nuclear auxiliary building is adjacent to the reactor building. It contains all rooms and systems that do not need to be installed in the reactor building:

- Control rooms for reactor and experiments;
- Workshops for preparation, repair and maintenance of non-irradiated equipment;
- Laboratories for, e.g., chemistry and radiology;
- Storage pools that are connected to the reactor pool by a water channel network penetrating through the reactor building;
- Hot cells for the handling of irradiated materials.

2.3. Reactor

The reactor is a 100 MW_{th} pool tank water reactor. It is cooled with forced convection through a pressurized primary circuit that measures 15 bars at the core inlet. The reactor, 60 cm in diameter and 60 cm height, is situated in a vertical cylindrical part of the primary circuit. Outside of the reactor tank, the reactor is surrounded by beryllium blocks that reflect neutrons (See Figure 2).

The 34 fuel elements, 60 cm of fissile length, of the reactor are inserted into holes in a massive aluminium structure situated in the vertical part of the primary circuit. Each fuel element is made of eight concentric cylindrical plates of U_3Si_2 of 95 mm in outer diameter. This configuration has been selected because it provides the highest fast neutron flux at the irradiation sites.

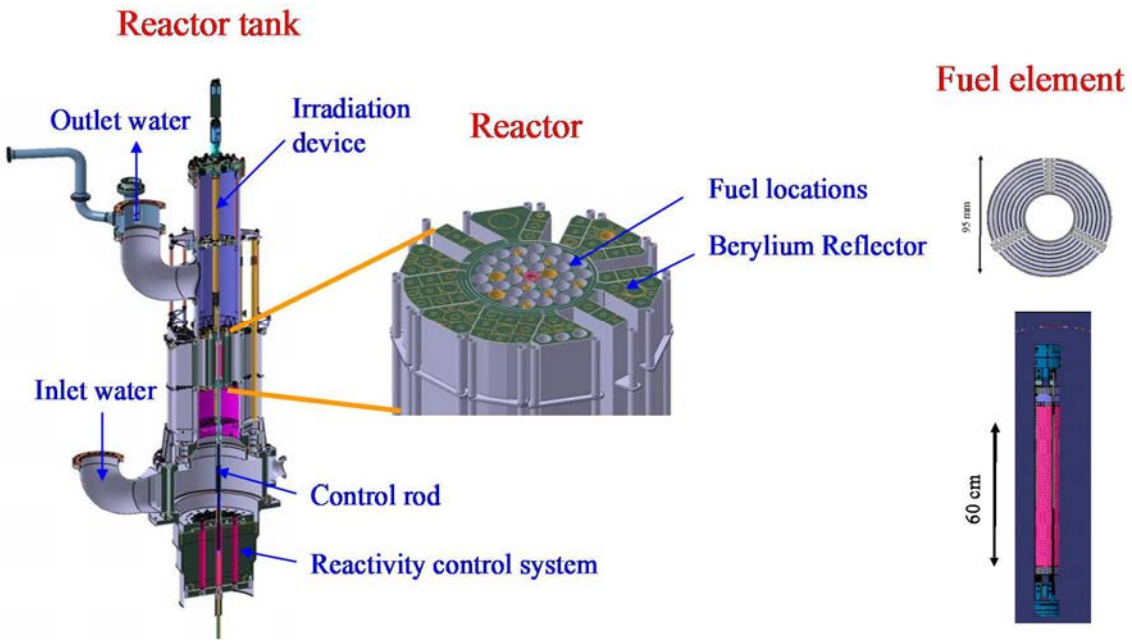

FIG. 2. JHR reactor tank and reactor.

In the central part of each fuel element, a 33 mm diameter location volume is available and allows implementation of or experimental devices of small diameter or control rods for the control of reactivity or safety purposes. The reactivity control system of the reactor is situated below the reactor core with absorbers penetrating through the core from the bottom.

The irradiation devices are inserted in the reactor core from the top of the reactor. The devices are tightly penetrating through the top cover of the reactor tank ensuring tightness of the primary circuit.

3. EXPERIMENTAL CAPACITY OF JHR

3.1. Irradiation locations

For the purpose of performing experimental irradiations of material or fuel samples, some locations are available in the reactor core and in the beryllium reflector. In these locations, experimental devices holding the sample and instrumentation can be installed. They consist of cylindrical containers located in the irradiation cavities with a sample holder for insertion.

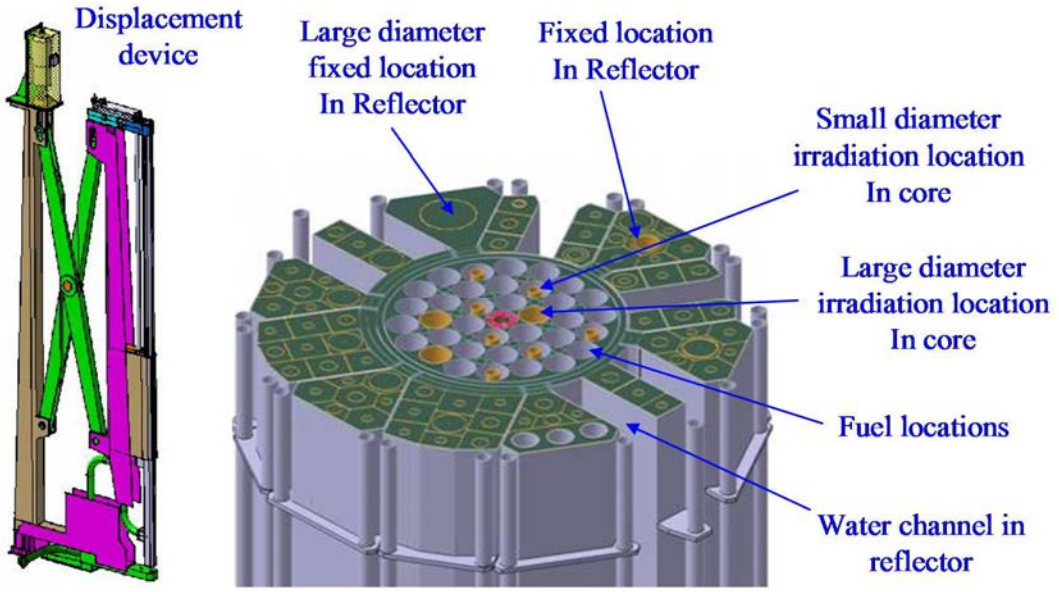

FIG. 3. Experimental locations in the reactor core and in the beryllium reflector.

In the reactor, the samples are submitted to a high fast neutron flux. These experimental locations are adequate for the irradiation of material samples, because high damage is induced on the samples. They can also be used for fuel experiments requiring a fast neutron flux. The design of the reactor allows two types of experimental locations:

- Some locations are located in the centre of fuel assemblies and can house an experimental device of small diameter, typically 33 mm. Among the 34 fuel assemblies of the reactor core, 7 can house such experimental devices (See Figure 3);
- Some locations replace a fuel assembly and can house an experimental device of large diameter, typically 95 mm. In the reactor core are three that can house such experimental devices (See Figure 3).

In the beryllium reflector, samples are submitted to a high thermal neutron flux. These experimental locations are adequate for the irradiation of fuel samples. They can also be used for material irradiation requiring a low fast neutron flux, pressure vessel steel testing for example. The JHR beryllium will be equipped with two location types:

- Fixed locations will be situated in vertical cylindrical holes in the beryllium. The JHR will have about 15 of these locations of 100 mm in diameter and one of 200 mm in diameter (See Figure 3); and
- Moving locations with displacement devices will be implemented in the water channel of the beryllium. These systems allow for holding the experimental devices and controlling their position within the reactor tank and hence regulating the neutron flux submitted to the samples. The JHR will have 6 of these moving locations with a 100 mm diameter (See Figure 3).

3.2. Experimental capacity of the reactor building

In addition to the experimental devices located in the reactor or the beryllium reflector, the JHR is equipped with an experimental zone, situated in one half of the reactor building (See Figure 4).

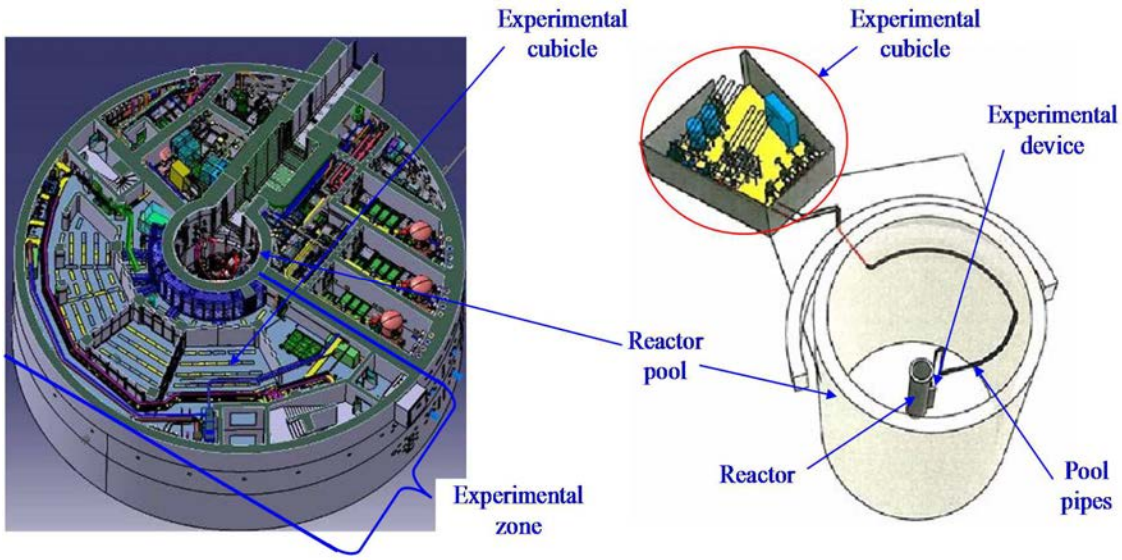

FIG. 4. View of the level 1 of the reactor building (left) and view of an experimental device in the reactor pool with an experimental cubicle connected (right).

This zone is made of 6 floors, 3 situated under the reactor pool water level and 3 above, and it is dedicated to the installation of equipment in support of the experimental programmes:

- From level 0 to level 2, a 490 m^2 area is available and dedicated to the implementation of instrumentation and control systems. Safety and experimental instrumentation and control equipment, e.g., control racks, calculators and actuators, must be implemented in this zone; and

- From level -1 to level -3, a 700 m^2 area is available and dedicated to the implementation of experimental cubicles in order to install mechanical equipment participating in the control of the samples environment conditions. This equipment is connected to the experimental device by pipes and electrical cables travelling in the reactor pool. This experimental zone can accept a pavement loading of up to 6 t/m^2. In addition, this zone is equipped with a total electrical power supply of 1.5 MW_e and a 2 MW cooling capacity.

In addition to all this experimental capacity in the reactor building, the JHR will be equipped with hot cells implemented in the nuclear auxiliary building. The main task of these hot cells is the handling and non-destructive examination of irradiated materials.

The JHR hot cells are made of four high cells, 10 m in height, that allow for the handling of an entire experimental device. These large hot cells can load and unload irradiated material coming from the water channel network. In these hot cells, the sample holder can be removed from the irradiation device.

Adjacent to these high hot cells, smaller cells are installed. They communicate with the large ones and allow precise handling and non-destructive examination of experimental samples pieces (See Figure 5).

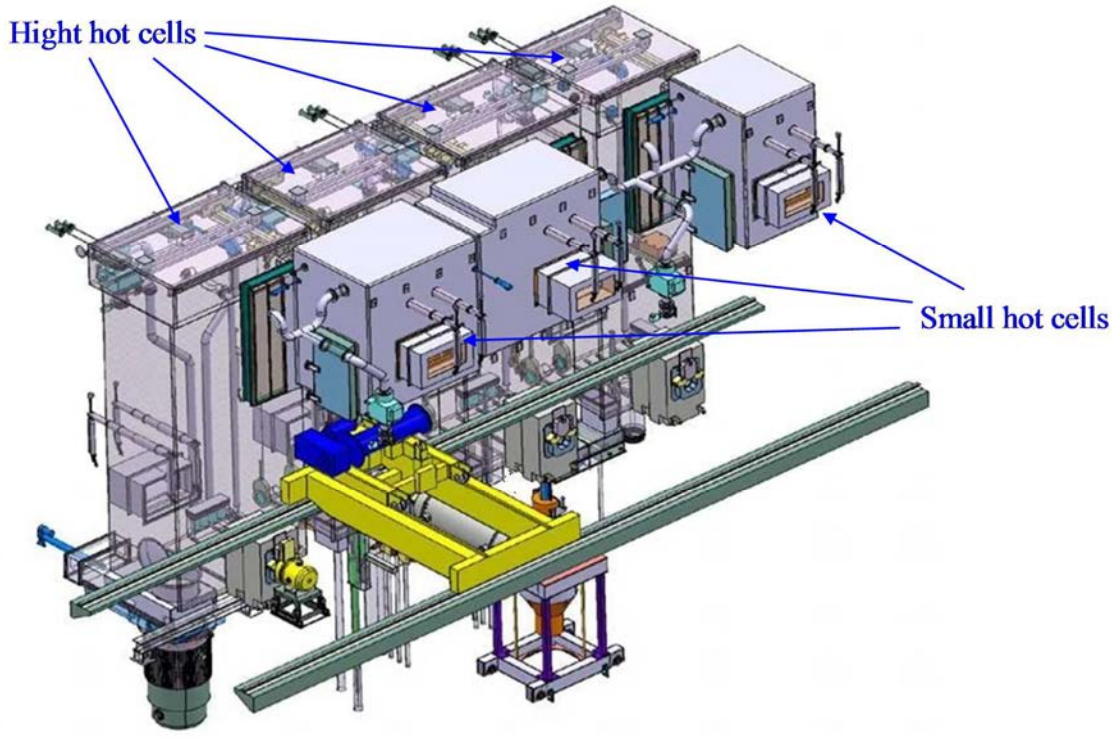

FIG. 5. Hot cells in the nuclear auxiliary building.

3.3. Sample examination

The experimental irradiation of samples in a material test reactor requires high performance examination of the samples online or at the end of the irradiation. For online examination, the

JHR facility will provide good flexibility in its experimental devices in order to adapt the instrumentation on the sample holder to specific needs that are required by customers.

For post irradiation examinations, the JHR is equipped with various non-destructive benches:

- A gamma spectrometry and X radiography bench (See Figure 6) will be located in the reactor pool. The examination will be performed through the structures of the experimental device and immediately after unloading the irradiation device from its irradiation location;
- A second gamma spectrometry and X radiography bench will be located in the storage pool in the nuclear auxiliary building. The examinations will be performed through the structures of the experimental device and with a delay after unloading the irradiation device from its irradiation location;
- A neutron imaging system could be installed in the reactor pool. The opportunity to install this bench will depend on customer needs. It will use the neutron flux from the reactor core. The examination will be performed through the structures of the experimental device and quite rapidly after unloading the irradiation device from its irradiation location;
- After unloading the samples from the experimental device in hot cells, other examinations such as visual inspections, metrological techniques, default characterization and corrosion layer determination can be performed in one of the small cells.

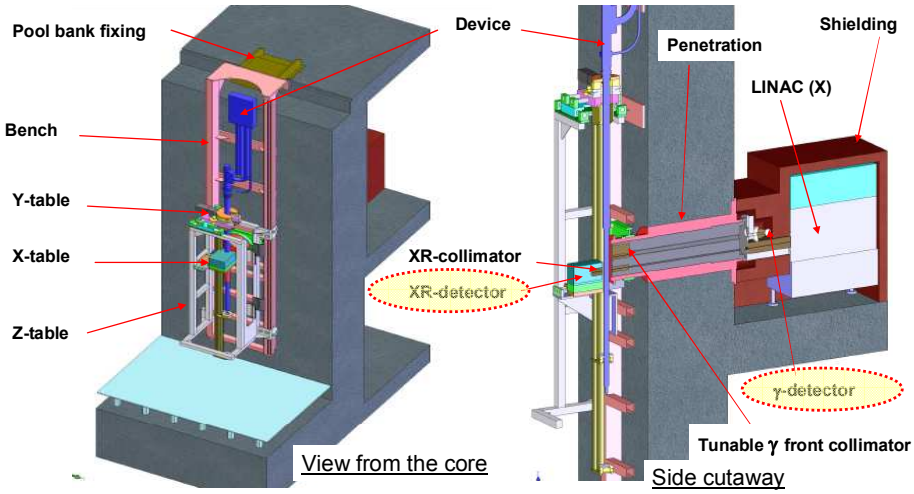

FIG. 6. X radiography and gamma spectroscopy bench in the border of the reactor pool.

4. GENERAL DESCRIPTION OF EXPERIMENTAL DEVICES UNDER DESIGN

In parallel to the building of the reactor, the first irradiation devices to be used in the JHR are under design phase. Other experimental devices are under a feasibility study in order to comply with all the needs of the nuclear industry, but only a limited number of these devices will be in operation at the initialization. Indeed, the design and manufacturing of this equipment is a long and complex process.

At the present time, CEA is focusing its efforts on the design of two families of experimental devices that correspond to the present needs of the nuclear industry and that will be available at JHR's initial operation:

- Light water reactor fuel irradiation devices for the selection, characterization and qualification of fuel products. These devices are not described in the present document because of the lack of direct application to fusion technology;
- Material irradiation devices of low embarking capacity and highly instrumented for testing under well controlled environment conditions in the reactor core. These experimental devices named CALIPSO and MICA will be described in the next section;
- Material irradiation devices in the beryllium reflector for light water reactor vessel steel qualification under low fast and low epithermal neutron fluxes. This experimental device named IRMA will be shortly described in the next section.

Other families of experimental devices are under a feasibility study. They will not be in operation at the start of JHR but should be in operation during the first decade:

- A material irradiation device of large embarking capacity called MATGAZ in the reactor core with little instrumentation and a limited control of environment conditions. This experimental device will be described in the next section;
- Experiments dedicated to Generation IV reactors. This includes sodium cooled or gas cooled reactors and transmutation experiments. These devices are not precisely described in the present document;
- A material irradiation device located in the beryllium reflector but close to the core and dedicated to investigation of irradiation assisted stress corrosion cracking. This device will not be described in the present document.

At the present time, one quarter of the area available in the experimental zone of the reactor building is used for the implementation of the first experimental devices under development. The remaining area can be used for the implementation of other experimental devices to meet the irradiation needs of other customers.

5. FOCUS ON MATERIAL IRRADIATION DEVICES UNDER DEVELOPMENT

This section describes the material irradiation devices that are under development and may interest researchers on fusion reactor technologies.

5.1. Low embarking capacity, highly instrumented devices

In the nuclear industry, research on materials is an important topic. In the past, numerous experimental irradiations have been performed, increasing the knowledge and performance of materials from the current light water power reactors under operation. At the present time, research on these materials is still under progress, but customers are interested in experiments requiring high accuracy and online instrumentation. Their purpose is obtaining good characterization of the physical properties of the products under a neutron flux.

For such experiments, CEA is developing two experimental devices to be inserted in the centre of a fuel assembly. Such a location allows for high fast neutron fluxes. They will have a small

diameter, 33 mm of outer diameter, effectively 24 mm for experimental purposes, and low embarking capacity. One main requirement of these experimental devices is ensuring a well-known and homogeneous temperature is applied to the samples. For this purpose a liquid metal, NaK, is used as coolant for samples. Indeed, this coolant has high thermal conductivity and is transparent to a neutron flux. Two versions of this experimental device are actually planned:

- The MICA device filled with static NaK. In this case the maximum temperature expected for the coolant, and hence for samples, is 450°C. Since NaK is static, one cannot ensure good homogeneity along the entire sample;
- The CALIPSO device with an integrated NaK forced circulation loop (See Figure 7). In this case the maximum operating temperature is also 450°C. Note that preliminary investigations to reach a higher temperature of around 650°C are under progress. Thanks to NaK circulation, it is possible to ensure less than 8°C of thermal gradient in the experimental samples. For monitoring NaK flow, CEA has developed an annular electro-magnetic pump.

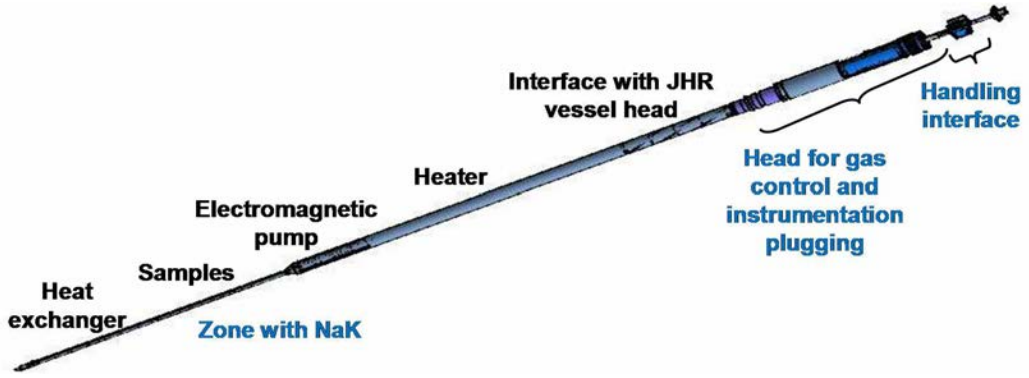

FIG. 7. View of the design of the CALIPSO experimental device with its main components.

In addition to very accurate control of thermal conditions, these two experimental devices allow for the loading of a panel of sample holders that can submit samples to specific stress conditions:

- Pressurized rodlets to investigate creep under irradiation;
- Bending tests;
- Tensile tests to investigate axial creep phenomena;
- Bi-axial loading to investigate phenomena on anisotropic materials (See Figure 8).

All sample holders can be instrumented with specific sensors allowing online measurements of sample elongation and diameter.

In the MICA experimental technology, it is possible to replace NaK coolant with He. In this case, one can investigate material irradiations under high temperatures up to 1000°C. At CEA, such experiments have already been performed in the Osiris reactor in order to test the behaviour of silicon carbide materials for fusion reactor technology in the FURIOSO experiment and for Generation IV reactor technology in CEDRIC, which is presented in Figure 9.

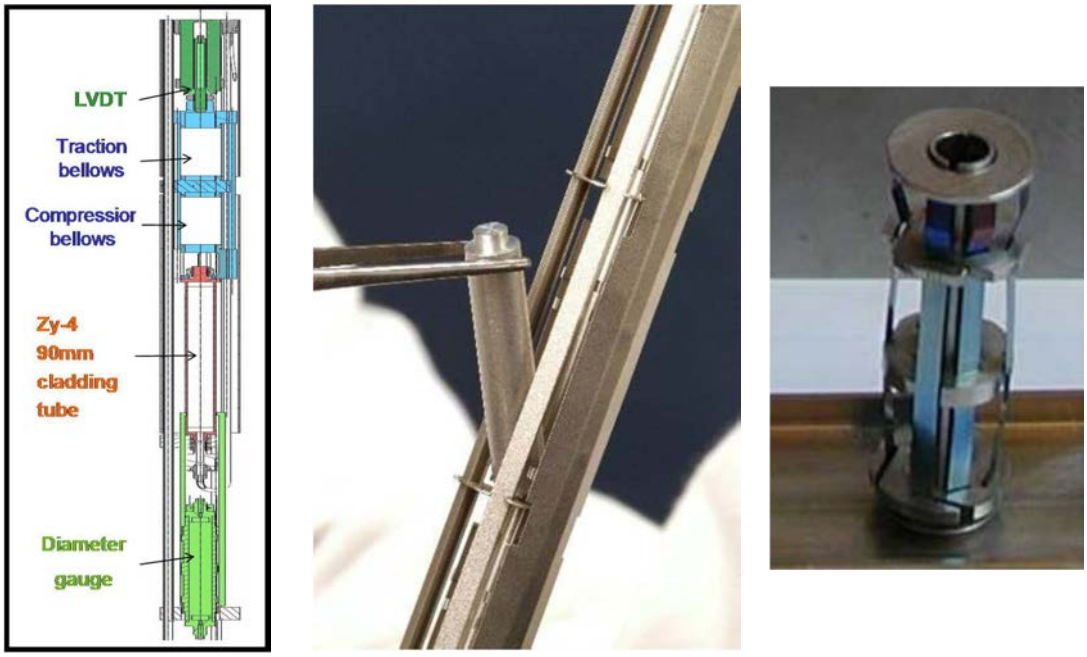

FIG. 8. Schematic view of the design of the Bi-axial loading sample holder (left) and view of two examples of samples, pressurized rodlets (centre) and bending tests samples (right), that were irradiated in another experimental reactor.

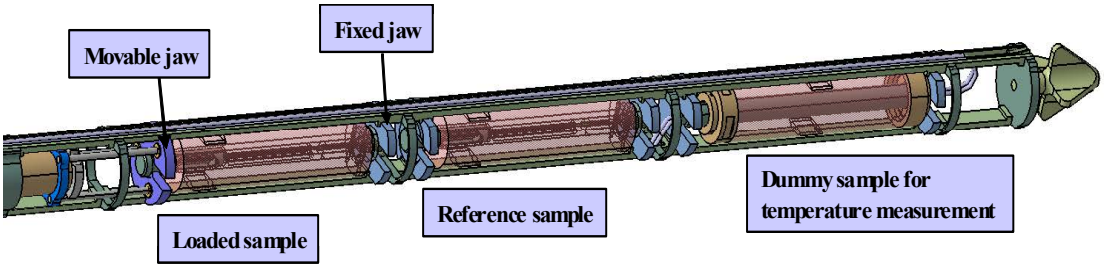

FIG. 9. View of the design of the CEDRIC experiment for the testing of SiC creep under irradiation and high temperature (1000°C). This experiment was performed in the Osiris reactor.

5.2. High embarking capacity with low instrumentation device

The present experimental device called MATGAZ is complementary to the ones mentioned above. Its purpose is the performance of irradiations of numerous samples with a limited level of instrumentation. Such an experimental device is more devoted to selection experiments in which customers want to select the most promising material for their application without online characterization. In this case, the examinations of the samples are performed after irradiation.

This experimental device will be installed in the reactor core, in place of one JHR fuel assembly in an experimental location of 95 mm in diameter.

The device is cooled by a natural convection circulation of slightly pressurized He. The samples, 3 stages of 20 samples of dimensions 3 mm×4 mm×8 cm, will be located in the central upward He vertical channel, and cooling will be performed in the downward vertical channels by the structures of the experimental device (See Figure 10).

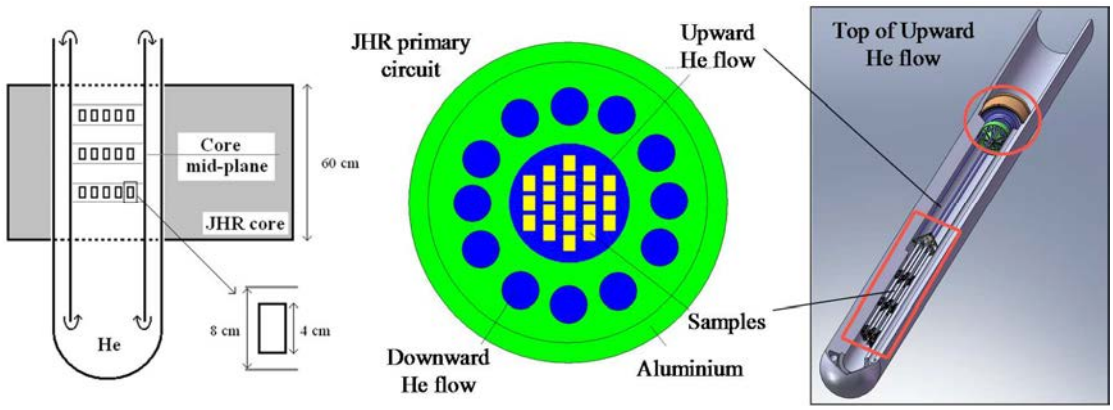

FIG. 10. Schematic view of the high embarking capacity device design. Left: View of the He natural convection loop. Centre: View of the location of the samples and the downward water flow channels. Right: 3D view of the experimental device with the sample holder.

The temperature of the samples will be monitored by regulation of the He flow from the natural convection loop. Upon reducing the helium flow, one increases the samples' temperature. This experimental device can provide investigation of samples in temperatures ranging between 600°C and 1000°C. Good homogeneity of the temperature among different samples, however, cannot be guaranteed, though 50°C heterogeneity is targeted.

If better precision in sample temperature monitoring is required, it is possible to propose an equivalent experimental device with forced circulation of He.

5.3. Material irradiation device in the JHR reflector

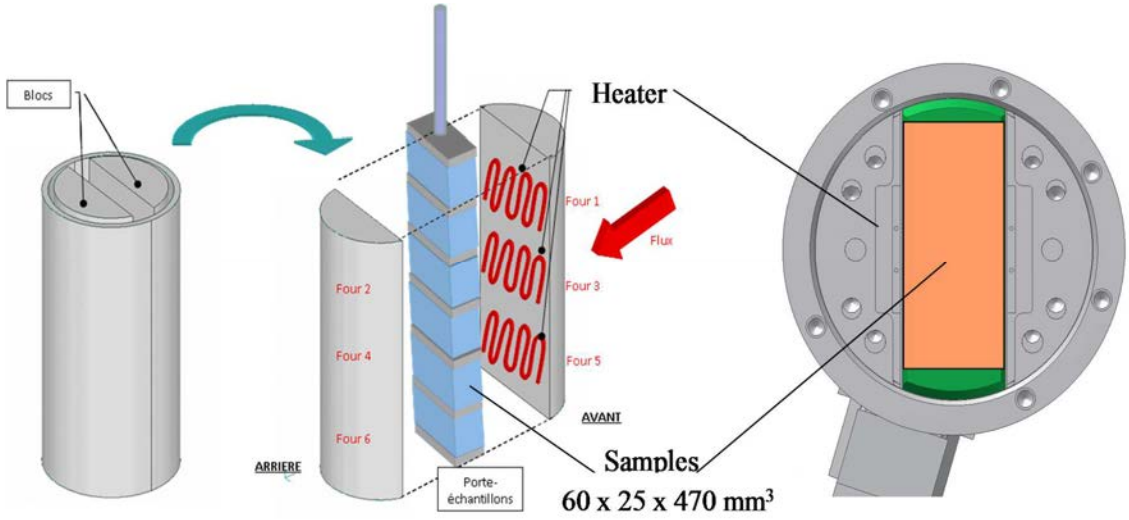

FIG. 11. Schematic view of the LWR reactor vessel steel device.

The material experimental devices presented in the previous sections are installed in the reactor core in order to take advantage of the high fast flux. For some applications like reactor vessel steel qualification, however, it can be relevant to investigate the effect of a low fast neutron flux on materials. One particularity of this device is the ability to install large material samples up to CT 25 (See Figure 11).

6. CONCLUSION: APPLICATION FOR FUSION REACTOR TECHNOLOGY

The design of the JHR aims to provide an experimental capacity for the nuclear industry. The experimental devices presented in this document focus on the experimental needs for fission power reactors, current light water or Generation IV reactors. Of course, the experimental tool can be used for some aspects of fusion reactor technology projects in spite of the large difference in neutron energy. For example, Figure 12 provides a typical neutron flux within a material test device located in the JHR core. Note that the neutron flux corresponding to neutrons of energy >10 MeV is about 4×10^{11} $cm^{-2}s^{-1}$.

But the experimental techniques for material behaviour under irradiation and stress with possible online measurement are probably of interest for materials dedicated to fusion technology.

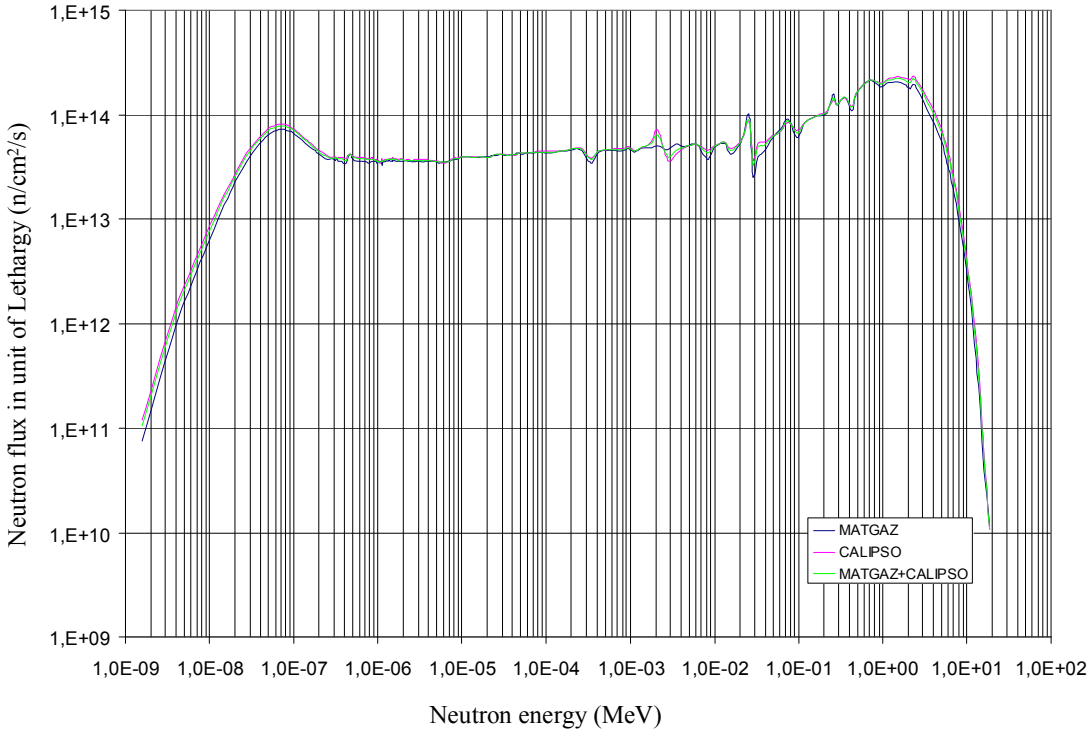

FIG. 12. Neutron flux spectrum in material irradiation devices given in unit of lethargy.

EVALUATION OF MICROSTRUCTURAL STABILITY OF RAFM ODS-EUROFER STEEL

H.R.Z. SANDIM, R.A. RENZETTI, K.D. ZILNYK
Escola de Engenharia de Lorena,
Universidade de São Paulo,
Lorena, Brazil
hsandim@demar.eel.usp.br

A.F. PADILHA
Escola Politécnica,
Universidade de São Paulo,
São Paulo, Brazil

R. LINDAU, A. MÖSLANG
Karlsruher Institut für Technologie (KIT),
Karlsruhe, Germany

Abstract

Oxide dispersion strengthened ferritic–martensitic steels are candidates for applications in future fusion power plants. High creep resistance, good oxidation resistance, reduced neutron activation and microstructural long term stability at temperatures of about 650°C are required in this scenario. Samples of reduced activation ferritic–martensitic 9%Cr ODS–EUROFER steel were cold rolled to 80% reduction in thickness and further annealed in vacuum at 800°C at exposure times varying from 5 min up to 4320 h (6 months). These conditions were chosen to simulate accelerated service conditions with emphasis on the likely softening mechanisms responsible for changing microstructure and properties: recovery, recrystallization and Ostwald ripening of Y-based particles. Nevertheless, these experimental conditions are far from those expected during service life in fusion reactors where a unique combination of high energy, high intensity fast neutron fluxes and high temperatures is present. The preliminary microstructural characterization of annealed samples was performed using scanning electron microscopy and Vickers microhardness testing. Further testing of deformed samples under neutron irradiation is a necessary step to understand how defects created by neutron irradiation interact with already existing dislocations and interfaces in the deformed material.

1. INTRODUCTION

The potential applications of reduced activation ferritic–martensitic (RAFM) steels in future nuclear fusion reactors depend very much on understanding how the microstructure evolves during life service. High creep resistance, good oxidation resistance and long term microstructural stability at temperatures of about 650–700°C are required in this scenario [1–3]. In particular, thermally activated softening mechanisms like recovery, recrystallization, grain growth and particle coarsening play an important role in changing the mechanical properties of structural materials during long term operation. Concurrently, solid state precipitation of equilibrium phases formed after long periods such as the Laves (Fe_2W) or Chi phase may also contribute to either harden or even embrittle these steels depending on the ageing temperature and irradiation conditions [4–7].

In the present paper, we present an overview of current activities of our research group regarding the annealing behavior of ODS–EUROFER steel. This steel contains a fine and stable dispersion of nanosized oxide particles that interact with dislocations and boundaries during straining and further annealing. The interaction of fine particles with mobile dislocations contributes to a higher degree of work hardening compared to other non-ODS candidate materials like EUROFER-97 steel [8, 9]. During annealing these particles are very effective to either retard or even prevent recrystallization. The preliminary results of long term annealing performed in this

steel and the reasons for doing further research on the underlying mechanisms concerning its recrystallization behavior under neutron irradiation are presented and discussed.

2. OVERVIEW OF RESEARCH ACTIVITIES ON RECRYSTALLIZATION OF ODS-EUROFER STEEL

Research activities on the annealing behavior of ODS–EUROFER steel started in 2006 in cooperation with the Karlsruher Institut für Technologie, formerly Forschungszentrum Karlsruhe. Since this steel undergoes martensitic transformation under air cooling after heating above 835°C (A_{c1}, the critical transformation temperature for a heating rate of 1 K/s), we decided to concentrate our efforts on understanding the softening mechanisms present in the ferritic phase field [10]. Static recovery was found to be the main softening mechanism in 9%Cr–ODS–EUROFER steel when annealed in the ferritic phase field. Recrystallization is strongly prevented due to the strong interaction between boundaries and the fine dispersion of stableY_2O_3 particles even after severe cold rolling to 80% reduction and annealing at 800°C for long periods. The few recrystallization nuclei were found predominantly at prior grain boundaries and surrounding coarse $M_{23}C_6$ carbide particles.

Another important finding was that nucleation for recrystallization occurs preferentially in grains belonging to the γ-fiber texture component. The γ–fiber refers to all grains with a common <111> axis parallel to the sheet normal, and grains belonging to the γ-fiber component tend to store many more dislocations during deformation compared to other orientations like rotated cube ({001}<100>), for instance. When nucleation occurs at grain boundaries, the recrystallization front tends to migrate towards the interior of γ-fiber grains due to their higher stored energy.

The annealing behavior in the austenitic phase field was also investigated, and the main results are summarized elsewhere [11]. Since the intended operating conditions of future candidates for structural applications in fusion reactors include temperatures below A_{c1}, our efforts were concentrated in understanding the annealing behavior of ODS–EUROFER steel in the bcc structure (ferritic phase field).

3. EXPERIMENTAL

3.1 Long term annealing

A 6 mm thick plate of ODS–EUROFER steel with nominal composition of 9Cr1W0.08Ta0.2V0.07C0.4Mn0.3Y_2O_3 (wt. %) in the tempered condition (750°C for 2 h) was cold rolled to 80% thickness reduction in multiple passes. Samples were annealed in vacuum at 800°C for times ranging from 5 min to 4320 h (6 months) under isothermal conditions. These conditions were chosen to simulate accelerated service conditions with emphasis on the softening mechanisms responsible for changing microstructure and properties: recovery, recrystallization and likely Ostwald ripening of Y-based particles. Scanning electron microscopy (SEM) was used to depict microstructures using a tungsten filament LEO 1450-VP microscope. Vickers hardness testing was performed using a load of 200 g for 30 s on the longitudinal section of polished samples.

It is worth mentioning that the experimental conditions herein investigated are far from those found in real operating conditions expected for fusion reactors, in which a unique combination of

high energy, high intensity fast neutron fluxes and high temperatures is present. Vickers microhardness testing was performed on the longitudinal section of polished samples to follow the softening behavior. SEM using a tungsten filament LEO 1450-VP microscope was used to display microstructures.

4. PRELIMINARY RESULTS AND DISCUSSION

The preliminary results of ongoing research can be summarized in Figure 1, which shows the softening behavior of ODS–EUROFER steel during long term annealing. In an earlier paper [10] we reported that after a small drop after the first 10 min hardness remained nearly unchanged even after 10 days at 800°C. The present results verify that this observation is valid even after annealing for two months. For longer periods, however, a slight hardening, about 6%, was observed after four months. The reasons for such hardening are still unclear and depend on further detailed microstructural characterization. Nevertheless, it must be noted that hardness values found in the annealed samples lie in between those given by the upper limit, i.e., the cold rolled state (425±5, HV-0.2), and the lower limit given by the material in the as received condition (367±5, HV-0.2). These numbers imply a rather good microstructural stability, at least in terms of hardness. Electron backscatter diffraction (EBSD) and transmission electron microscopy (TEM) are necessary to determine the recrystallized volume fraction and the nature of the precipitates including their size, chemical composition, structure, and volume fraction after long term annealing. These activities are already in progress.

EBSD allows the observation of much larger areas compared with TEM in addition to better statistics [12, 13]. The preparation of samples is much easier, and mapping of large areas is fast depending on the chosen step size. The use of EBSD with small step sizes in the range of 50–100 nm enables the quantification of the recrystallized volume fraction more accurately by using kernel average misorientation maps. For a given data point, the average misorientation between the data point and all of its nearest neighbours is calculated while excluding misorientations greater than a given value. Low misoriented regions indicate a higher degree of recrystallization, whereas highly misoriented regions can be related either to “deformed” or to recovered regions. When Vickers microhardness testing is used to estimate the volume fraction of recrystallized grains, both recovered and recrystallized regions are accounted at every indentation mark.

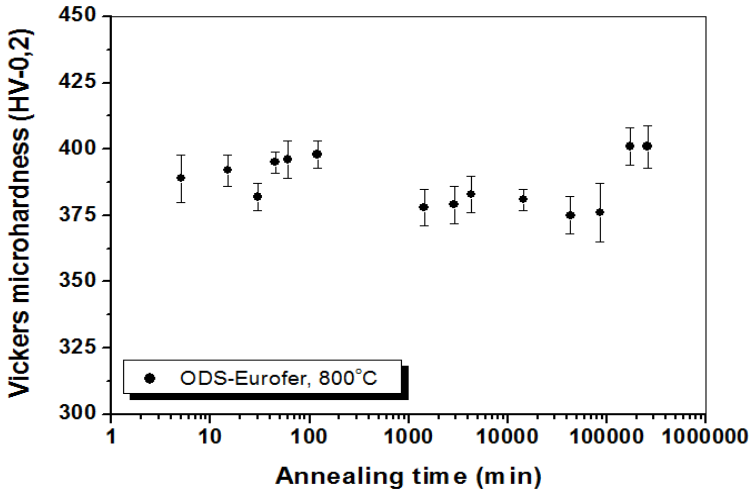

FIG. 1. Softening behavior of ODS-EUROFER annealed at 800°C for long periods.

SEM micrographs of long term annealed samples revealed the presence of coarse and elongated $M_{23}C_6$ carbide particles growing parallel to the rolling direction, as shown in Figure 2. Figure 2a also shows an array of fine recrystallized grains close to a coarse carbide particle (see arrow). These elongated carbides have an aspect ratio of about 5–10. In Figure 2b, the microstructure is still very fine, and only a coarse carbide particle can be noticed in the center of the micrograph. These features suggest that discontinuous recrystallization did not occur with full extent. On the other hand, coarsening of carbide particles due to Ostwald ripening is evident.

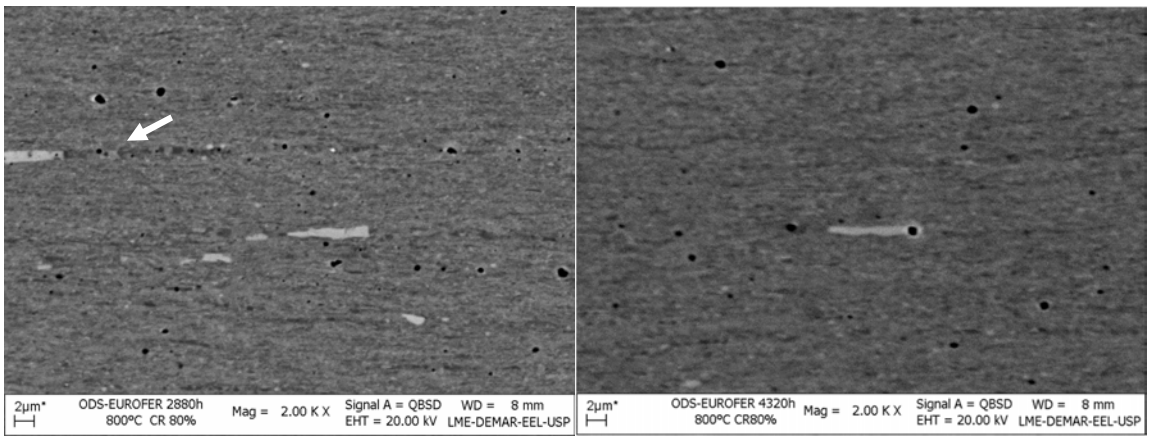

a) b)

FIG. 2. SEM micrographs of ODS-EUROFER steel annealed at 800°C for: a) 4 months (2880 h); b) 6 months (4320 h). Backscattered electron images.

4.1. Recrystallization in irradiated materials

Future collaborative efforts aiming at understanding the recrystallization behavior of ODS Eurofer steel or any other structural material for applications in fusion reactors must be directed towards the investigation of irradiated samples. In-situ neutron irradiation would be the best choice; however, the scarcity of experimental facilities to perform such investigations for long periods cannot be disregarded. Moreover, experimental conditions in terms of both neutron and thermal fluxes resembling those expected during operation of the ITER or DEMO fusion reactors are not available at existing research reactors.

The interaction of neutrons with matter has been reported in many publications [14–17]. Lattice defects are created and may have detrimental effects on the mechanical properties of metals and alloys. Annealing at high temperatures produces either annihilation of these defects or their recombination to more stable defects. There are many studies reporting the mechanical behavior of ferritic–martensitic steels irradiated at moderate to low temperatures [18–21], but none have investigated recrystallization issues.

Recrystallization is a diffusion controlled, solid state reaction driven by the elastic stored energy in particular dislocations in deformed metals that contribute to the softening of the material. Point defects are also created during plastic deformation; however, they are easily annihilated at low annealing temperatures. A high angle boundary with enough mobility is necessary to migrate towards the deformed microstructure. As a result, lattice defects are removed, resulting in a lower energy configuration.

The extent of discontinuous recrystallization in a particle containing material like ODS Eurofer steel results from the balance between driving (P_D, elastic energy provided by dislocations) and retarding pressures given by Zener pinning (P_Z). These quantities can be estimated as follows:

$$P_D \approx \alpha G b \rho^{0.5} \quad (1)$$

$$P_Z \approx (3f\gamma_B)/2r \quad (2)$$

where $\alpha \approx 0.5$, G is the shear modulus, ρ is the dislocation density, f is the particle volume fraction, γ_B is the grain boundary energy and r is the particle radius [9]. In a simplistic analysis, recrystallization occurs when $P_D > P_Z$ during annealing. In ODS–EUROFER steel, in which a fine and stable dispersion of Y_2O_3 particles is present, P_z is very high. Concurrent dislocation recovery is favored in α–Fe matrix because of its high stacking fault energy (SFE) and lower P_D. In consequence, $P_D - P_Z \leq 0$, and the resulting microstructure is partially recrystallized as reported earlier [10].

Recrystallization under neutron irradiation is a much more complex phenomenon. Depending on neutron dose and annealing temperature, important changes in terms of the driving pressure for recystallization may occur. At low temperatures, P_D increases due to excess vacancies produced in the metal. Contrastingly, P_D decreases with time due to vacancy annihilation when annealing is performed at high temperatures. Since recrystallization depends also on the diffusivity, D changes to D* due to excess vacancies during irradiation. Usually, D*>D, a situation in which the recrystallization process could be accelerated.

The presence of helium and its interaction with point defects may cause void swelling at very high neutron doses, increasing P_Z [22]. Last but not least is the possibility of precipitate dissolution or its amorphization, lowering P_Z even at low annealing temperatures [23]. Understanding how these effects interact with each other during annealing depends on intensive experimental research coupled to modelling. Due to the intrinsic complexity, collaborative efforts are necessary to have a clear picture of how recrystallization occurs in bulk samples under neutron irradiation.

5. SUMMARY AND CONCLUSIONS

The preliminary results of the microstructural characterization of long term annealing of unirradiated specimens of 80% cold rolled ODS–EUROFER steel have been presented. Vickers microhardness testing was used to follow the softening behavior of samples annealed in vacuum at 800°C for times ranging from 5 min to 4320 h. A slight hardening of about 6% was observed in samples annealed for 2880 and 4320 h. Discontinuous recrystallization remains strongly prevented by particle pinning. Carbide particle coarsening was also observed. Further detailed EBSD and TEM microstructural characterization are still needed to evaluate the extent of recrystallization and the nature of the precipitates.

A tentative list of the inherent difficulties to fully understand recrystallization or any other phase transformation under neutron irradiation and its potential effects on the mechanical properties of structural materials during its expected lifetime was also provided.

ACKNOWLEDGMENTS

The authors would like to acknowledge the support provided by Brazilian agencies São Paolo Research Foundation grants 07/56.436-0 and 08/54.064-1 and Council of Scientific and Technological Development grant 484.355/2007-4 for the development of this work. Funding provided by IAEA to attend the meeting is also deeply acknowledged.

REFERENCES

[1] LINDAU, R., et al., Present development status of EUROFER and ODS-EUROFER for application in blanket concepts, Fus. Eng. Des. **75–79** (2005) 989.

[2] RENSMAN, J., et al., The European integrated materials and technology programme in fusion, J. Nucl. Mater. **329–333** (2004) 20.

[3] TAVASSOLI, A.A.F., Present limits and improvements of structural materials for fusion reactors — a review, J. Nucl. Mater. **302** (2002) 73.

[4] MURATA, Y. et al., Dependence of *solvus* temperature of the Laves phase on (Mo+W+Re) contents in high Cr ferritic steels**,** ISIJ Int. **45** (2005) 101.

[5] LI, Q., Precipitation of Fe2W laves phase and modeling of its direct influence on the strength of a 12Cr-2W steel, Metall. Trans. 37A (2006) 89.

[6] KLUEH, R.L., NELSON, A.T., Ferritic/martensitic steels for next-generation reactors, J. Nucl. Mater. **371** (2007) 37.

[7] GELLES, D.L., HSU, C.Y., LECHTENBERG, T.A., Effects of irradiation on tungsten stabilized martensitic steels, J. Nucl. Mater. **155-157** (1988) 902.

[8] HÄUSSLER, D., REPPICH, B., BARTSCH, M., MESSERSCHMIDT, U., Interaction processes between dislocations and particles in the ODS nickel-base superalloy INCONEL MA 754 studied by means of in situ straining in an HVEM, Mater. Sci. Eng. A **309–310** (2001) 500.

[9] HUMPHREYS, F.J., HATHERLY, M., Recrystallization and Related Annealing Phenomena, Elsevier, New York (2004).

[10] SANDIM, H.R.Z., et al., Annealing behavior of ferritic–martensitic 9%Cr–ODS–Eurofer steel, Mater. Sci. Eng. A **527** (2010) 3602.

[11] RENZETTI, R.A., et al., Annealing effects on microstructure and coercive field of ferritic–martensitic ODS Eurofer steel, Mater. Sci. Eng. A **528** (2011) 1442.

[12] HUMPHREYS, F.J., Characterisation of fine-scale microstructures by electron backscatter diffraction (EBSD), Scripta Mater. **51** (2004) 771.

[13] DAVUT, K., ZAEFFERER, S., Statistical reliability of phase fraction determination based on electron backscatter diffraction (EBSD) investigations on the example of an Al-TRIP steel, Metall. Trans. **41A** (2010) 2187.

[14] DUNNING, J.R., PEGRAM, J.B., FINK, G.A., MITCHELL, D.P., Interaction of neutrons with matter, Phys. Rev. **48** (1935) 265.

[15] BLEWITT, T.H., COLTMAN, R.R., The effect of neutron irradiation on metallic diffusion, Phys. Rev. **85** (1952) 384.

[16] BRINKMAN, J., On the nature of irradiation damage in metals, J. Appl. Phys. **25** (1954) 96l.

[17] SCHILLING, W., Radiation induced damage in metals, J. Nucl. Mater. **72** (1978) l.

[18] KITAJIMA, K., ABE, H., AONO, Y., KURAMOTO, E., Effects of low temperature neutron irradiation on mechanical properties of bcc metals, J. Nucl. Mater. **108-109** (1982) 436.
[19] KLUEH, R.L., KAI, J.J., ALEXANDER, D.J., Microstructure-mechanical properties correlation of irradiated conventional and reduced-activation martensitic steels, J. Nucl. Mater. **225** (1995) l75-186
[20] KATOH, Y., ANDO, M., KOHYAMA, A., Radiation and helium effects on microstructures, nano-indentation properties and deformation behavior in ferrous alloys, J. Nucl. Mater. **323** (2003) 251.
[21] KLUEH, R.L., SHIBA, K., SOKOLOV, M.A., Embrittlement of irradiated ferritic/martensitic steels in the absence of irradiation hardening, J. Nucl. Mater. **377** (2008) 427.
[22] MANSUR, L.K., COGHLAN, W.A., Mechanisms of helium interaction with radiation effects in metals and alloys: a review, J. Nucl. Mater. **119** (1983) l-25
[23] MARTIN, J.W., DOHERTY, R.D., CANTOR, B., Stability of Microstructure in Metallic Systems, Cambridge University Press, Cambridge (1997).

RADIATION EFFECTS IN FUNCTIONAL MATERIALS FOR NUCLEAR FUSION APPLICATION

TATSUO SHIKAMA, HIROKAZU KATSUI, SHINJI NAGATA, AKIRA HASEGAWA
Tohoku University,
Sendai, Japan
shikama@imr.tohoku.ac.jp

ARATA NISHIMURA, TAKEO MUROGA
National Institute for Fusion Science,
Toki, Japan

HIROSHI KAWAMURA
Japan Atomic Energy Agency,
Oarai, Japan

BUN TSUCHIYA
Meijo University,
Nagoya, Japan

YUTAI KATOH
Oak Ridge National Laboratory,
Oak Ridge, Tennessee,
United States of America

Abstract

Radiation effects can be grouped into three major events: atomic displacement, electronic excitation and nuclear transmutation. In the meantime, radiation effects have two aspects, accumulation and dynamic effects. The diagnostic components developing group of the ITER Engineering Design Activities clearly declared that the only in-situ type radiation effects studies, preferably with a fission reactor, will be relevant to nuclear fusion development. As a background, the evolution of radiation effects as functions of time and environmental parameters such as temperatures, chemical potentials, and electrical and magnetic fields could be categorized into several domains: linear radiation effects dominating, environment effects dominating, synergistic effects modifying, multi-scale modelling effective and finally non-linear effects dominating. Among major irradiation tools such as spallation and fusion neutron sources charged particle accelerators, gamma ray facilities and fission reactors, as well as computer based simulations, only fission reactor irradiation can give an overall perspective of radiation effects in nuclear fusion materials with abundant and uniform irradiation volumes. In the meantime, fission reactor irradiation is handicapped by relatively low neutron fluence except for some very high neutron flux reactors, which will be needed for evaluation of structural materials. For the study of functional materials, some handicaps of fission reactor irradiation can be neglected such as primary knock-on cascade profiles, and the demanded neutron fluence is within the attainable range. The paper will describe some examples of irradiation tests of nuclear fusion functional materials in fission reactors, the electrical conductivity of ceramic insulators and hydrogen isotope mobility in solid breeders. Also, a recent attempt to evaluate nuclear fusion relevant irradiation effects in superconductive magnets will be briefly reported, noting that a cryogenic irradiation and post irradiation examinations in a high magnetic field is crucial.

1. INTRODUCTION

It is unanimous that nuclear fission reactors are the only irradiation tool relevant to actual nuclear fusion irradiation environments until some advanced nuclear fusion irradiation facilities such as International Fusion Materials Irradiation Facility (IFMIF) are realized. In particular for nuclear fusion functional materials, fission reactor irradiation is indispensable, as ion irradiation, being more convenient, far less expensive and much more reproducible due to high controllability of irradiation conditions, could often substitute for fission reactor irradiation but would sometimes cause peculiar and exotic irradiation effects that could jeopardize results.

In the meantime, it is mandatory for realizing effective fission reactor utilization to have intense cooperation among reactor specialists who maintain and operate fission reactors. In principle, interests and concerns of reactor specialists and reactor users will not concur, because their major working principles are different. Coordination between reactor specialists and users could be done while both belong to the same institution; however, the reactor users will emerge from nuclear fusion institutions as nuclear fusion developments proceed. Herein, the importance of a bridging mechanism between them is highlighted. The relationship between reactor specialists and users is schematically depicted in Figure 1. This paper describes the role of the Oarai Branch of the Institute for Materials Research (IMR) of Tohoku University in coordinating reactor users with specialists for effective utilization of research reactors for nuclear fusion developments. Some recent research activities will be presented as examples of effective cooperation under recent new cooperative frameworks. One is bilateral international collaboration, and the other id bidirectional collaboration led by the National Institute for Fusion Science (NIFS) of Japan.

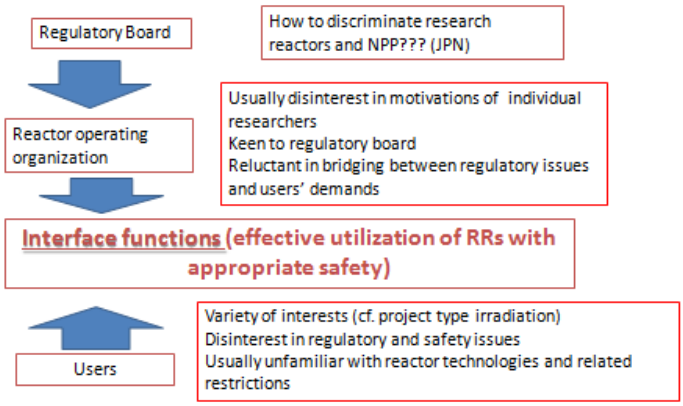

FIG. 1 The relationship between reactor specialists and reactor users.

2. COORDINATING ROLE OF THE OARAI BRANCH

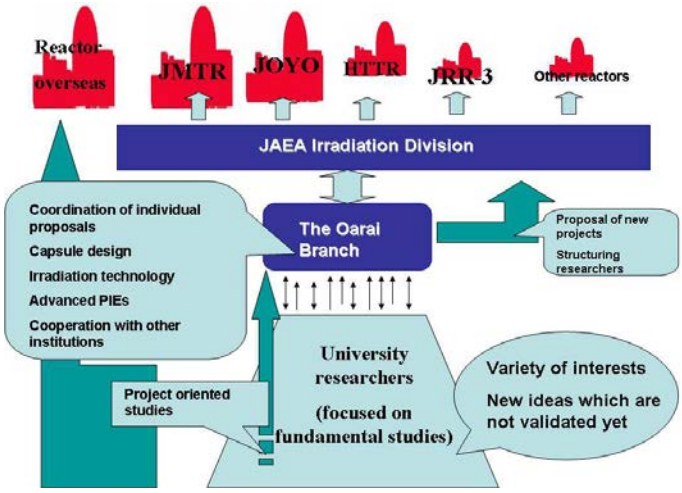

FIG. 2. Role of the Oarai Branch in utilization of research reactors.

The Oarai Branch of the Tohoku University IMR was established in 1971 to connect university researchers and the Japan Materials Testing Reactor (JMTR) of the Japan Atomic Energy

Research Institute, now Japan Atomic Energy Agency (JAEA), with annual financial support from the Ministry of Education; now the Ministry of Education, Culture, Sports, Science and Technology (MEXT). Initially, the major role was to support individual university small laboratories without many financial resources in their utilization of JMTR. Their interests were in general divergent among a variety of research fields. In the 1980s, the Ministry of Education endorsed a large scale grant-in-aid for development of nuclear fusion materials by utilizing fission reactors, and the Oarai Branch was recognized as the major post-irradiation facility for reactor irradiation. Also, development and steady deployment of nuclear power plants based on the light water reactors proceeded under the control of the Ministry of International Trade and Industry, now the Ministry of Economy, Trade and Industry (METI). These streams tended to organize individual and small university laboratories into purpose oriented research groups. Following this trend, the Oarai Branch tried to shift its role to a more project oriented style. Figure 2 shows the present schema of the role of the Oarai Branch. However, the Fukushima disaster in 2011 causes us to reconsider an important role of individual and fundamental researches spread among a variety of research fields, though there is a serious difficulty in obtaining financial support from the government and industries. The role of research in universities in nuclear engineering fields must be seriously re-evaluated, especially in Japan.

In the meantime since the early 1980s, the Oarai Branch has participated in the US Department of Energy and Japanese Ministry of Education Scientific Collaborative Program on Nuclear Fusion Science to utilize the US irradiation facilities Rotating Target Neutron Source (RTNS-II) of Sandia National Laboratories, Fast Flux Test Facility/Materials Open Test Assembly of Pacific Northwest National Laboratory and High Flux Isotope Reactor (HFIR) of Oak Ridge National Laboratory, among others. The role of the Oarai Branch there is depicted in Figure 3. The initial baseline of the collaboration was to give Japanese university researchers an opportunity to utilize nuclear facilities in the US; however, the Oarai Branch has increased its role as a post-irradiation examination facility in Japan for not only Japanese researchers but also US researchers. In 2010, another new cooperative research framework was proposed by the NIFS, namely the bidirectional collaboration program, to the Oarai Branch. Under this plan, whose scheme is schematically shown in Figure 4, the Oarai Branch is expected to have close collaboration with other major nuclear fusion research centres in Japanese universities.

3. IRRADIATION EFFECTS IN NUCLEAR FUSION FUNCTIONAL MATERIALS

Development of reliable materials and correct evaluation of materials performance including their life limit is essential for development of any nuclear power systems. Irradiation effects will affect the performance of materials substantially, and extensive studies have been accumulated in this research field for more than 60 years. Phenomena of irradiation effects could be categorized into several areas depending on irradiation parameters. Figure 5 shows one example of this categorization as a function of the irradiation dose or rate and environmental parameters such as temperature, chemical potential and magnetic field. Up to now, the major efforts of researches have been dedicated to the development of structural materials for any nuclear power system. However, any serious troubles in nuclear power systems stem from malfunctions of minor components composed of structural and functional materials. Also, the recent severe accident re-highlights the importance of diagnostic components in any nuclear system, not only in a normal steady state condition but also much more in transient and troubled conditions.

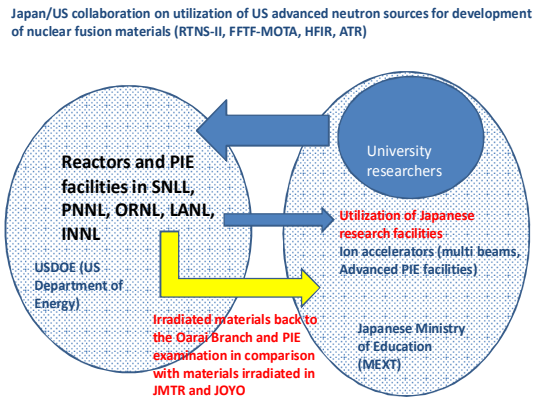

FIG. 3. Japan/US collaboration utilizing US facilities for development of nuclear fusion materials.

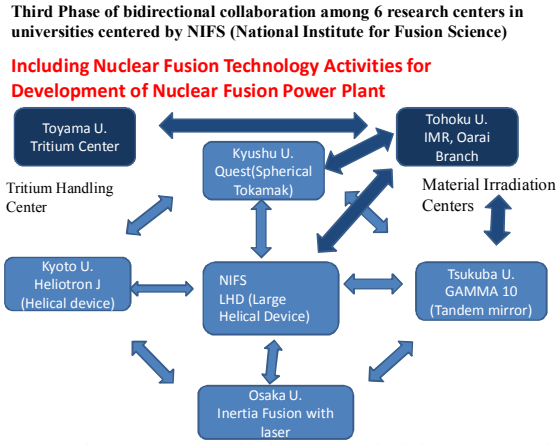

FIG. 4. Bidirectional collaboration led by NIFS. The Oarai Branch plays a role as irradiation response facility for nuclear fusion materials developments.

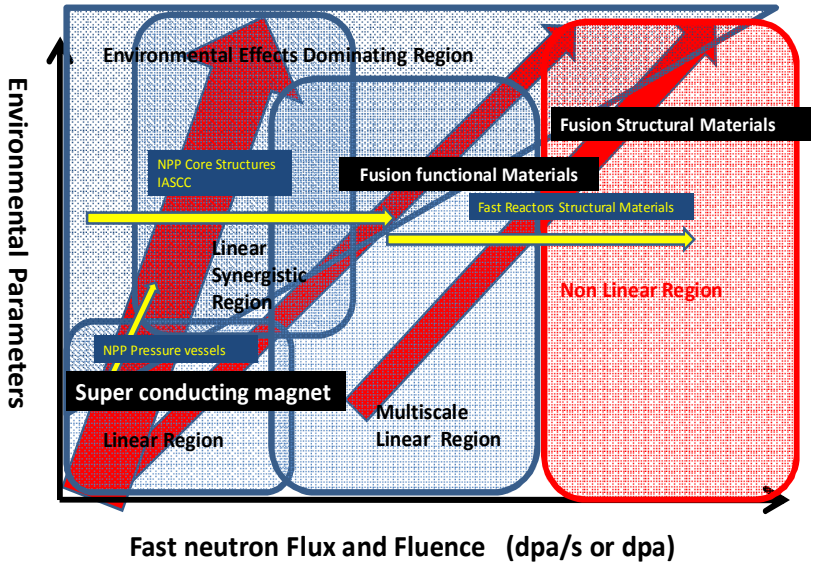

FIG. 5. Categorization of irradiation effects as a function of irradiation dose or rate and environmental parameters.

In fission systems, diagnostic or dosimetric systems were not given appropriate concern because fission systems are, in principle, an exponential system and can adapt a scale law. In contrast, fusion systems demand a sophisticated diagnostic system, as they need active control of plasma, which behaves in a complicated manner. It has been widely recognized that irradiation effects upon functional materials is one among many key issues for the successful completion of ITER, but the present financial situation is hampering an appropriate allocation of efforts toward such studies. For studies of irradiation effects in functional materials, fission reactor irradiation, especially in situ type irradiation experiments, is very important. The irradiation effects in functional materials are schematically summarized in Figure 6. From a fission reactor utilization point of view, the following could be summarized:

- High flux reactors, e.g., JHR, HFIR, BOR-60, JOYO, MBIR, MYRRHA:
  - Good for high flux and high fluence irradiation for development of structural materials;
  - Difficulties in desirable instrumentation;
  - Limited ability for in-situ type experiments and controlled environment experiments;
- Medium flux reactors, e.g., JMTR and BR-2:
  - Handicapped with attainable dpa;
  - Good for detailed instrumentation;
  - Feasible access for in-situ type experiments and controlled environment experiments.

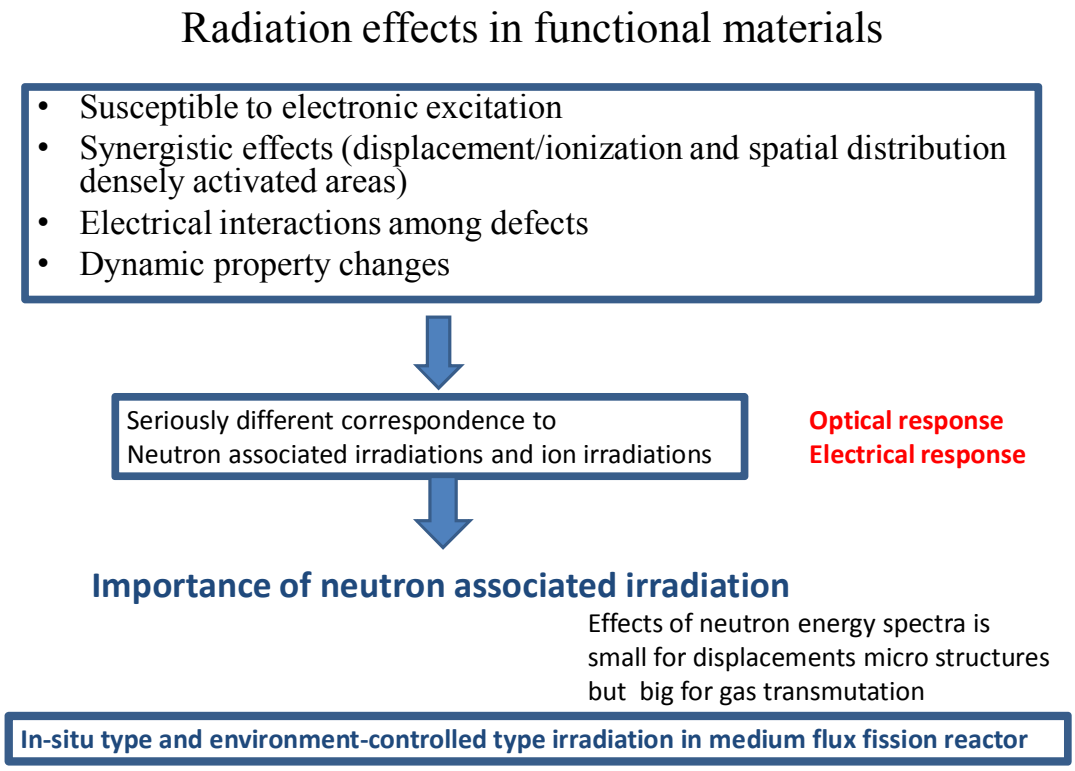

FIG. 6. Irradiation effects in functional materials for nuclear fusion application.

4. RECENT RESEARCH ACTIVITIES

In addition to the baseline coordinated works shown in Figure 2, the Oarai Branch has conducted the following research activities recently:

- Neutron irradiation effects on plasma materials interaction:
  - Japan/USA collaboration, bidirectional collaboration among NIFS and Tohoku, Toyama and Tsukuba Universities;
- Irradiation effects in ceramic breeders and silicon carbide materials, including tritium behaviour studies:
  - Japan/USA collaboration, bidirectional collaboration among NIFS and Tohoku and Toyama Universities;

- In-situ irradiation for studying dynamic irradiation effects in diagnostic and functional materials:
  - — Bidirectional collaboration between Tohoku University and NIFS with potential contribution from Osaka University;
  - — Possible expansion to international collaborations like SCK/CEN, CIEMAT and ITER;
- Irradiation effects in superconductive magnet materials:
  - — Bidirectional collaboration between Tohoku University and NIFS;
  - — Cooperation from industries, universities and other national institutions;
- Cryogenic irradiation in JMTR:
  - — Collaboration among JAEA, NIFS, Tohoku other universities.

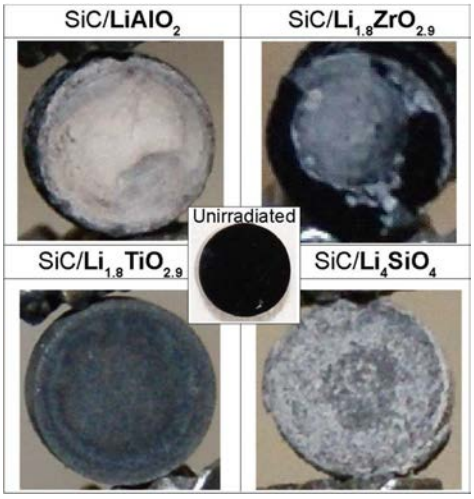

FIG. 7. Compatibility test of lithium containing oxide and silicon carbide in HFIR at 800–900°C.

Figure 7 shows the results of compatibility testing of lithium containing oxide, a solid breeder, with silicon carbide irradiated in HFIR at 800–900°C up to several dpa [1]. The results showed good compatibility between $LiAlO_2$ and Li_2ZrO_2 and chemical instability of Li_4SiO_4, which formed Li_3SiO_3 following the evaporation loss of Li through chemical reaction with SiC. Lithium containing oxides produce tritium in the course of reactor irradiation. In the case of the HFIR irradiation up to several dpa, the ^6Li was almost exhausted in the formation of tritium through the (n,α) nuclear reaction. The profile of tritium injected into SiC is shown in Figure 8. The injected tritium stayed very near to its projected range and did not diffuse deeply. This result is a good standing point to analyze accumulated ion irradiation results and a controversial but important result reported in the Japan/US collaboration [2].

For the study of irradiation effects in superconductive materials, a high magnetic field test facility must be installed in a hot laboratory. The Oarai Branch has just installed a 15.5 T helium free superconductive magnet and 500 A test insert in its hot laboratory. Figure 9 shows the installed facility. With this facility, superconductive Nb_3Sn irradiated in JRR-3, with a fluence of 10^{22} m^{-2}, was examined. As a general tendency, the critical magnetic field decreased by irradiation at temperatures as low as 9 K, but the data imply that the critical magnetic field may increase below 9 K when compared with an unirradiated one. The estimated critical magnetic field of the irradiated sample was 27.1 T, as compared with 25.4 T of the non-irradiated one [3, 4].

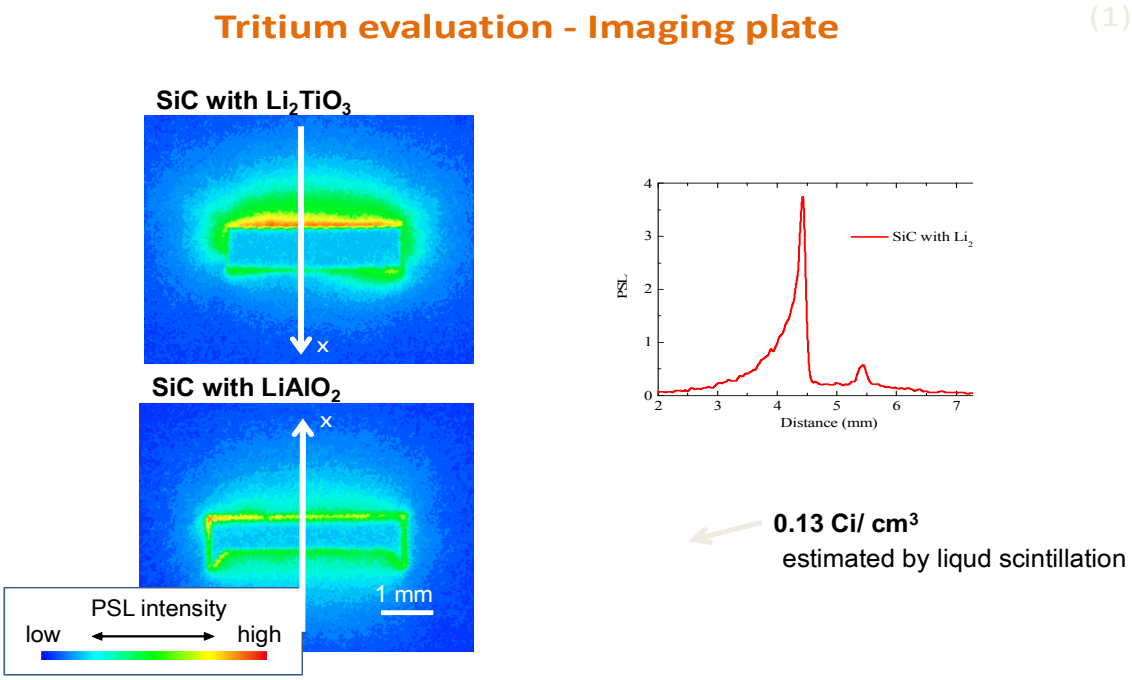

FIG. 8. Tritium profile through (n,α) reactions in silicon carbide (SiC) injected with lithium containing oxides in the course of HFIR irradiation at 800°C [1].

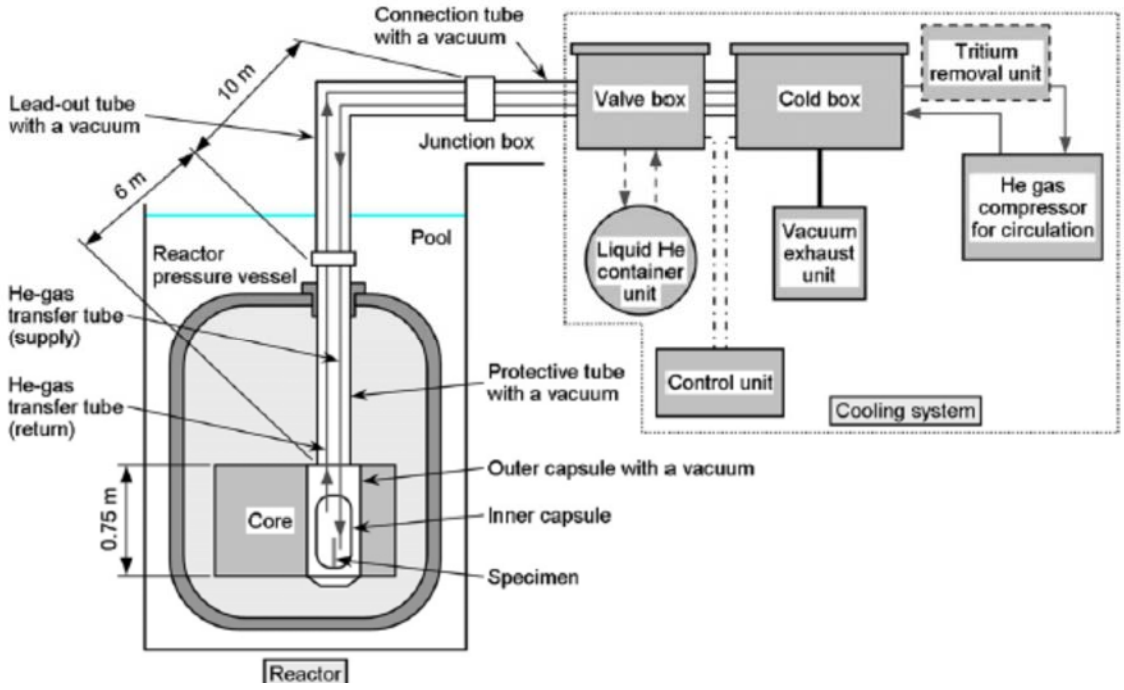

FIG. 9. Cryogenic irradiation system in JMTR without using liquid heliums proposed by JAEA Oarai [5].

For further study of irradiation effects in superconductive materials, a cryogenic irradiation facility is needed. JAEA is proposing the cryogenic facility beyond the gamma shielding wall of JMTR as shown in Figure 9 [5]. The proposed facility will enable irradiation at 20 K with a neutron flux in the range of 10^{15} $m^{-2}s^{-1}$. The system will have an ability of exhausting 12 W of

heat, and the system can be also used for vacuum or reductive environment irradiations of functional ceramics, which will be essential for validating application of ceramics in nuclear fusion systems [6].

5. CONCLUSIONS

The importance of the mechanism bridging between the reactor sections and users for effective utilization of research reactors has been described. The Oarai Branch of Tohoku University IMR of Japan has been functioning as a coordinator of research reactor users in Japanese university sections since 1971 under a financial support from the Japanese Government. In the course of its bridging, the Oarai Branch has expanded its role through new collaborative frameworks:

- Government based Japan/US collaboration on studies of nuclear fusion reactor materials since the early 1980s;
- IMR based bilateral international collaborations with SCK/CEN for utilization of the research reactor BR-2 and collaborative research in nuclear materials, and with the ORNL, USA, for utilization of HFIR and collaborative research on nuclear fusion materials;
- Bidirectional collaboration led by NIFS of Japan. Collaboration among multiple nuclear fusion research centres in Japanese universities, such as plasma research centres in Tsukuba University and Kyushu University and a tritium research centre in Toyama University, are now underway.

Based on these new collaborative frameworks, new research instruments were installed in the Oarai Branch such as a thermal desorption analyzer for studying H, D, T and He desorption behaviours in reactor irradiation materials and a liquid helium free 15.5 T superconductive magnet for study of radiation effects in superconductive materials for nuclear fusion application. In conjunction with these activities, a new irradiation facility for cryogenic irradiation is proposed in JMTR by JAEA Oarai in collaboration with the Oarai Branch.

REFERENCES

[1] KATSUI, H., HASEGAWA, A., NAGATA, S., SHIKAMA, T., presented at the 14th International Conference in Fusion Reactor Materials (ICFRM-14), Sapporo, 2009.

[2] HATANO, T., presented at the 14th International Conference in Fusion Reactor Materials (ICFRM-14), Sapporo, 2009.

[3] SHIKAMA, T., NISHIMURA, A., presented at the 26th Symposium on Fusion Technology, Porto, 2010.

[4] NISHIMURA, A., et al., presented at the 14th International Conference in Fusion Reactor Materials (ICFRM-14), Sapporo, 2009.

[5] INABA, Y., TSUCHIYA, K., SHIKAMA, T., NISHIMURA, A., KAWAMURA, H., Feasibility Study on Cryogenic Irradiation Facility in JMTR, Fusion Eng. Design **86** (2011) 134–140.

[6] HODGSON, E.R., SHIKAMA, T., NISHITANI, T., presented in IEA Workshop on Radiation Effects in Nuclear Fusion Insulating Materials, Porto, 2010.

NON-DESTRUCTIVE EVALUATION OF PERSPECTIVE STEELS FOR FUSION TECHNOLOGIES

V. SLUGEŇ, J. VETERNÍKOVÁ, M. PETRISKA, S. SOJAK, R. HINCA, P. BALLO, J. DEGMOVÁ, M. STACHO
Institute of Nuclear and Physical Engineering,
Slovak University of Technology,
Bratislava, Slovakia
Vladimir.Slugen@stuba.sk

S. KILPELÄINEN, F. TUOMISTO
Department of Applied Physics,
Aalto University School of Science and Technology,
Aalto, Finland

J. RÄISÄNEN
Department of Physics,
University of Helsinki
Helsinki, Finland

V. KRŠJAK
Institute for Energy,
Joint Research Centre of the European Commission,
Petten, Netherlands

Abstract

This paper focuses on microstructure study of 9% chromium steels (T91, P91) and observation of microstructure changes with open volume defect accumulation or residual stress growth after radiation damage, which was simulated by helium ion implantation. Investigated materials were observed by non-destructive experimental techniques based on positron annihilation in the matter, positron annihilation spectroscopy and Doppler broadening spectroscopy, and magnetic properties of iron alloys, magnetic Barkhausen noise measurement. Results indicated higher radiation resistance of T91 than P91, although T91 shows higher residual stress in its microstructure before irradiation.

1. INTRODUCTION

In comparison to recent commercial reactors, thermonuclear fusion facilities will be operated at higher neutron and gamma fluence [1]. Thus, their materials must withstand more exacting conditions without exhibition of cracking or fracture.

In the world, research and development of high chromium steels is still ongoing for applications in advanced nuclear facilities. Steels with 9% chromium in content usually achieve advanced requirements for mechanical and thermal properties [2].

In our research, the radiation resistance of two similar 9%Cr steels, T91 and P91 [3], were investigated with the use of three different experimental techniques. An emphasis was put on microstructure features such as open volume defect concentration and level of residual stress. These parameters have significant influence on mechanical properties like material embrittlement and fatigue, which had already been described in a state before irradiation, even after radiation treatment [4].

In this paper, residual stress of non-implanted steels was studied by magnetic Barkhausen noise measurement (MBN). After helium implantation simulated radiation damage, changes of defect

size and concentration were observed by two different positron annihilation techniques, positron annihilation lifetime spectroscopy (PALS) and Doppler broadening spectroscopy (DBS).

2. EXPERIMENT

2.1. Investigated materials

In this paper, two advanced commercial high chromium steels developed by Oak Ridge National Laboratory in the US were investigated in detail:

- T91 is a low carbon 9Cr1MoVNb steel alloyed with a small amount of tungsten that was developed initially for thin walled components;
- P91 is a 9Cr1MoVNb steel with a negligible addition of aluminium and higher content of silicon than for T91 that was designated especially for thick walled components.

The chemical composition of these steels is listed in Table 1.

TABLE 1. CHEMICAL COMPOSITION OF HIGH CHROMIUM STEELS T91 AND P91 IN %WT. [5, 6]

	T91	P91
C	0.1	0.1
Mn	0.5	0.5
Si	0.15	0.45
Ni	0.09	0.05
Cr	8.32	9.12
Mo	0.86	0.96
Al	-	0.004
W	0.01	-
Nb	0.06	0.06
V	0.2	0.2
N	0.055	0.04

The microstructure of both steels was formed by similar thermal treatment. It was firstly annealed at about 1050°C for three hours in order to support the formation of an austenitic structure. After austenitizing, the steels were quenched, and the structure was changed to a ferritic–martensitic one.

Subsequently, steel ingots were treated by hot rolling into a plane shape and partly tempered in order to minimize internal stress and remove an amount of defects that had accumulated during quenching and hot rolling. Further cooling was done in air at room temperature.

Finally, the samples were prepared by cutting steel sheets into suitable pieces. After cutting, the sample surfaces were polished for the purpose of removing surface impurities.

2.2. Experimental techniques

The samples of T91 and P91 were investigated by the three following experimental techniques:

- MBN measurement at the Joint Research Centre of the European Commission, Petten, Netherlands [7];
- PALS at the Department of Nuclear Physics and Technology, Slovak University of Technology, Slovakia [8]; and
- DBS with a slow positron beam at the Department of Applied Physics, Aalto University, Finland [9].

The experimental technique MBN is based on an electromagnetic field passing through a ferromagnetic material. During the measurement, the structure composed of disordered domains starts to reorganize according to the external field. This phenomenon requires domain movement, which is made by discontinuous jumps that are recorded as an MBN signal [10]. The typical resultant MBN signal is given as a time function of the MBN voltage (See Figure 1A).

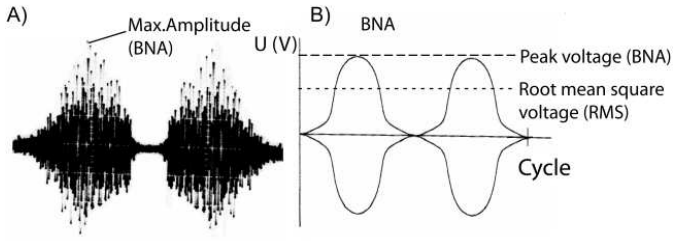

FIG. 1. Barkhausen noise signal (A) and the signal envelope (B).

Results acquired by this experimental technique can be given as determined by either:

- In absolute values, root mean square (RMS) (See Equation 1) and Barkhausen noise amplitude (BNA):

$$RMS = \sqrt{\frac{1}{n}\sum_{i=0}^{n-1} x_i^{\,2}} \tag{1}$$

  Where x_i is individual signal calculated from a complete cycle of Barkhausen emission; or
- By the shape of the signal envelope, as shown in Figure 1B.

RMS is calculated by measuring and evaluating software, in our case, commercial system Stresstech AST µScan 500, that analyzes the integral of the spectra. BNA characterizes the maximum value of the voltage in the MBN signal.

RMS and BNA correspond with the signal envelope. The envelope is plotted as a function of the applied magnetic field, or current.

RMS, BNA and the envelope decrease with defect concentration, residual stress and hardness growth [10]. The envelope has usually one peak, but in special cases it can contain two peaks, e.g., dual ferritic–martensitic structures with higher carbon content [10]. In our case, we were

studying tempered ferritic–martensitic steels; therefore observation of two distinctive peaks was not expected.

In this paper, MBN measurement was performed for applied magnetizing frequencies up to 50 Hz and a magnetizing peak-to-peak voltage of 10 V_{pp}. The sampling frequency was set up to 2–2.5 kHz. The signal of the pick-up coil was filtered from 5–500 kHz and amplified with a gain of 10.

The second used technique, PALS [11], can determine the concentration and size of vacancy type defects in samples. When positron lifetime grows, defect concentration or defect size also increases.

As a positron source, we used β^+ radioactive ^{22}Na with an activity of around 100 μCi (3.7 MBq). ^{22}Na emits positrons and gamma particles with a probability of 90.4 %.

The measuring equipment used in this work consisted of 2 BaF_2 scintillation detectors and 2 discriminators (See Figure 2). The first discriminator, START, was set to ~1.2 MeV, which is the energy of the characteristic gamma ray emitted along with a positron during the beta decay of ^{22}Na. The second discriminator, STOP, records the 511 keV annihilation gamma radiation. The time difference between these two signals, START and STOP, was converted to a voltage pulse in a time to amplitude converter, TAC, and stored in a multi-channel analyser.

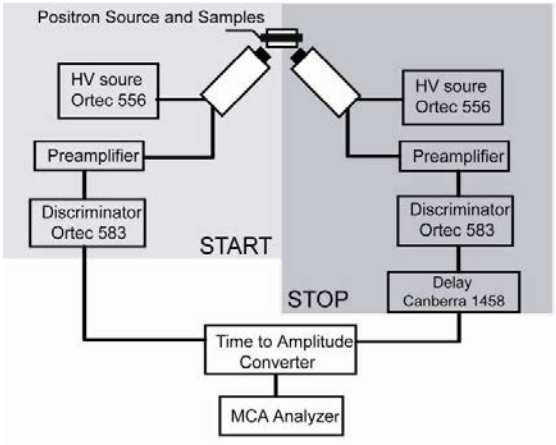

FIG. 2. PALS equipment.

The resulting spectrum evaluated by the programme LifeTime9 [12] can usually be fitted with one or more Gaussian functions describing the positron lifetimes in width and intensity, or height. In the case of a perfect lattice, the spectrum is characterized by only one positron lifetime, and this value corresponds to the defect free structure, or so called bulk. The bulk value for metals is usually around 110 ps. A higher value of positron lifetime indicates defect presence or positronium formation. PALS is also sensitive to changes in defect concentration and the size of the sample before and after implantation.

The last used technique, DBS [11], associated with a slow positron beam (See Figure 3), can observe the defect depth profile in surface and subsurface layers of samples.

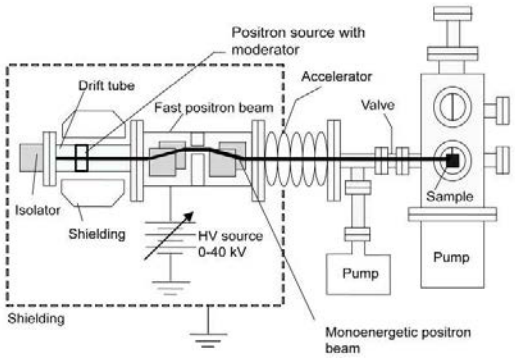

FIG. 3. Scheme of slow positron beam.

The same isotope as for PALS, ^{22}Na, was used as a positron source for a slow positron beam with an activity around 20 mCi (740 MBq). Positrons emitted by the source were moderated using a tungsten foil and separated by a fast positron filter. Subsequently, the monoenergetic beam was accelerated, and positrons were injected to the sample.

Positron trapping in samples can be described by following exponential function [13]:

$$P(x,E) = \frac{mx^{-1}}{x_0^m} \exp\left[-\left(\frac{x}{x_0}\right)\right] \tag{2}$$

in which x is the mean positron stopping depth, x_o maximal positron stopping depth and m an environmental parameter.

The implantation energy range of the used positron beam was from 0.5–36 keV; therefore the maximal investigated depth, calculated according Equation 3 [13], slightly exceeds 1.5 μm.

$$x = \frac{4 \cdot 10^{-2}}{\rho} \cdot E^n \qquad [\mu m] \tag{3}$$

in which n=1.6, ρ is material density in g/cm^3 and E is kinetic energy of the positron beam in keV.

DBS uses semiconductor detectors to measure a conventional spectrum of the annihilation energy, nominally around 511 keV, and its shift obtained by a change in the momentum space of the electron distribution annihilated with the positron [14].

Experimental data were evaluated with application of the S parameter (See Figure 4), which is calculated by using Equation 4 [15]:

$$S = \frac{\int_{511keV-\Delta E_\gamma}^{511keV+\Delta E_\gamma} I.dE}{\int_0^{E_\gamma} I.dE} \tag{4}$$

in which I is the intensity of the detected signal and E is the energy in keV of a measuring channel in the multi-channel analyser.

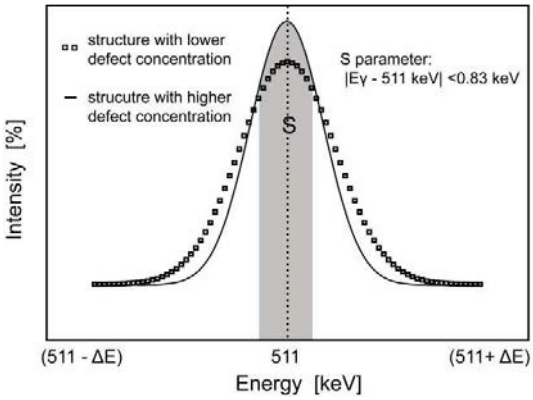

FIG. 4. A positron Doppler broadening spectrum and the difference in the S parameter on the defect concentration in a sample.

2.3. Experimental treatment

Samples of T91 and P91 with dimensions of about 15 mm×10 mm×0.8 mm were observed in the basic non-implanted state and consequently irradiated for the purpose of radiation resistance study of these steels. The radiation damage of the samples was experimentally simulated by helium ion implantation performed at the Kilo Electron Volt Ion Implantation Accelerator at the University of Helsinki, Finland.

The energy used for helium implantation was at most 500 keV and the implantation level 0.3 C/cm^2 for ~20 dpa and a neutron fluence of 1.87×10^{18} per cm^2 per ion. The depth profile of the collision events is demonstrated in Figure 5 as a result of application of simulation software SRIM [16].

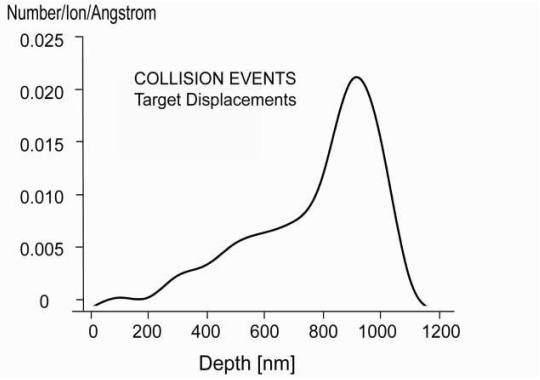

FIG. 5. The depth profile of the helium implantation of 9CrMoVNb simulated by SRIM.

3. RESULTS AND DISCUSSION

MBN measurement is presented by the MBN signal envelopes as well as BNA and RMS values, according to which the residual stress for both materials can be compared. By reason of a statistic improvement, four samples of both materials were investigated.

When the peak of the envelope grows, the defect concentration in the structure or the residual stress decreases. Figure 6 shows resultant envelopes for non-implanted materials P91 and T91.

The results indicate that the signal envelope is higher for samples of steel P91, which demonstrates lower defect concentration in this non-implanted steel in comparison with steel T91.

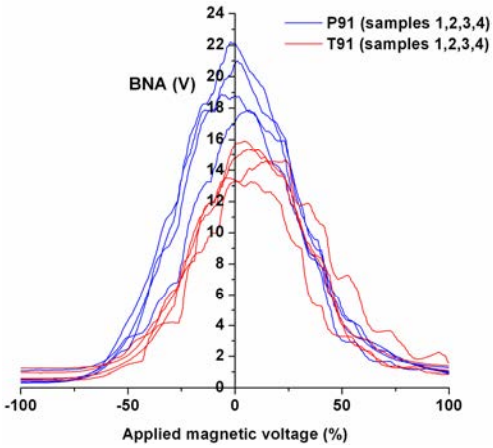

FIG. 6. The MBN signal envelope.

Results introduced by absolute values RMS and BNA, as shown in Figures 7 and 8, confirm our estimation based on the signal envelopes. The RMS value is proportional to the envelope; therefore the samples of T91 have lower values, with an average RMS of ~12.5 V, than P91, ~15.2 V.

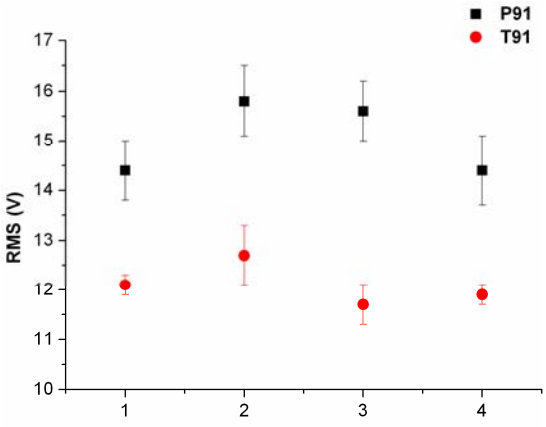

FIG. 7. RMS for four samples of T91 and P91.

The value of the BNA characterizing the maximum value of the peak is also in accordance with the envelope or RMS; i.e. for T91 the average value is 16 V and for P91 ~20 V (See Figure 8).

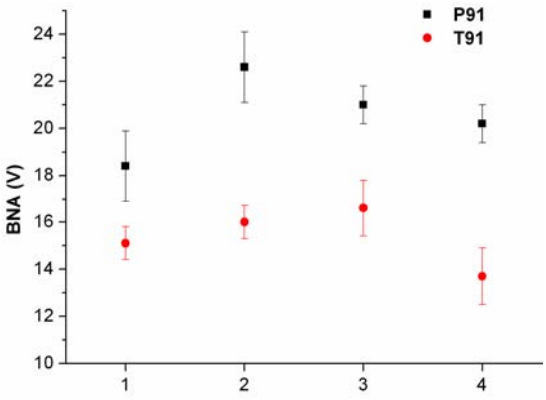

FIG. 8. BNA for four samples of T91 and P91.

Deviation of RMS and BNA up to 20% for the same kind of material is due to the limited dimensions of the samples, which causes a weaker response in BNS. Another reason is inhomogeneity of steels and the effects of sample cutting and selection for measurement.

Results from MBN measurements proved higher residual stress in T91 steels than in P91, which should be proportional to defect presence.

The spectra measured by PALS were comprised of two positron lifetimes for the implanted samples as well as for the non-implanted samples. According to the standard trapping model, the short lifetime, (LT1 of ~100 ps, describes mostly a defect free structure together with some impurities and very small defects. A longer lifetime, LT2 between 140 and 180 ps, represents defects, in our case mono-vacancies together with likely high edge dislocations, as in Figure 9.

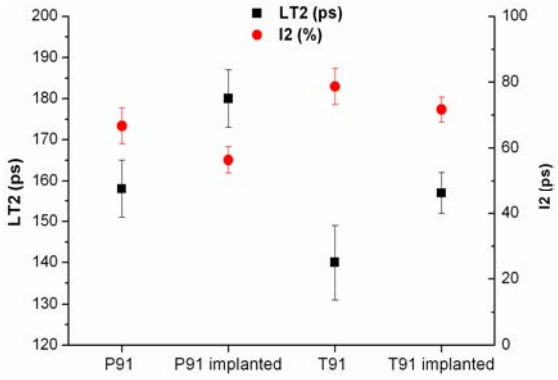

FIG. 9. Lifetimes (LT2) and intensities (I2) characterising defects in T91 and P91 before and after helium implantation.

Implanted samples contain more defects than non-implanted samples (See LT2 in Figure 9) due to defect accumulation during irradiation. Some amount of defects, mostly in non-implanted samples, is the impact of untransformed martensite.

The mean lifetime (MLT) for non-implanted samples indicates that the material T91 contains a higher concentration of these defects or bigger defects than P91 (See Figure 10). The difference in MLT is 3 ps, which is not high but significant for very similar materials. The systematic error of the PALS technique is less than 2 ps. On the contrary, after helium implantation, MLT of

material P91 is higher than for T91, which can demonstrate better radiation resistance of steel T91.

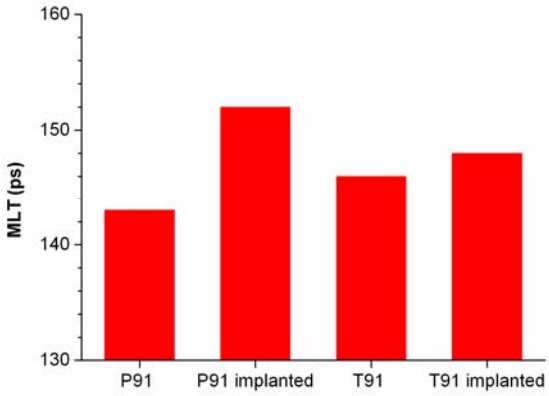

FIG. 10. MLT of non-implanted and implanted samples P91 and T91.

The DBS method was used for a graphic illustration of the differences in surface and subsurface layers between the non-implanted samples and implanted ones. Results are expressed by the parameter S, which describes positron annihilation by valance electrons mostly in open volume defects. When the S parameter grows, defect density increases.

In Figure 11, the results for the non-implanted and implanted steels are shown. This DBS measurement is a verification of the previous measurements by PALS. The difference between T91 and P91 in non-implanted state can lead to the conclusion that T91 contains either more or larger defects than P91 before implantation. The results for the implanted steels demonstrate higher S parameter for P91 than for T91. Implanted material P91 probably contains more or larger defects than T91.

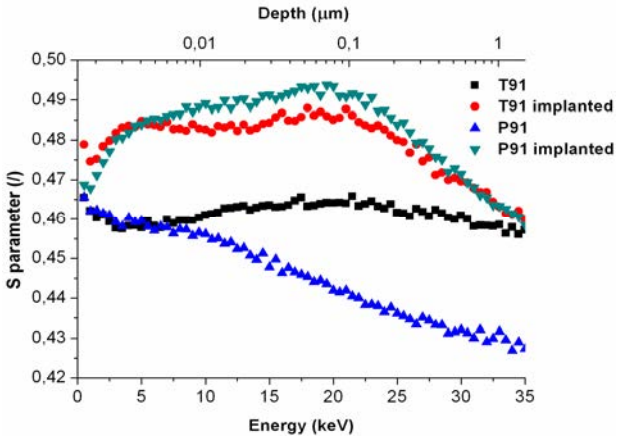

FIG. 11. DBS results, the line shape S parameter as a function of positron implantation energy and depth.

4. CONCLUSION

Our measurements demonstrate that two almost identical ferritic–martensitic steels, T91 and P91, that contain negligibly different chemical composition and undergo similar thermal treatments can have different microstructures from the viewpoint of defect concentration and residual stress.

These types of steels have not the same radiation resistance, as was proven by our three different experimental techniques.

On the basis of the results from PALS and DBS, a higher concentration of defects was registered in non-implanted steel T91 than in P91. This statement is supported by MBN measurements, in which the residual stress, which should be proportional to defects concentration or size, was also higher for T91. Furthermore, both positron annihilation techniques show that T91 has fewer suspected defect formations during helium implantation than P91. This in turn means that T91 has a higher resistance to radiation damage, and the radiation induced changes in its mechanical properties will in all likelihood be smaller as well.

Observed differences between T91 and P91 can be due to different amounts of untransformed martensite, which supports defect occurrence and structure hardness. This needs to be further investigated with application of microhardness tests and a technique that is able to determine the atomic structures of iron such as Mössbauer spectroscopy.

ACKNOWLEDGEMENT

Financial contributions from the European Atomic Energy Community Fusion Association EURATOM.CA and grant VEGA 1/0129/09 are acknowledged. This work was also partially supported by the Academy of Finland.

REFERENCES

[1] CARRÉ, F., YVON, P., "Outlook on GEN IV nuclear systems and related materials R&D challenges", Proc. Conf. Materials for Generation IV Nuclear Reactors (MATGEN-IV), Cargese, 2007.

[2] HOFFELNER, W., "Materials for high temperature components", Proc. Eurocourse 3 on Safety, Materials and Components, Aix en Provence, 2008.

[3] MORIN, F., et al., "Status of the ETDR preconception design studies", Proc. 18th International Conference on Structural Mechanics in Reactor Technology (SMiRT 18), Beijing, 2005.

[4] KLUEH, R.L., HARRIES, D.R., High Chromium Ferritic and Martensitic Steels for Nuclear Applications, ASTM International, Bridgeport (2001) 221 pp.

[5] MALAPLATE, J., et al., Characterization of He embrittlement of a 9Cr-1Mo steel using local approach of brittle fracture, J. Eng. Fract. Mechanics **75** 11 (2008) 3570–3580.

[6] ENNIS, P.J., et al., The mechanical properties and microstructures of 9% chromium steel P92 weldments, OMMI **1** 2 (2002).

[7] DEGMOVA, J., DEBARBERIS, L., Magnetic Barkhausen Noise Measurement of As-Cast Model Steels with Parametric Variation of Ni, Mn and Si Content, Rep. EUR 22512 EN, Joint Research Centre, European Commission, Petten (2006).

[8] PETRISKA, M., et al., Application of fast-digitizer card Acqiris DP-240 in positron lifetime spectroscopy, Phys. Stat. Solidi C **60** (2009) 2465–2467.

[9] LAHTINEN, J., et al., High-intensity variable-energy positron beam for surface and near-surface studies, Nuc. Instr. Meth. Phys. Res. B **17** (1986) 73–80.

[10] KLEBER, X., et al., Evaluation of the proportion of phases and mechanical strength of two-phases steels using Barkhausen noise measurements: application to commercial dual-phase steel, Metalurg. & Mater. Trans. **39A** (2008) 1308–1318.

[11] KRAUSE-REHBER, R., LEIPNER, H.S., Positron Annihilation in Semiconductors: Defect Studies, Springer-Verlag Berlin Heidelberg, New York (1999) 379 pp.
[12] KANSY, J., Microcomputer program for analysis of positron annihilation lifetime spectra, Nucl. Instr. Meth. Phys. Res. A **374** (1996) 235–244.
[13] PUSKA, M.J., SANKU, P., NIEMINEN, R.M., Positron affinities for elemental metals, J. of Phys.: Condensed Matter **1** 35 (1989) 6081–6094.
[14] ITO, Y., Dependence of the Doppler-broadening of the positron-annihilation radiation in C_{60} fullerenes on the temperature, Rad. Phys. & Chemistry **6** 4 (2002) 273–275.
[15] SLUGEN, V., What Kind of Information we can Obtain from Positron Annihilation Spectroscopy, Rep. EUR 22468 EN, Joint Research Centre, European Commission, Luxembourg (2006).
[16] ZIEGLER, J.F., The Stopping and Range of Ions in Solids, Pergamon, New York, (1985) 321 pp.

TRITIUM GENERATION AND MIGRATION IN Li BASED MATERIALS FOR A FUSION SOLID BLANKET

I. TAZHIBAYEVA, T. KULSARTOV, E. KENZHIN
Institute of Atomic Energy,
National Nuclear Center of the Republic of Kazakhstan,
Kurchatov, Kazakhstan
tazhibayeva@ntsc.kz

Abstract

The paper describes the main results of experiments on tritium and helium release from irradiated lithium ceramic Li_2TiO_3 enriched with ^6Li (96%). Mass spectrometry was used for in-situ registration of residual gas spectra from lithium ceramics and in post-radiation studies of residual tritium and helium. Tritium release kinetics was studied depending on irradiation conditions under constant temperature and thermo cycling. Post-radiation studies of residual tritium release from lithium ceramics were carried out by thermo-desorption technique. The effects of lithium burn-up up to 23% on tritium release from lithium titanate during long-term reactor irradiation were studied. It was discovered that tritium release was mainly controlled by bulk diffusion; however, a specific role was played by lithium trapping by point defects and the reaction of tritium molization at the material surface. The temperature dependence of tritium diffusion coefficients in lithium ceramics was obtained for various levels of ^6Li burn-up. Mechanisms were proposed for description of tritium and helium release from irradiated ceramic Li_2TiO_3. The main parameters of tritium and helium interaction were calculated, and total quantity of accumulated tritium was defined as well.

1. INTRODUCTION

Modern concepts of solid blankets propose to use lithium ceramics as a tritium generating material. Accumulation and migration of tritium is one important parameter in the selection of materials for fusion reactors. Absence of experimental data on the parameters of tritium interaction with such materials restricts development of fusion facilities. Thus, study of the processes of tritium and helium accumulation and release from irradiated breeder materials is an important contribution to solve material testing issues of future fusion facilities.

Work on lithium ceramics as a tritium breeding material for future fusion facilities have been carried out in Europe [1], Japan [2, 3] and the Russian Federation [4]. Experimental data have been gathered on generation and release of tritium under reactor irradiation conditions, but irradiation experiments were only carried out for samples with low enrichment in ^6Li and only up to low levels of lithium burn-up. Since breeder ceramics must be the tritium source for long periods of time, the processes of lithium burn-up, which is accompanied by stoichiometry changes and complex phase–structural transformations, can affect the mechanical, thermal–physical and diffusion characteristics of irradiated ceramics. Also, the mechanisms of tritium release from lithium ceramic granules are so far unknown.

The objective of this work was in-pile studies of lithium ceramic Li_2TiO_3 with lithium burn-up to a maximum of ~20%, "in situ" registration of tritium release for various temperatures up to 900°C and assessment of the prospects for using ^6Li enriched lithium metatitanate as a breeder material for controlled fusion facilities with respect to possible long term effective generation of tritium. The irradiation was carried out at the thermal research reactor WWR-K at the Institute of Nuclear Physics (INP NNC RK) for 5350 hours under a power rating of 6 MW. The paper describes the conditions and main results of the experiments on tritium and helium release from irradiated lithium ceramic Li_2TiO_3 enriched to 96% ^6Li. Experimentally obtained TDS spectra showed that tritium release kinetics exhibited complex behaviour and in many respects depended on the type of pebbles. Nevertheless, the total integral amount of tritium released is of a similar order of magnitude for all types of pebbles and comprises about 10^{11} Bq/kg. It was shown that for

the temperature range from 250–1100°C tritium, the release process is determined by bulk diffusion and thermo-activated release of tritium from radiation induced accumulation centres.

2. EQUIPMENT AND STUDY TECHNIQUE

The techniques and methods of the experiments to study tritium generation and release from lithium ceramics (Li_2TiO_3+5 mol% TiO_2) enriched to 96% ^6Li under long term thermal neutron irradiation (5350 hours, 15 campaigns, 2 year experiment, WWR-K reactor) were reported earlier [5]. In these experiments lithium burn-up was about 23%. Temperature and tritium release were automatically and continuously measured [6]. Characteristics of the samples, apparatus and experimental technique, as well as results of post-radiation studies of the changes in physical and mechanical properties of lithium ceramics due to long term reactor irradiation are given in additional references [7, 8]. The techniques for producing the test materials are given in a Japan Atomic Energy Agency paper [9].

The irradiation was carried out in two irradiation channels of the WWR-K reactor. Three active capsules were equipped with a system for continuous in-situ measurement of tritium release; the other capsules, labelled passive, were equipped with a tritium accumulation system. Passive capsules were meant to accommodate 20% burn-up in lithium ceramic samples enriched in ^6Li under constant sample temperature. The universal loop facility allowed control and maintenance of the operating temperature of each capsule during the entire irradiation period of 220 days, or 5350 hours [10]. Mass spectrometry was used for in-situ registration of residual gas spectra from lithium ceramics and in post-irradiation studies of residual tritium and helium. Tritium and helium release was studied by the thermodesorption method using the VIKA device (See Figure 1). Tritium release kinetics was studied for given irradiation conditions under constant temperature and thermal cycling. Post-irradiation studies of residual tritium release from lithium ceramics were carried out by the thermo-desorption technique. The obtained results were compared with tritium activity measurements by the liquid scintillation beta spectrometer TRICARB-3100TR.

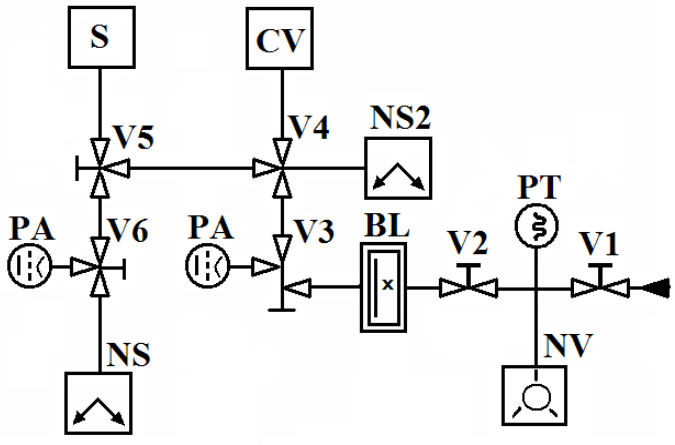

FIG. 1. Schematic diagram of the device VIKA:

NV: pump NVR-5DM; NS2: ion pump NORD-250; BL: nitrogen trap; PT: thermocouple vacuum gage; PA: vacuum ionization gage; CV: working chamber; V: vacuum valve; S: omegatron detector RMO-13 of mass spectrometer IPDO-2.

3. MAIN EXPERIMENTAL RESULTS

During reactor irradiation we could mark the following processes that occurred in lithium metatitanate based ceramics:

- Generation of tritium and α particles in the course of the nuclear reaction of neutrons, mainly thermal ones, and ^{6}Li:

$$^{6}Li + n \rightarrow {}^{3}H + {}^{4}He + 4.78\ MeV \quad (1)$$

- Lithium burn-up, which resulted in a shift of stoichiometric composition of Li_2O_3 in the direction to titanium, and increase of defects in the crystal lattice;
- Release of thermal energy due to reaction (1), which resulted in local heating, even melting, of the material under study;
- Generation of radiation defects due to tritium and helium release;
- Generation of radiation defects due to fast neutron bombardment;
- Generation of radiation defects due to the influence of intense fields of gamma irradiation;
- Tritium accumulation in the ceramics' volume and following mechanical degradation, indicated by a rise in gas porosity and material smelling during thermo-cycling.

Practically all of these processes influenced the chemical composition of the sample material and its structure, initiated a wide range of defects from point to multidimensional ones such as cracks and gas bubbles and activated such processes as blistering and flaking. As a result gas release kinetics changed considerably, which may result in worse operation characteristics of the breeder material as a stable supplier of tritium for fusion facilities.

3.1. Changes of physical–mechanical properties

Integrated material studies of lithium ceramics Li_2TiO_3+5%TiO_2 before and after long term irradiation in the WWR-K reactor for 5350 h at 490 and 650°C showed a significant impact of radiation–thermal effects on its structure and properties [7, 8]. After reactor irradiation the pebbles became dark, i.e., the quantity of the dark component having a lower density and microhardness, increased. Element analysis led to the conclusion that the dark impregnations in lithium ceramics were lithium oxide, and the light component was titanium oxide.

The lithium ceramics were softened under irradiation, and the effect is more pronounced at 490°C than at 650°C. The value of the maximum permissible load, above which the granule is deformed, is about ~40 N. The ceramics with higher content of the light structure are stronger that material with more dark structure. The most probable reason for this is the gaseous products of lithium fission, helium and residual tritium, as the ^{3}H content was higher in the samples irradiated at 490°C than at 657°C.

Measurement of tritium in the samples under study showed the content is higher in the ceramics irradiated in capsule P1 at 490 ºC, $6.6\pm0.6\times10^{11}$ Bq/kg, than in the samples irradiated in capsule A3 at 657ºC, $1.7\pm0.3\times10^{11}$ Bq/kg. These results agree well with data from sample measurements, in which the average diameter of granules increased slightly as a result of irradiation; bigger for T_{irr}=490°C than for T_{irr}=657°C. This is possibly due to partial release of tritium and helium

during the higher temperature irradiation. X ray analysis showed changes in phase composition of Li_2TiO_3+5%TiO_2 with the formation of new phases $LiTi_2O_4$, $LiTiO_2$ and $Li_4Ti_5O_{12}$ during irradiation.

3.2. Changes in chemical composition of irradiated ceramics and burn-up level calculations

Changes in the chemical composition of Li_2TiO_3 and in the ratio of lithium isotopes were studied using an inductively coupled plasma mass spectrometer with ELAN 9000. The mass and isotope ratios of $^6Li/^7Li$ were determined using the following procedure: preliminary measurement of an unirradiated sample; measurement of a comparison standard, a solution with 100 ppb Li with a natural ratio of lithium isotopes, i.e., 7.59%^6Li and 92.41%^7Li; and then measurement of the irradiated sample.

A correction factor for mass discrimination was calculated using a programme of the isotope ratio technique. Results obtained from the comparison standard were used for calculation of the isotope ratio correction factor $RSF=S_{measured}/S_{standard}$, in which $S_{measured}$ is the measured isotope ratio in the standard minus that of the idle sample and $S_{standard}$ is the known isotope ratio in the standard. The burn-up level of ^6Li was calculated by the formula:

$$\text{Burn-up level}=((^6Li/^7Li)_{initial}-(^6Li/^7Li)_{irradiated}))/(^6Li/^7Li)_{initial}\times 100\% \quad (2)$$

in which isotopic Li ratios are compared before and after irradiation. The resulting burn-up level calculated was 20–22%, which agrees well with the measurements.

The ceramic samples irradiated at a lower temperature are characterized by a small degree of ^6Li burn-up. It was established that the irradiation resulted in softening of the lithium ceramics, and that the effect is more pronounced for lower irradiation temperatures. The quantity of tritium released during a reactor campaign increased with an increase in campaign length, but the quantity of tritium released from lithium titanate per hour did not depend on the duration of irradiation. Thus, despite lithium burn-up, tritium flow from lithium titanate did not change for long term irradiation, since a reduction of the strength of the tritium source due to lithium burn-up is compensated by an increase in mobility of tritium in the ceramic. These results show that a breeder material based on ^6Li enriched lithium titanate can be a practical source of tritium for at least one year of reactor operation.

3.4. Tritium accumulation during irradiation of lithium ceramics with thermal neutrons in the WWR-K reactor

As was mentioned above, tritium generation in lithium ceramics occurs due to the nuclear reaction of neutrons and the isotope ^6Li. With irradiation time, tritium generation rate diminishes due to ^6Li burn-up (See Figure 2).

During the initial reactor campaigns, nuclear reaction (1) occurred in the near surface layer of a pebble sample, and as a result the surface was depleted of ^6Li, whereas the lithium isotope ratio inside a pebble was practically invariable. With an increase in the number of campaigns there were increases in burn-up in the near surface layer, expansions of the depleted layer and greater distribution of (n,^6Li) interactions deep into the sample. In neutron physics and chemistry this process is named kinetics of the shrinking sphere.

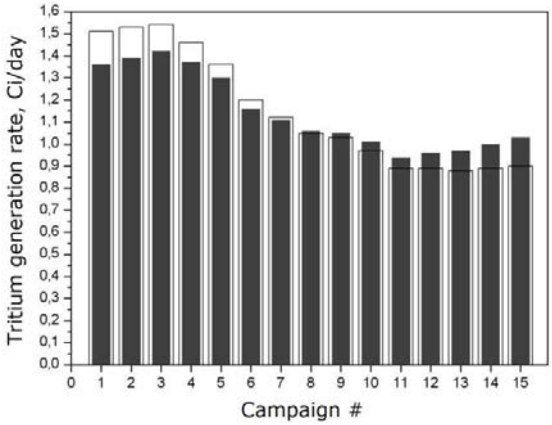

FIG. 2. Tritium generation in continuous campaigns during irradiation in WWR-K reactor: white areas are theoretical calculations of tritium release by MCNP software and dark areas are experimental data.

3.5. Kinetics of tritium release from Li_2TiO_3 during reactor irradiation

Tritium release kinetics was studied according to irradiation conditions of constant temperature and thermo-cycling. As an example, let's consider the experimental results obtained during campaign #2. Time dependences of temperature and tritium flux are given in Figure 3. For analysis a curve was divided into sections or steps (See Figure 4) that were graphed in Arrhenius coordinates. Then activation energy of tritium diffusion in lithium titanate was calculated by a slope ratio of the straight line portion. All sections of the initial curve were treated similarly. Obtained data are given in Table 1. Similarly processed were all tritium release curves from each of the campaigns.

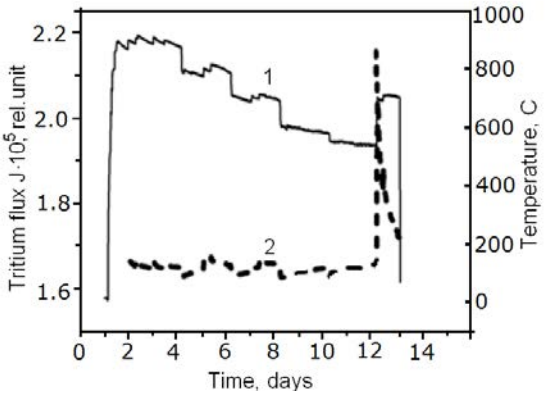

FIG. 3. Changes of temperature (1) and tritium flux (2) depending on time.

TABLE 1. ACTIVATION ENERGY OF TRITIUM DIFFUSION CALCULATED FOR STEP SEQUENCE

Step #	1	2	3	4	7	10
Activation energy (kJ/mol)	375.601	126.252	18.48	56.379	97.019	54.338

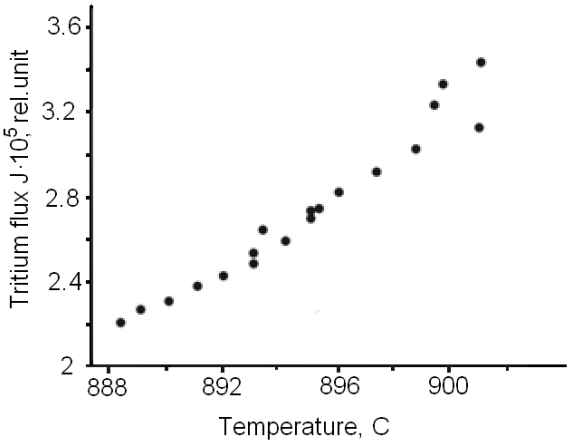

FIG. 4. Typical dependence of tritium flux from lithium ceramic's temperature for section 1 (sample A1, campaign 2).

The obtained results showed that activation energy decreased by a factor of ~6, as lithium was expended and the defectiveness of the material increased. Though this tendency remained, for the following campaigns the level of decrease in activation energy was reduced, demonstrating dependence on the duration of the reactor experiment. For example, for campaign #14 the tritium release activation energy decreased by a factor of ~2 only. Thus it may be expected that tritium release from lithium titanate will increase with a decrease of lithium concentration in the breeder material.

Mathematical simulation of tritium generation and release from lithium ceramics under reactor irradiation showed that in the beginning of reactor irradiation tritium concentration increased linearly and progressively to neutron fluence and ^{6}Li concentration. Subsequently the increase slowed, and finally tritium generation rate became a constant value — the rate was balanced by the insignificant tritium radioactive decay rate and release rate from a sample.

3.6. Tritium release kinetics during thermo-cycling

The experiments showed that tritium flow apparently depends on temperature; changes of temperature were accompanied by changes in tritium flux from a sample. Let's consider changes in gas flow from a sphere under stepped change of the sample's temperature, both heating and cooling.

3.6.1. Stepped heating of the ceramic

As an example, Figure 5 shows the time dependence of the tritium flux that was continuously generated from a sphere under a sharp rise of temperature and, correspondingly, diffusion coefficient. At first, the flux monotonically increased towards a constant value. In the moment of sharp temperature rise, the flux jumped then monotonously fell to a value that exceeded the value of the first temperature step. During the next temperature rise the behaviour of the flux was similar, but the values of the jump and subsequent stationary flux exceeded previous ones.

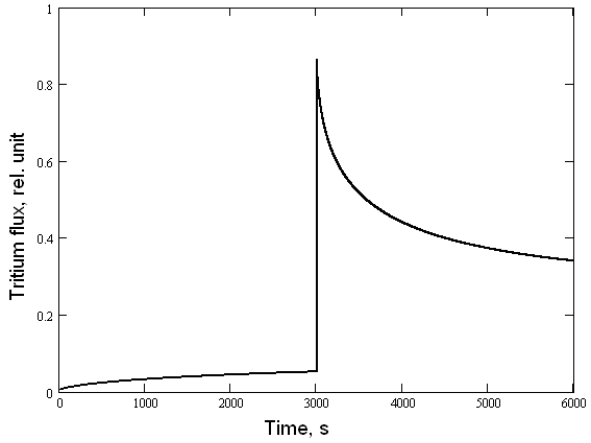

FIG. 5. Time dependence of the tritium flux continuously generated from a sphere under a sharp temperature rise.

3.6.2. Stepped cooling of a sample

As an example, Figure 6 shows the time dependence of the tritium flux from a sphere under step decreases in temperature. Evidently, under a sharp drop of temperature there was a sharp, almost vertical decrease of the flux.

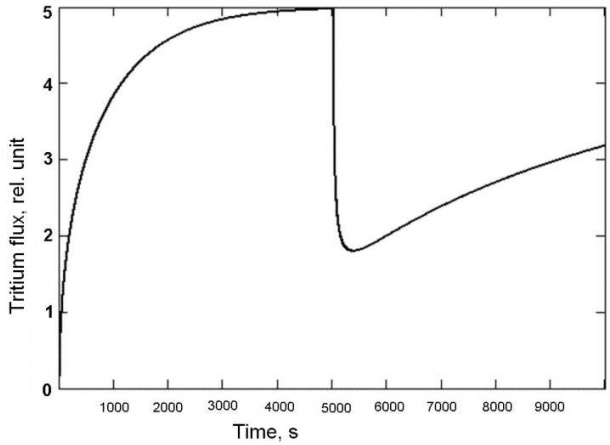

FIG. 6. Release of tritium generated in a sphere taking into account tritium generated during previous temperature steps (stepped cooling).

If partial degassing of tritium in a sample under higher temperature steps were taken into account, then flux decreased monotonically in the area of temperature change. However, the period of flux decrease was short and did not have significant influence on the form of a curve following the rise in generated tritium flux during the new temperature step.

Analysis of the dependence of flow with time allows not only the determination of the diffusion coefficient at low temperatures under stepped cooling but also the ratio D_2/D_1 under stepped heating and the diffusion coefficient at high temperatures using stepped heating curves. Data on H–^{3}H and $^3H_2$ release, the data of stepped cooling from high temperatures, at which degassing of

the granules was rather large, were converted to the diffusion coefficient of tritons in the crystal lattice of lithium metatitanate as defined by the stepped heating data.

Processing of the experimental data in the framework of the classical diffusion model showed that during the one year irradiation of lithium ceramics in the reactor, the diffusion activation energy significantly decreased. This is evidence of a decrease in the depth of potential wells, along which triton diffusion and tritium release in the form of H–^{3}H and $^3H_2$ is realized. The value of the pre-exponential or entropic factor decreased as well, which is evidence of a decrease in diffusion paths available, probably due to the creation of radiation defects acting as traps for diffusing tritium.

We assumed that the temperature dependence of tritium bulk diffusion can be described by the Arrhenius law. This dependence of the diffusion coefficient of $^3H^+$ showed the following values: D_{01}=0.1 cm^2/s and E_{D1}=130 kJ/mol during initial lithium burn-up and D_{02}=0.006 cm^2/s and E_{D2}=69 kJ/mol during the last phase of the irradiation experiment. Thus, long term irradiation of lithium ceramics resulted in the decrease of activation energy of tritium diffusion by a factor of 2 and a decrease in the pre-exponential or entropic factor of diffusion of more than one order of magnitude.

Graphically the temperature dependencies of tritium diffusion coefficient for two stages of tritium burn-up are given in Figure 7. The same dependencies in the Arrhenius scale are given in Figure 8. Some typical values of tritium diffusion coefficients in lithium metatitanate for various temperatures and various times are given in Table 2.

TABLE 2. DIFFUSION COEFFICIENTS IN LITHIUM METATITANATE UNDER VARIOUS TEMPERATURES AND TIMES

Irradiation initial stage		Irradiation final stage	
Temperature, °C	Diffusion coefficient	Temperature, °C	Diffusion coefficient
300	1.35×10^{-13}	300	3.0×10^{-9}
500	1.59×10^{-10}	500	1.28×10^{-7}
700	1.02×10^{-8}	700	1.17×10^{-6}

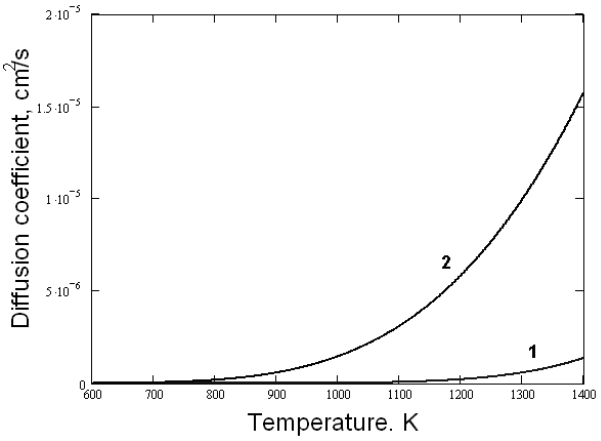

FIG. 7. Temperature dependence of tritium diffusion coefficient by lithium ceramic volume for the initial (1) and final (2) stages of ^{6}Li burn up.

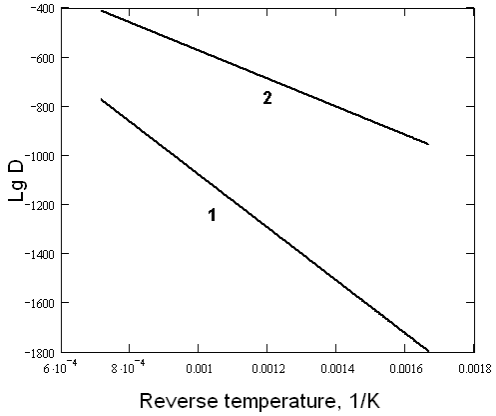

FIG. 8. Data of Figure 7 displayed in Arrhenius coordinates.

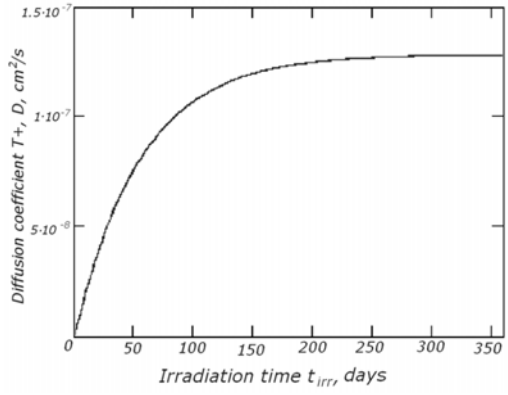

FIG. 9. Tritium diffusion coefficient change in Li_2TiO_3 during long term reactor irradiation.

For the semi-quantitative estimation of diffusion coefficient changes during constant temperature reactor irradiation we used an empirical formula. For example, at 500°C this dependence to a first approximation can be described by:

$$D(t_r) = 1.59\times10^{-10} + 1.28\times10^{-7}[1 - e^{-0,018t_r}] \quad (3)$$

in which t_r is the irradiation time.

The graph of this function $D(t_r)$ is given in Figure 9. From this dependence we conclude that the diffusion coefficient increases only during the first 10 months of reactor irradiation, then effectively stabilizes at 1.3×10^{-7} cm^2/s without significant change. Reaching this limiting value of the diffusion coefficient comes from the balance of two opposing factors: lithium burn-up resulting in reduced tritium production and radiation induced defects that trap diffusing tritium. As a result of this balance, the diffusion coefficient does not depend on the irradiation duration in long irradiation times.

3.7. Measurement of residual tritium

Residual tritium was measured using liquid scintillation spectroscopy with a beta spectrometer TRICARB-3100TR. This showed that retained tritium is higher in the ceramics irradiated in capsule P1 at 490ºC, $6.6\pm0.6\times10^{11}$ Bq/kg, than in the samples irradiated in capsule A3 at 657ºC,

$1.7\pm0.3\times10^{11}$ Bq/kg. These results agree well with data on sample measurements, in which the average diameter of granules slightly increased as a result of irradiation; larger for T_{irr}=490°C than for T_{irr}=657°C. This is possibly due to partial release of tritium and helium from ceramics during high temperature irradiation.

3.8. Measurement of tritium release from irradiated samples using thermodesorption spectrometry (TDS)

The experiments showed that tritium release kinetics have a complex nature and are mainly defined by bulk diffusion from traps or pores. Analysis of the thermodesorption spectrum showed that tritium was a first order chemical reaction. The activation energy of tritium gas release is in the range of 110–150 kJ/mol. Characteristic thermodesorption curves of residual tritium and helium release from irradiated ceramic samples (capsule A3) are given in Figure 10.

Several common effects are illustrated in the figures. For most TDS spectra of various types of pebbles from different capsules the peak tritium release was observed at ~550°C with a heating rate of 6°C/min. Activation energy of tritium release for this peak is in the range of 120–150 kJ/mol. For dark pebbles the "peak content" was about 50% of the total amount of released tritium and for dark grey pebbles about 90%. This peak was narrow and accounted for tritium release from accumulation centres, including macro defects and micro pores resulting from both irradiation and production technology.

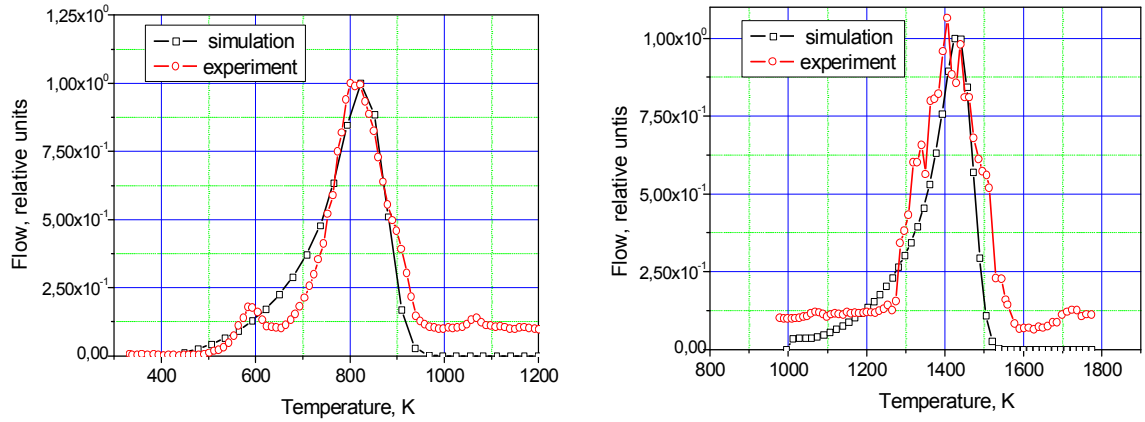

FIG. 10. Simulation results of, respectively, tritium and helium release from irradiated lithium ceramics.

Moreover, most of the samples had peaks of tritium and helium release below a temperature of about 1150°C at a heating rate of 6°C/min. This peak was broad and accounted for diffusion release of residual tritium and helium from the irradiated lithium ceramic bulk. The integral quantity of residual tritium and helium released from similar pebbles irradiated at high temperature was less than the quantity released from pebbles irradiated at low temperatures. For light grey pebbles from capsule A3 at $T_{irradiation}$~657°C, the integral value of residual tritium, ~0.8×10^{11} Bq/kg, is only half that for light grey pebbles from capsule P2, ~1.7×10^{11} Bq/kg at $T_{irradiation}$~595°C.

TABLE 3. RESULTS OF SIMULATION OF TRITIUM AND HELIUM RELEASE FROM IRRADIATED LITHIUM CERAMICS

Element	D_0 (m^2/s)	E_D (kJ/mole)
Tritium	1.6×10^{-6}	63
Helium	1.5×10^{-2}	215
Tritium [11]	6×10^{-7}	69

3.9. Mechanisms of tritium generation and release from lithium ceramics during long term reactor irradiation

Degassing of the pebble sample was analyzed in the framework of the classical diffusion mechanism, complying with Fick's law for diffusion and Henry's law for solubility and taking into account the presence of the sources and sinks under type 1 boundary conditions.

The following factors affecting tritium release were taking into account:

- Generation of tritium during irradiation;
- Tritium radioactive decay;
- Tritium depletion of the near surface layer, layer thickness being the tritium atom recoil distance;
- Generation of tritiated water due to ion exchange between H_2O and $^3H^+$;
- Possible impact of ^4He as a product of the nuclear reaction $^6Li+n\rightarrow{}^3H+{}^4He$ on the tritium diffusion mechanism; any impact of ^3He from ^3H decay was neglected;
- Molization of atomic tritium to molecular tritium, $2\,{}^3H\rightarrow{}^3H_2$, at open surfaces of a sample;
- The role of radiation effects related to irradiation with fast neutrons and gamma irradiation will be considered in future publications.

The temperature of the sample and tritium flow from lithium metatitanate was continuously measured during long term reactor irradiation. Experimental results were analyzed based on a degassing model for a spherical sample by classical diffusion mechanisms, taking into account the sources, generation from nuclear reactions, and losses, radioactive decay of tritium, under type 1 boundary conditions. Analysis of the time dependence of flow from determination of the diffusion coefficient at low temperatures under stepped cooling determined the ratio D_2/D_1 for stepped heating, as well as the diffusion coefficient at high temperatures using stepped heating curves. Data on H–^{3}H and $^3H_2$ release from stepped cooling from high temperatures, during which degassing was large, were converted to the diffusion coefficient of triton in the lattice of lithium metatitanate, as defined by the stepped heating data.

Assessment of the Arrhenius dependence of the diffusion coefficient for triton gave the following values: D_{01}=0.1 cm^2/s and E_{D1}=130 kJ/mol for initial lithium burn-up during the initial campaign of reactor experiments and D_{02}=0.006 cm^2/s and E_{D2}=69 kJ/mol during the last campaigns. Thus, long term irradiation of lithium ceramics resulted in a decrease of activation energy of tritium diffusion by a factor of two and decrease of the pre-exponential or entropic factor of more than an order of magnitude.

4. CONCLUSION

Diffusion coefficients and activation energies of tritium release from irradiated ceramics were calculated. The diffusion coefficient increased only during the first 10 months of reactor irradiation and then effectively stabilized at 1.3×10^{-7} cm^2/s without significant variation. This limiting value of the diffusion coefficient comes from the balance of two opposing factors: lithium burn-up resulting in reduced tritium production and radiation induced defects that trap diffusing tritium.

The tritium release process is mainly controlled by tritium diffusion, but a certain role is played by lithium trapping by point defects and the reaction of molization of tritium at the material surface. The total integral amount of tritium released is on a similar order of magnitude for all types of pebbles and comprises about 10^{11} Bq/kg.

When lithium is exhausted, the activation energy of tritium release decreases, tending to reach a constant value at high burn-up levels. The effect is explained by a decrease of lithium ion concentration and the presence of lattice defects acting as additional diffusion barriers. Low retention levels and times lead to low tritium concentrations in pebbles under irradiation at rather moderate temperatures. This allows us to recommend ceramics based on lithium metatitanate as a breeder material for fusion reactors, provided the physical and mechanical properties are conserved during irradiation.

REFERENCES

[1] FISCHER, U., et al., EU blanket design activities and neutronics support efforts, Fusion Science and Technology **47** (2005) 1052–1059.

[2] TSUCHIYA, K., et al., In-situ tritium release behavior from Li2TiO3 pebble-bed, Fusion Engineering and Design **58–59** (2001) 679–682.

[3] TSUCHIYA, K., et al., Integrated experiment of blanket in-pile mockup with Li2TiO3 pebbles, Fusion Engineering and Design **51–52** (2000) 887–892.

[4] KAPYCHEV, V., TEBUS V., FROLOV V., Influence of neutron irradiation on the strength characteristics of lithium ceramic pellets for fusion reactor blankets, J. Nucl. Mater. **307–311** (2002) 823–826.

[5] TAZHIBAYEVA, I., et al., VANT, Fusion Series 2 (2007) 3–10.

[6] CHIKHRA, Y., et al., Study of Li2TiO3+5 mol% TiO2 lithium ceramics after long-term neutron irradiation, J. Nuclear Materials **386–388** (2009) 286–288

[7] TAZHIBAYEVA, I., et al., VANT, Fusion Series 1 (2008) 3–12.

[8] TAZHIBAYEVA, I., et al., Measurement system for in-pile tritium monitoring from Li2TiO3 ceramics at WWRK reactor, J. Nuclear Materials **367–370** (2007) 1028–1032.

[9] TSUCHIYA, K., KAWAMURA, H., Fabrication and characterization of ^{6}Li-enriched Li_2TiO_3 pebbles for High Li-burnup irradiation test, JAEA Technology (2006).

[10] TAZHIBAYEVA, I., et al., VANT, Fusion Series 1 (2008) 3–12.

[11] BECKMAN, I.N., et al., Diffusion of tritium generated in lithium metatitanate Li_2TiO_3 under thermal neutron irradiation in WWR-K reactor, VANT, Fusion Series 2 (2009) 83–92.

FEASIBILITY STUDY AND INSTALLATION OF THERMAL NEUTRON DRIVEN 14 MEV NEUTRON CONVERTER INTO THE TRIGA RESEARCH REACTOR

A. TRKOV, L. SNOJ, G. ŽEROVNIK
Jožef Stefan Institute
Ljubljana, Slovenia
Andrej.Trkov@ijs.si

Abstract

Tentative design and implementation of an irradiation facility that will add a 14 MeV component to the neutron spectrum in a thermal research reactor irradiation facility are described. The idea is to exploit the ^{6}Li(n,^{3}H)^{4}He reaction in a blanket of lithium in a deuterated environment placed in a thermal reactor irradiation channel. Existing literature describing similar devices is reviewed, the theoretical basis is presented, and plans for the design and implementation are described. Potential uses of such a device are activation studies of new materials under development for fusion reactors like ITER and DEMO, evaluated nuclear reaction data validation at energies above 10 MeV and fast neutron activation analysis, among others.

1. INTRODUCTION

The demand for experimental devices capable of irradiation with 14 MeV neutrons, which are very important for fusion applications, is increasing. Conventional neutron generators require laboratory space and maintenance. In the literature one can find documents that pursue the idea of using a deuterated environment in a blanket of lithium placed in a thermal reactor irradiation channel in order to obtain a neutron source with an enhanced 14 MeV component in the neutron spectrum from the ^{6}Li(n,^{3}H)^{4}He reaction. The sample is placed in a container lined with a blanket material containing ^{6}Li and deuterium (D). The container with a sample is irradiated in one of the conventional irradiation channels in a reactor. The tritium (T) produced in the reaction interacts with deuterium in the blanket, thus adding 14 MeV neutrons from the ^{2}H(^{3}H,n)^{4}He reaction to the reactor spectrum inside the container. Design and installation of such a device in a thermal reactor would provide the following enhanced capabilities:

- Validation and improvement of evaluated nuclear reaction data at energies above 10 MeV;
- Irradiation and testing of low activation fusion reactor candidate materials to verify:
  - — Activation properties of the new materials;
  - — Radiation damage;
- Fast neutron activation analysis.

The proposed irradiation facility enhancement is a low cost facility complementary to International Fusion Material Irradiation Facility (IFMIF), which is intended for testing mechanical properties of materials under extreme irradiation damage conditions. IFMIF is a large and expensive facility, and construction requires much time. Neutron generators with a D–T source are another possibility, but these require auxiliary structures like shielding, collimators, a power supply and control instrumentation, in addition to the infrastructure for the maintenance and operation of the facility. In comparison, a 14 MeV neutron converter in an existing fission research reactor is an attractive alternative.

The specific objective of the investigation is the feasibility of installation of a thermal neutron driven 14 MeV neutron converter in the TRIGA research reactor at the Jožef Stefan Institute (JSI)

in Ljubljana that would enable irradiation of various small samples in a close to fusion neutron spectrum and allow more users to have access to an intermediate energy neutron irradiation facility. Although the neutron flux levels will not be comparable to the levels in facilities such as IFMIF, the facility will support a number of experiments that require 14 MeV neutron spectra but do not need a high neutron fluence.

At JSI we have long term experience with the production of radioisotopes, neutron activation analysis, irradiation of various samples for external customers, handling of radioactive material from radioactive samples to spent fuel element, neutron transport calculations, radiography, among other nuclear activities. We are planning to develop and install a 14 MeV converter that will extend our capabilities in the area of reactor physics, neutron activation and nuclear data validation by exploiting the potential in manpower and existing expertise at the Institute with the support of the International Atomic Energy Agency (IAEA).

2. EXISTING TECHNOLOGY AND KNOW-HOW

The idea of a thermal neutron driven neutron generator has been addressed by various authors. One of the earliest reports is by Frigerio [1], who proposed to use such a device for neutron activation studies. In 1976 Napier, et al., [2] described an operating device, including construction details. Two years later Eckhoff, et al., referring to Napier's work, reported [3] that such a device is not as effective as initially believed, and Wysocki, et al., argued [4] that the flux magnitudes reported for a LiOD–D_2O converter indicate that such a device offered little if any advantage over fission spectrum neutrons. Both statements are probably true, in light of the authors' objectives to use irradiation devices for analytical work and considering the status of nuclear data at the time. Since then, the activation method has been greatly improved for routine applications, and the status of nuclear data is incomparable. Limitations of the activation method have been reached such that complementary information from high threshold reactions could be useful to extend the range of applicable elements and increase the reliability and detection limits of the method. Furthermore, the present objectives also include studies of the activation properties of new structural and special purpose materials in complex spectra that include a 14 MeV component as well as neutrons at lower energies from slowing down in surrounding materials and coolants. The spectrum of the 14 MeV converter device is quite representative of many such environments.

Napier's device was operated and tested on a TRIGA reactor similar to the one at JSI so the construction details and results of experimental measurements are highly relevant and valuable. A more detailed theoretical investigation was reported by Miller, et al., [5], including some optimisation studies. These can serve as the starting point and guideline for further studies using state of the art computational methods and nuclear data.

3. DEVICE DESIGN AND OPTIMISATION

Design optimisation requires verified and validated software tools and nuclear data. The optimisation process must consider not only the neutronic properties of the device but also safety aspects, since the heat dissipation and neutron activation in such a device might be considerable.

3.1. Validation of computational tools and nuclear data

The most accurate treatment of particle transport can be achieved by the Monte Carlo method. Unfortunately, none of the generally available Monte Carlo codes can treat coupled transport of neutrons and tritons for neutron production. The well known MCNPX code [6] can perform such calculations using nuclear data from models that are only valid at high incident energies. The SRIM code [7] adequately treats charged particle transport but does not calculate neutron emission, which in this case is of primary interest. A two stage computational scheme will therefore be needed. In the first stage the source term of tritons and their energy distribution will be calculated, followed by the reaction rate calculation of the D-T reaction and the associated neutron source term as a function of energy and position. It is expected that some code development will be needed, particularly if detailed triton slowing down turns out to be important. The research team at JSI already has some experience with such calculations through the development of the source routine for the MCNP family of codes to model the neutron source in a tritiated titanium target bombarded with accelerated deuterons [8].

Experimental setup and the measured data reported by Napier [2] and Miller [5] will be used for the validation of calculations. Their experiments will be simulated with the developed code system, and the calculated results compared to the reported measurements.

3.2. Definition of operational parameters

Using validated computational tools, sensitivity to the spectral parameters of different thermal channels in the TRIGA reactor will be determined. This will allow for the preliminary design of the sample container with regards to the dimensions and material composition, namely the chemical form, layout and quantity of lithium and deuterium. The tentative design could differ for different irradiation positions. Locations in the reactor at which the device could be implemented include the central channel, the triangular channel, the irradiation channel in the F-ring, the pneumatic post transfer system, the carousel facility in the reflector (See Figure 1), the dry cell, radial and tangential channels, and the thermal column (See Figure 2). The criteria for the first selection will be:

- Ease of container insertion and withdrawal;
- Influence on the neutronics of the reactor core;
- Additional safety implications;
- The fraction of 14 MeV neutrons in the spectrum.

Based on the above criteria a short list of candidate locations will be made, each of which will undergo a second round of design optimisation. At this stage, detailed operational parameters will be determined regarding the necessary reactor power level for operation, maximum irradiation time, and anything else that might influence the safety of the reactor or the personnel, e.g., induced activity of the container and cooling time.

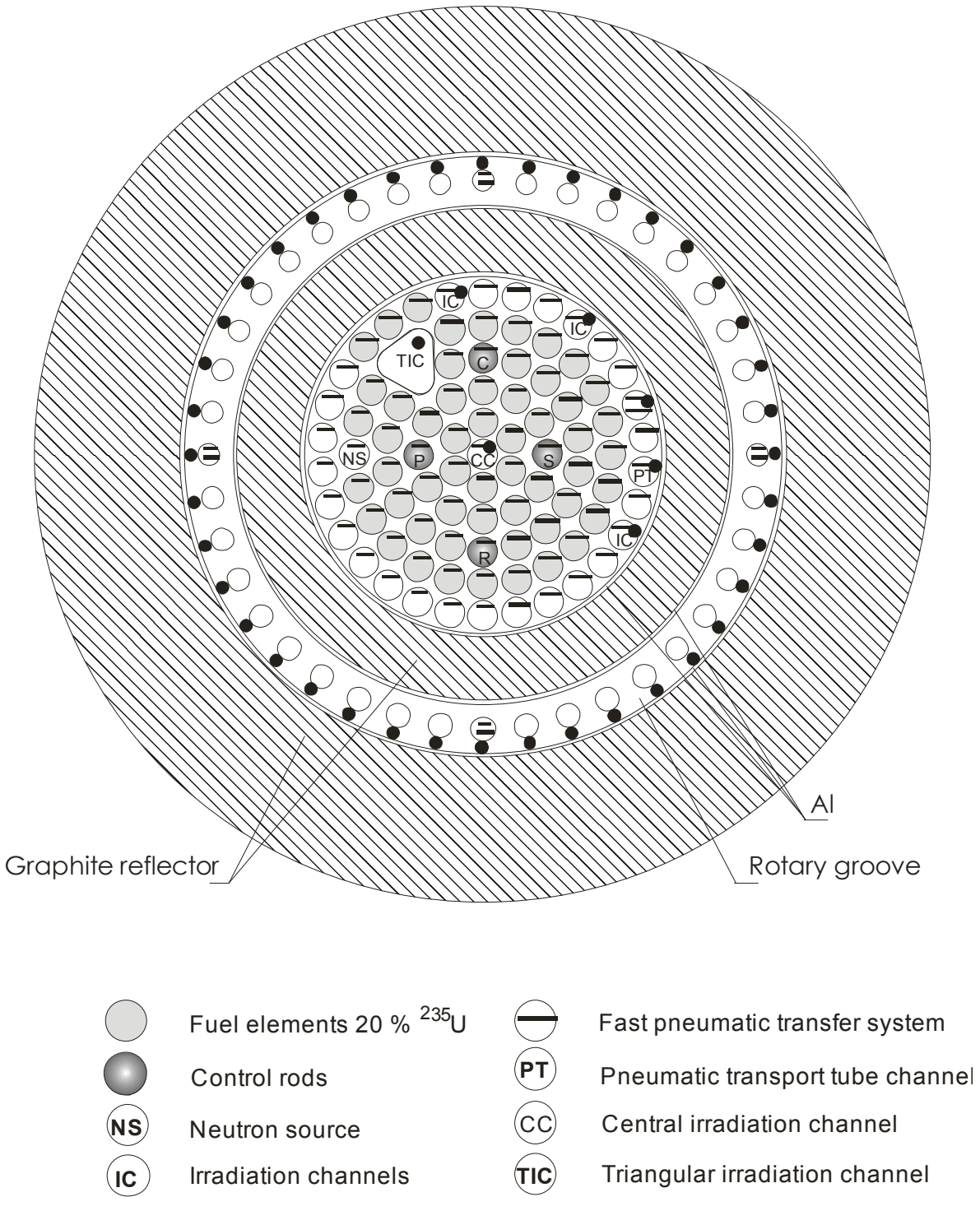

FIG. 1. Schematic top view of the TRIGA reactor core and reflector. The possible locations of the D–T converter are marked with black dots.

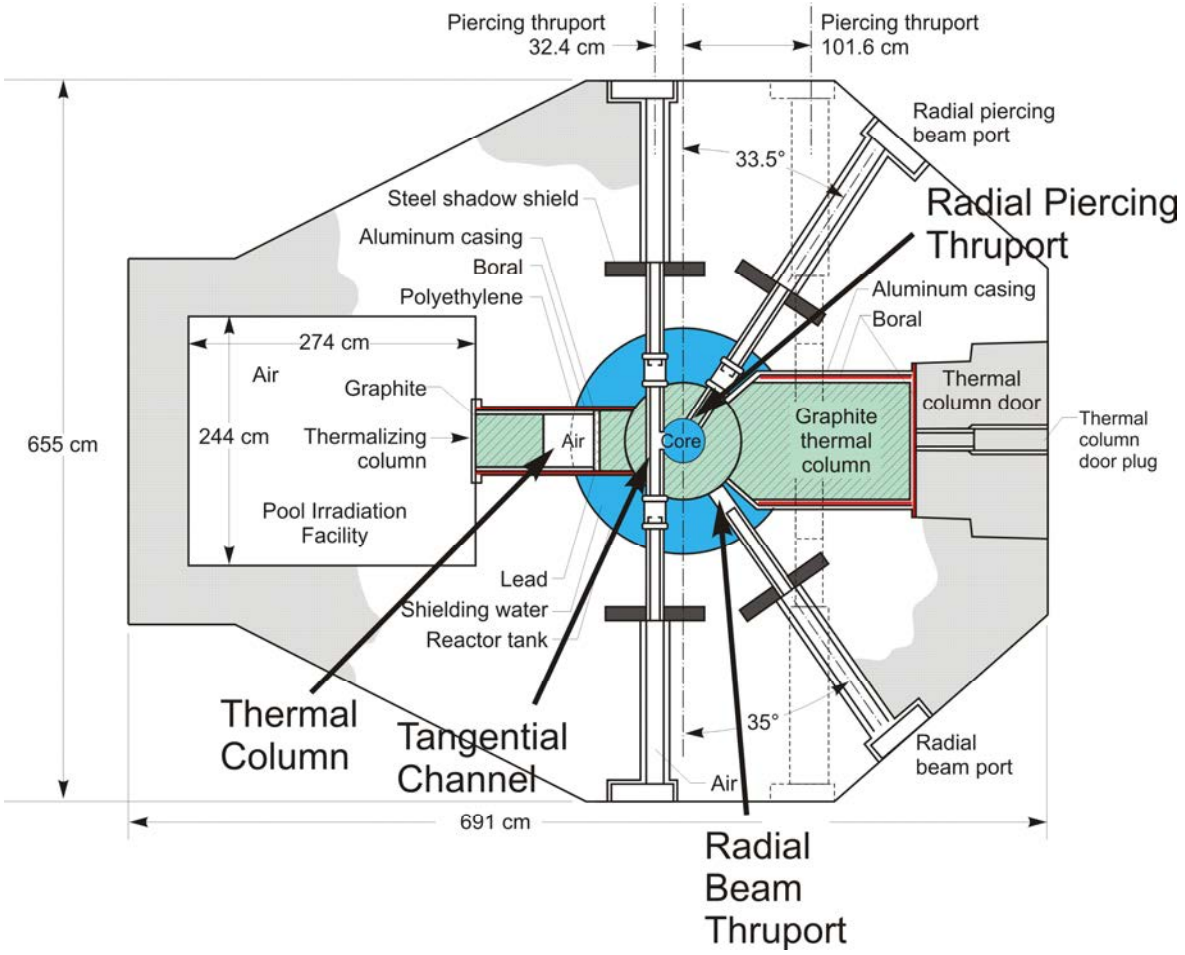

FIG. 2. Schematic top view of the TRIGA reactor. The possible locations for the D–T converter outside the reactor core are indicated by large black arrows.

3.3. Design optimisation

The chosen irradiation location in the reactor will determine the outer dimensions of the device. The minimum dimensions of the sample compartment are defined by the users. It is expected that the inner radius should be at least 1 cm in diameter. The length will depend on the position.

The chemical form of the lithium and deuterium compounds will be constrained by the safety considerations of the device. A detailed sensitivity analysis will be performed to allow the optimisation of the quantities and composition of the materials, including the canning materials, as needed. The objective is to maximize the 14 MeV component in the neutron spectrum. The limiting criteria for the optimisation will include:

- Heating related to the chemical stability of the compounds, phase transitions, etc.; and
- Induced activation of the container itself.

4. DEVICE CONSTRUCTION AND TESTING

The results of the optimisation stage will be sufficient to proceed with the mechanical design of the device. This will determine the precise quantities of materials. Since these quantities will not be large, some of the tasks of chemical conversion can be done at JSI. Materials that are not available at JSI must go through procurement procedures. Some capabilities for the machining of components are available at the JSI workshops but might be insufficient for the full implementation of the design.

Since this is a nuclear irradiation device, first tests will be made at low power to check activation. Heat release could be the next test, the scope of which will depend on the safety report. The next series of tests will be with activation monitors to perform spectrum unfolding, which will determine the neutronic characteristics of the device.

After the completion of the testing phase, the device will be commissioned for use in the applications mentioned in the introduction.

5. CONCLUSIONS

The rationale for the design and construction was presented for an irradiation device that will include a 14 MeV component in the neutron spectrum. This will be a low flux, low cost device for testing low activation material samples, validation of nuclear reaction data and other activation studies that require a component of the neutron spectrum with energies above 10 MeV. The steps for design optimisation, implementation and testing were described. Some of the tasks will be performed by the JSI staff, but support is also requested from the IAEA.

REFERENCES

[1] FRIGERIO, N.A., "Conversion of reactor neutrons to 15 MeV with LiD", Panel Proc. Radiobiological Applications of Neutron Irradiation, 1971, IAEA STI/PUB 325, IAEA, Vienna (1972) 51–56.

[2] NAPIER, B.A., et al., Design of an in-core fast neutron generator, Nuclear Instruments and Methods **138** 3 (1976) 463–465.

[3] ECKHOFF, N.D., MERKLIN, J.F., On the utility of an in-core fast neutron generator — a response, Nuclear Instruments and Methods **156** 3 (1978) 607.

[4] WYSOCKI, C.M., GRIFFIN, H.C., On the utility of an in-core fast neutron generator, Nuclear Instruments and Methods **156** 3 (1978) 605–606.

[5] MILLER, W.H., LAW, W.S., BRUGGER, R.M., Thermal neutron driven, 14.1 MeV neutron generators, Nuclear Instruments and Methods in Physics Research **216** 1–2 (1983) 219–226.

[6] PELOWITZ, D.B. ed., MCNPX User's Manual, Version 2.6, LA-CP-07-1473, Los Alamos National Laboratory, Los Alamos (2007).

[7] ZIEGLER, J.F., BIERSACK, J.P., ZIEGLER, M.D., SRIM — The Stopping and Range of Ions in Matter, SRIM Co., Chester (2008).

[8] MILOCCO, A., TRKOV, A., "Production of source neutrons by low voltage accelerated deuterons on titanium-tritium targets", Proc. Int. Conf. Nuclear Energy for New Europe 2007, Nuclear Society of Slovenia, Ljubljana (2007).

IRRADIATION DAMAGE IN CHINA LOW ACTIVATION MARTENSITIC (CLAM) STEEL

Farong WAN, Yi LONG
School of Materials Science and Engineering,
University of Science and Technology Beijing,
Beijing, China
wanfr@mater.ustb.edu.cn

Abstract

In order to fabricate the test blanket module for ITER, China Low Activation Martensitic steel is being developed with the composition of 9Cr1.5WVTa. This paper investigates the behaviour of irradiation damage and the effect of transmutation gas atoms in the materials. Ion implantation to materials by hydrogen or deuterium was carried out by an ion accelerator. Electron irradiation by high voltage electron microscope was used to simulate the procedure of irradiation damage. In addition to CLAM steel, irradiation enhanced precipitation was also studied using some binary model alloys such as Fe–Cr, Fe–V, Fe–Ta and Fe–Si. Electron irradiation at 723 K formed many voids in CLAM steel without silicon addition, whereas no voids were observed in CLAM steel added with 0.2% silicon. Silicon was found to be a good alloying element for increasing the irradiation swelling resistance of the CLAM steel. Both the growth and shrinkage of the dislocation loops produced by deuterium ion implantation may be observed in CLAM steel under electron irradiation. The growing loops were of interstitial type and formed at lower temperatures. However, the shrinking ones were of vacancy type and formed at higher temperatures. Vacancy type loops absorbed more interstitial atoms than vacancies, so they shrank and disappeared during electron irradiation.

1. INTRODUCTION

As a part of work toward the development of fusion energy, the study of structural materials, especially activation characteristics, is an important issue. The research of appropriate materials has been carried out around the world since the 1980s with three potential candidates: vanadium alloys, SiC/SiC composites, and reduced activation ferritic–martensitic (RAFM) steel [1–4]. Although vanadium alloys and SiC/SiC composites have many attractive properties, such as superior thermal and physical properties [5], RAFM steel is now considered the primary candidate due to its low cost and excellent resistance to swelling and embrittlement under irradiation [6–8]. For this reason, many countries are doing RAFM steel research for developing their own RAFM steel. For example, the US is studying 9Cr2WVTa, while the EU is focusing on EUROFER97 [9], and Japan on JLF-1 and F82H [10].

After joining the International Thermonuclear Experimental Reactor (ITER) project and becoming a port master of a test blanket module, China is also developing its own RAFM steel, called China low activation martensitic (CLAM) steel as the structure material for the module. It is based on JLF-1 and EUROFER97 designs (See Table 1). The mechanical properties of CLAM steel have been determined to be comparable to 9Cr2WVTa and EUROFER97. The thermal and physical properties have been measured by other researchers, and the data indicate that CLAM steel could be a primary candidate among the structural materials to be tested by the ITER project. [11]

TABLE 1. COMPOSITIONS OF DIFFERENT RAFM STEEL

RAFM	Cr	W	V	Ta	Mn	Si	C	N	B
F82H	8.0	2.0	0.2	0.04	0.5	0.2	0.10	<0.01	0.003
JLF-1	9.0	2.0	0.2	0.07	0.45	0.08	0.10	0.05	-----
EUROFER97	8.5	1.1	0.2	0.1	0.4	0.05	0.12	0.02	<0.001

9Cr2WVTa	9.0	2.0	0.25	0.07	0.4	0.30	0.10	0.02	-----
CLAM steel	9.1	1.5	0.21	0.16	0.41	-----	0.10	-----	-----

On the other hand, 14 MeV neutrons produced by the fusion reaction cause nuclear transmutations reactions such as (n,p) or (n,α), inducing huge amounts of hydrogen and helium. Deuterium and tritium from the fusion reaction will enter the structural materials. Combined with irradiation defects this may cause a dramatic change in the mechanical properties of their materials.

The interaction between hydrogen and irradiation induced defects in iron has been studied [12]. CLAM steel, however, is a much more complicated structural material than pure iron. In addition, in a real fusion reactor hydrogen, deuterium and tritium all exist simultaneously, but unfortunately until now there has not been any research on the irradiation effects on the vacancy loop formation.

Electron irradiation produces the same number of single vacancies and interstitial atoms. Because of the high mobility of interstitial atoms, the reaction of interstitial atoms dominates during the early state of the electron irradiation. If self-interstitial atoms react with defect clusters stronger than vacancies, clusters of interstitials are expected to grow while the clusters of vacancies to shrink and disappear [13, 14].

Previous research has been done using data simulation calculations regarding hydrogen and vacancies, but a real fusion reactor would involve deuterium and tritium, as well. [15, 16]

As yet, few reports about the interaction between the isotopes of hydrogen and irradiation induced defects can be found. This research focuses on the impact of deuterium and vacancies. Microstructural changes of deuterium ion implanted CLAM steel induced by electron irradiation are investigated at constant and varying temperatures.

2. EXPERIMENTAL PROCEDURE

CLAM steels were prepared according the composition shown in Table 1. The alloying effect of silicon was investigated by using two different CLAM steels, without silicon and with 0.2% Si. The steels were normalized at 1253 K for 30 minutes before quenching in water at room temperature. The tempering was conducted at 1023 K for 90 minutes and then air cooled. Pure iron samples were also used for irradiation experiment.

For transmission electron microscopy (TEM) investigation samples 3 mm in diameter were punched out from a 0.1 mm thick strip. They were prepared from a thick plate of CLAM by spark erosion and chemically polished to their final thickness. The TEM samples were polished using a twin jet electro-polisher with a 5%HClO4+95%C2H5OH solution at room temperature under 50 V.

The CLAM steel samples were implanted with deuterium ions by an ion accelerator at room temperature. The electron beam irradiation was carried out with a damage rate of about 2×10^{-3} dpa/s at room temperature, 773 K, 823 K and 873 K up to a dose of around 0.48 dpa at 1250 kV using the high voltage electron microscope JEM-ARM 1300 located at Hokkaido

University, Japan. The microstructure was observed in situ during the electron irradiation process.

3. RESULTS AND DISCUSSION

Figure 1 shows the microstructure of CLAM steel without silicon addition, the first sample, during electron irradiation at 723 K. It is known that many voids formed after irradiation to 10 dpa. Two small voids, marked A, combined and developed into a large void. On the other hand, Figure 2 shows the microstructure of CLAM steel with 0.2% silicon addition under the same irradiation as in Figure 1. No void could be observed in Figure 2, meaning that silicon addition may improve the resistance to swelling in CLAM steel.

Figure 3 shows the change of defect clusters in deuterium ion implanted CLAM steel during election irradiation at 823 K. It is found that the loops marked A, B and C shrank under electron irradiation.

According to our previous report [15], hydrogen implantation induces interstitial atoms (I) and vacancies (V), and also some interstitial atom clusters (Is) and vacancy clusters (Vs). Thus, four complexes of hydrogen and defects in the deuterium ion implanted samples could be identified, namely, H–I, H–V, H–Is, and H–Vs.

When ageing at lower temperatures, around 573 K to 723 K, H–I and H–Is complexes may move and cluster to form interstitial loops, but once the temperature approaches 723 K, H–V complexes may start to move and cluster to form vacancy loops. When the temperature is around 793 K, H–Vs complexes begin to move and cluster to form voids.

The deuterium ion implantation induces interstitial atoms (I), vacancies (V), interstitial atom clusters (Is), and vacancy clusters (Vs) in CLAM steel. These defects would form D–I, D–V, D–Is, and D–Vs complexes with D^+.

When ageing at low temperatures, D–I and D–Is complexes may move freely and cluster to form interstitial loops, but once the temperature reaches 823 K, D–V complexes begin to move and form vacancy loops.

Just as in the case of hydrogen implanted pure iron, the vacancy loops in the deuterium ion implanted CLAM steel seized interstitial atoms and then shrank and disappeared under high energy electron irradiation.

The temperature at which vacancy loops formed in CLAM steel was 823 K. There are only interstitial loops when electron irradiation temperature is 773 K. However, in pure iron implanted with hydrogen, vacancy loops had already formed at 723 K. The temperature difference in vacancy loop formation may be due to different types of sample materials or ions.

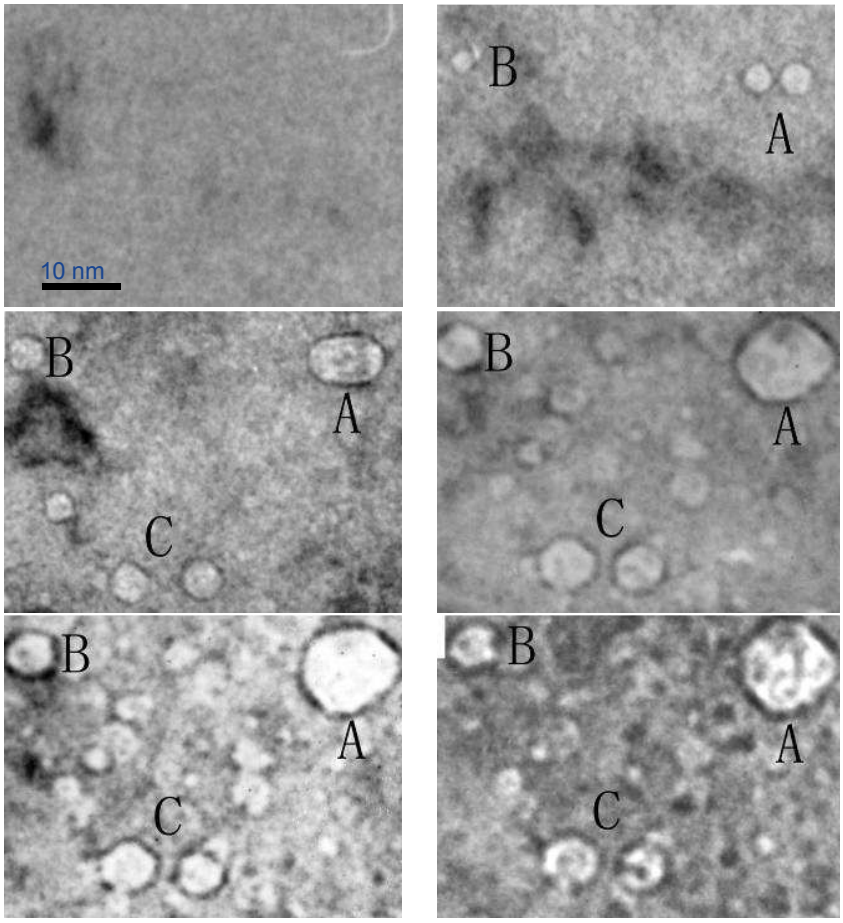

FIG. 1. Change of microstructure during electron irradiation at 723 K of CLAM steel without silicon addition. Damage rates are 0, 1.4, 3.6, 10.1, 11.5 and 13.8 dpa.

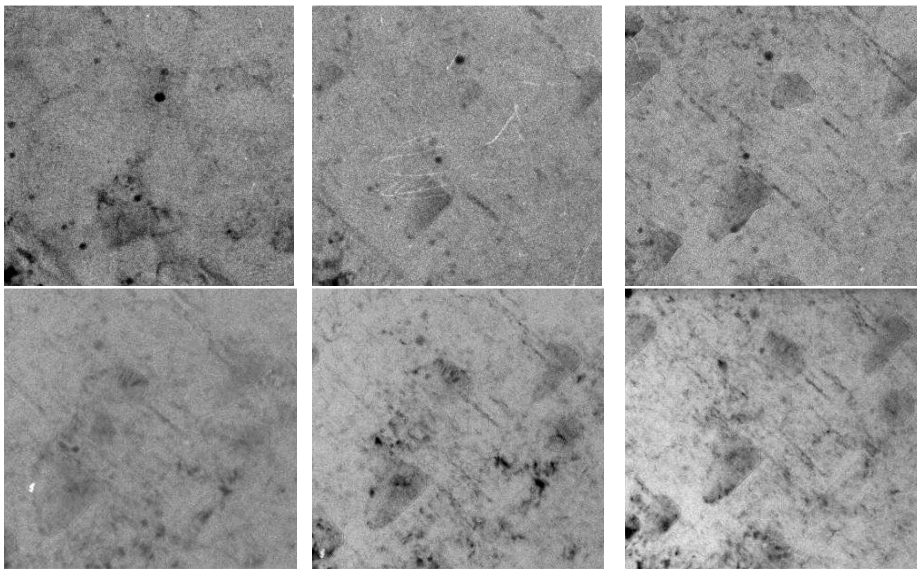

FIG. 2. Change of microstructure during electron irradiation at 723 K in CLAM steel with 0.2% silicon addition. Damage rates are 0, 1.2, 3.8, 7.6, 11.4 and 16.0 dpa.

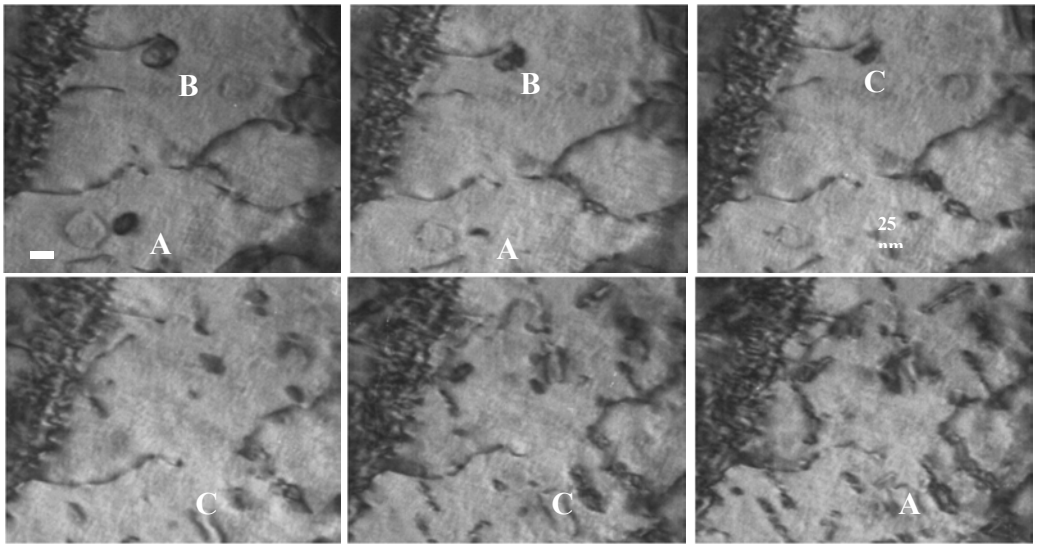

FIG. 3. Microstructural change of deuterium implanted CLAM steel during electron irradiation at 823 K for 0, 0.03, 0.06, 0.21, 0.24 and 0.36 dpa

4. SUMMARY

Silicon addition may improve the resistance to irradiation swelling of CLAM steel. In the CLAM steel implanted with deuterium ions at room temperature, interstitial loops formed by annealing at low temperature. When the annealing temperature reached 823 K, vacancy loops began to form. During electron irradiation, the interstitial loops grew continuously, but the vacancy loops shrank to disappearance under electron irradiation.

ACKNOWLEDGEMENTS

This work is supported by the National Natural Science Foundation of China with Grant Number 50971030 and by the National Basic Research Program of China with Grant Numbers 2008CB717802 and 2009GB109004. The authors gratefully acknowledge the support of the Core University Program in Japan.

REFERENCES

[1] MANSUR, L.K., et al., Materials needs for fusion, Generation IV fission reactors and spallation neutron sources — similarities and differences, Journal of Nuclear Materials **329–333** (2004) 166–172.

[2] GUEBALY, L.E., MASSAUT, V., TOBITA, K., CADWALLADER, L., Goals, challenges, and successes of managing fusion activated materials, Fusion Engineering and Design **83** (2008) 928–935.

[3] DOERNER, R.P., The implications of mixed–material plasma–facing surfaces in ITER, Journal of Nuclear Materials **363–365** (2007) 32–40.

[4] KATOH, Y., HASHIMOTO, N., KONDO, S., SNEAD, L.L., KOHYAMA, A., Microstructural development in cubic silicon carbide during irradiation at elevated temperatures. Journal of Nuclear Materials **351** (2006) 228–240.

[5] BARABASH, V., Role and contribution of ITER in research of materials and reactor components, Journal of Nuclear Materials **329–333** (2004) 156–160.

[6] MUROGA, T., GASPAROTTO, M., ZINKLE, S.J., Overview of materials research for fusion reactors, Fusion Engineering and Design **61–62** (2002) 13.
[7] SCHAAF, B.V., et al., The development of EUROFER reduced activation steel, Fusion Engineering and Design **69** (2003) 197–203.
[8] KIMURA, A., et al., Recent progress in US–Japan collaborative research on ferritic steel R&D, Journal of Nuclear Materials **367–370** (2007) 60–67.
[9] DYCK, S.V., BOSCH, R.W., Environmentally assisted cracking of Eurofer97 in water, Fusion Engineering and Design **75–79** (2005) 973–977.
[10] WAKAI, E., et al., Mechanical properties of small size specimens of F82H steel, Fusion Engineering and Design **81** (2006) 1077–1084.
[11] YU, J., HUANG, Q.Y., WAN, F.R., Research and development on the China low activation martensitic steel (CLAM), Journal of Nuclear Materials **367–370** (2007) 97–101.
[12] WAN, F.R., ZHU, X.F., XIAO, J.M., YUAN, Y., Effect of hydrogen on the behavior of irradiated defects in iron, Physics Transaction **39** (1990) 1093 (in Chinese).
[13] KIRITANI M. Recoil energy spectrum effects and point defect processes characteristic of cascades. Journal of Nuclear Materials **179–181** (1991) 81–86.
[14] YOSHIIE, T., KIRITANI, M., The variation of the cascade localization induced bias effect with material parameters and irradiation conditions, Journal of Nuclear Materials **191–194** (1992) 1088–1091.
[15] WAN, F.R., Irradiation damage in metal materials, Science Publisher, Beijing (1993) (in Chinese).
[16] TATEYAMA, Y., OHNO, T., Stability and clusterization of hydrogen–vacancy complexes in α-Fe: an ab initio study, Physical Review B **67** (2003) 1–10.

EFFORTS TOWARDS THE NEUTRON IRRADIATION BEHAVIOR STUDY OF RAFM STEEL AT SWIP

Pinghuai WANG, Jiming CHEN, Zengyu XU
Southwestern Institute of Physics,
Chengdu, China
wangph@swip.ac.cn

Abstract

In China, remarkable efforts are being made by several institutes and universities for characterization and optimization of reduced activation ferritic–martensitic steels. A neutron irradiation campaign was planned by the Southwestern Institute of Physics in the High Flux Engineering Test Reactor. The materials for irradiation are a type of RAFM steel named CLF-1 in various size samples for mechanical properties testing and microstructural observation. In 2012, the target dose level for the irradiation will be 1 dpa and the irradiation temperature 300°C. To establish a test standard in China for the preparation of studying irradiation effects, small specimen test techniques for mechanical property measurements of CLF-1 steel are under development. In addition, the irradiation hardening mechanism and helium effects on microstructural evolution were studied by means of heavy ion irradiation.

1. INTRODUCTION

Despite the variety of proposed concepts for the International Thermonuclear Experimental Reactor (ITER) Test Blanket Modules (TBM), reduced activation ferritic–martensitic (RAFM) steel was selected as the only candidate for the structural material [1] as well as the primary candidate for the DEMO fusion reactor. RAFM steel has good thermo-physical and mechanical properties, low sensitivity to radiation induced swelling and helium embrittlement under neutron irradiation, and good compatibility with major coolants and breeders [2] over other material candidates for a fusion blanket structural material. Based on the Chinese development strategy for the fusion DEMO reactor [3], China is implementing the TBM design and R&D plan. Two major blanket concepts were addressed, the dual functional liquid lithium–lead (DFLL) and the helium cooled solid breeder (HCSB), both of which select RAFM steel as structural material. Today, remarkable efforts are being made by several institutes and universities in China for the characterization and optimization of RAFM steel, mainly focusing on steel development, mechanical properties characterization and joining techniques.

High energy (14 MeV) neutron irradiation causes damage in a material by generating He and H via transmutation and by displacing atoms from their lattice positions, thereby forming various types of defects such as interstitials and vacancies [4]. The displacement damage in terms of displacement per atom and helium production by neutron irradiation induces microstructure change and degradation of mechanical properties, which are critical issues for RAFM steel, and extensive experiment data is required for a full understanding of fusion neutron irradiation behaviour.

Neutron irradiation campaigns have been carried out for several years on RAFM steels such as EUROFER97 and F82H, and the experimental irradiation damage is up to 70 dpa [5]. In order to assemble fully qualified TBMs at the beginning of the operation of ITER, the properties database as well as neutron irradiation properties up to 1 dpa are required for chosen RAFM steels. Thus, an irradiation campaign has been started by Southwestern Institute of Physics (SWIP) in the High Flux Engineering Test Reactor (HFETR) in China.

2. MATERIALS

RAFM steel was chosen as the structural material for the Chinese helium cooled solid tritium breeder TBM (CH HCSB TBM), and then a type of RAFM steel named CLF-1 was developed at SWIP in China. One of the objectives of CLF-1 steel R&D is to provide materials to fabricate CH HCSB TBM and to provide the properties database and technical information required for blanket fabrication such as strength, ductility, ductile to brittle transition temperature (DBTT), physical properties, heat treatment conditions, joining conditions and more.

CLF-1 steel has been developed since 2003, starting from small ingots of 5~50 kg used to determine compositions and to improve mechanical properties by optimizing smelting technologies and heat treatment. Processing routes like smelting, forging and rolling have been developed for CLF-1 steel. These research activities have led to a better understanding of the correlation among alloy composition, processing behaviour, heat treatment, microstructure and resulting mechanical properties. Based on the results obtained from the small heats, the chemical composition of CLF-1 steel was finalized as Fe8.5Cr1.5W0.25V0.5Mn0.1Ta0.1C (wt%), and in addition 0.025 wt% N is added to enhance the thermal stability of its microstructure and mechanical properties.

A 350 ingot of CLF-1 steel has been produced using vacuum induction melting and the consumable electrode re-melting method. The content of oxygen was kept below 0.005 wt%, and the radiologically undesirable trace elements in the CLF-1 steel were controlled to low level. The mechanical and thermo-physical properties required for the design and fabrication of the blanket have been well characterized, and the base mechanical properties were comparable to the small heats of CLF-1 steel in a second study [6].

The ingot was hot forged and hot rolled into different plates with thickness of 4 mm, 12 mm and 30 mm and rods with diameter of 65 mm. The material was used in normalized and tempered conditions. The heat treatment for all CLF-1 plates consists of an normalization at 980 K for 45 min, actual time depending on the size of steel being treated, followed by an air cooling and then tempering at 740 K for 90 min. The microstructure of the steel in the as received state was fully martensitic with equiaxed prior austenitic grain size of 13 μm consisting of thin plates of laths of 300±100 nm width, while M23C6 (M=Cr, W, Fe) carbides were distributed mainly along lath and grain boundaries and MX (M=Ta, V; X=C, N) particles distributed in matrix. Such microstructures have high initial dislocation density as well as many lath/grain boundaries which act as recombination centres for diffusing Frenkel pairs to suppress the formation of He bubbles down to the nanometer range and restrict swelling to a very low level. The mechanical property test results showed that CLF-1 steel has good high temperature tensile and creep properties and good mechanical property stability during long time thermal ageing.

3. NEUTRON IRRADIATION CAMPAIGN

Although the irradiation conditions of temperature and dose in a fission reactor are not representative of the fusion service conditions and neutron spectrums are not as highly energetic, irradiation experiments in a fission reactor are still considered to be important steps in the characterization of the fusion structural materials. Due to a limited number of neutron irradiation facilities and the different neutron fluxes and energies in existing reactors, however, most of the critical issues are not quite understood such as flux and energy effects on neutron irradiation

behaviours. Even the establishment of the International Fusion Materials Irradiation Facility (IFMIF) seems unlikely to fulfil the extensive need of fusion materials irradiation experiment due to a limited experimental volume [7–9]. Consequently, more experimental data is needed for a full understanding on the irradiation behaviours.

An irradiation experiment will be performed in the HFETR, which has a power of 125 MW and a maximum fast neutron flux of 1.7×10^{15} $cm^{-2}s^{-1}$ [10], at the reactor operation research centre in China. The irradiated materials will be CLF-1 steel with different size samples for mechanical properties test and microstructural observation, including miniature tensile, Charpy-V impact, pre-cracked Charpy-V specimens and TEM specimens. All specimens will be machined from a 12 mm thick plate in the as received state, 980°C/45 min+740°C/90 min. In 2012, the target dose level for the irradiation is 1 dpa, and the nominal irradiation temperature is 300°C, which can be controlled within ±15°C of the actual measured specimen irradiation temperature.

In fusion applications, neutron not only produce displacement damage, but also generate transmutation products like H, D and He, among which the most important is the so-called He/dpa ratio. However, there is no adequate simulation of He effects in present reactors, so while using fission reactors as an irradiation source, artificial He sources are still needed. Several methods are widely used to simulate helium production, including production of steels containing certain Fe (^{54}Fe) and B (^{11}B and ^{10}B) isotopes. After irradiation such materials show increasing helium content due to transmutation processes during neutron irradiation. The problem with these approaches is that these isotopes' content in existing steel is extremely low, requiring the production of new steel, which may affect the smelting process and other performance characteristics. In the experiment, we prefer the use of ^{58}Ni and Hf cladding for the thermal neutron irradiation, such that the desired helium can be generated by neutron spectrum adjustment based on the proper container design for helium production and the accurate calculation and analysis of helium production.

The irradiation experiments are characterized to provide the basic irradiation database required for fusion blanket design, including the effects of neutron irradiation on the mechanical properties, microstructures and additional data. After irradiation, the mechanical properties including tensile, Charpy impact and fracture toughness will be tested to obtain an experimental assessment of the main effects of neutron irradiation on the irradiation hardening and embrittlement. Tensile tests are performed in the temperature range from room temperature to 600°C. The DBTT is derived from the impact properties test using miniature V-notch specimens. Charpy tests are conducted in a temperature range from room temperature to 173 K. The DBTT is defined here as the temperature corresponding to half of the sum of upper shelf and lower shelf energy.

4. SMALL SPECIMEN TEST TECHNIQUES (SSTTs)

Due to the small available irradiation volume in a nuclear reactor and to facilitate the control of irradiation conditions and reduction of radioactive waste, the samples used for the neutron irradiation experiment should be reduced to small sizes. SSTTs have been considered one of the key technologies for the development of fusion structural materials. A variety of tests have been devised to extract mechanical property data from existing small size specimens. The results show that the sample size has a small effect on the tensile, hardness, fatigue and creep test results, with large effects on fracture toughness, Charpy impact and crack growth test results [11–14].

The tensile properties of CLF-1 steel at elevated temperatures were investigated for standard and miniature specimens to clarify the effect of specimen size. Figure 1 shows the results of the tensile tests on miniature specimens with a gauge section of 5 mm×1.2 mm×0.25 mm compared with those of standard specimens which have a gauge size of φ=5 mm×25 mm. It can be seen that the specimen size effects on the tensile strength appear quite small, but the total elongation of standard specimens is almost twice that of miniature specimens. It may be due to the difference in the stiffness of the samples, such that the standard samples have more resistance to plastic deformation instability, especially after the uniform deformation.

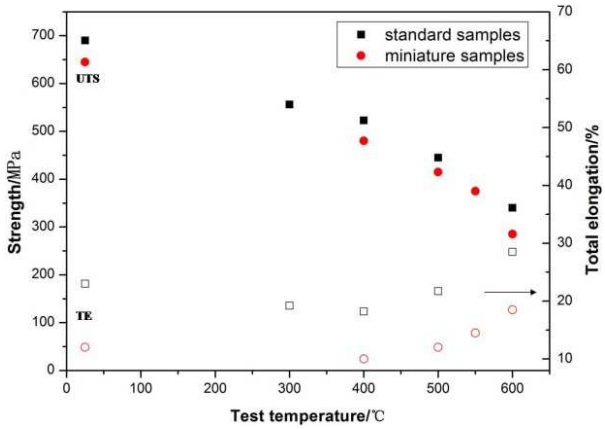

FIG. 1. Tensile properties of CLF-1 by using miniature samples and standard samples.

For the preparation of studying the irradiation effect, it is necessary to determine the mechanical properties of the CLF-1 steel using small size specimens to provide the mechanical property data before irradiation for the design of ITER TBM. A test standard for the qualification of the irradiation behaviour for the fusion structural materials needs to be established in China. Firstly, it is important to study the sample size effect on different mechanical properties and establish a standard size of the small specimens. Secondly, based on the existing test standard, some modification and further details evaluation are needed for the process of specimen preparation. Thirdly, the mechanical testing machines for small specimens need development. Currently, a fatigue test machine and a creep test machine have been developed for the small specimens test at SWIP.

5. HEAVY ION IRRADIATION

The effects of displacement damage and helium production on mechanical properties of RAFM steel are the most important subjects to be clarified, and irradiation in a fission reactor is the most effective way currently. However, due to the insufficiency of irradiation facilities and the excessive time required to reach the expected dpa in a fission reactor the behaviour of structural materials under irradiation conditions can hardly be fully tested in a real reactor. Irradiation experiments with energetic particles, especially high energy heavy ions, may be a very useful alternative technique for simulating the irradiation hardening mechanism and helium effects on microstructural evolution. For fusion material research and development, it is necessary to find the correlation between the damage produced by heavy ions and that expected to be produced by neutrons in a fusion reactor.

Experimental results and theoretical analysis suggest that irradiation with energetic heavy ions is a very useful technique for the study of some fundamental aspects of irradiation damage like cascade damage structures or helium effects on fusion reactor structural materials. Since Ne atoms have been proven to behave similar to helium in irradiated metals, high energy Ne ion irradiation is used to simulate helium effects [15] that are expected to produce the same displacement damage and the same amount of He to be reached under neutron irradiation in fusion facilities. In addition, heavy ion irradiation presents an important advantage of easy achievement of long penetration depth. The penetration depth in pure iron by Ne ions with the energy of 80 MeV/u and 120 MeV/u is respectively 2.0 mm and 4.0 mm, which can fulfil a requirement of mechanical properties testing using miniature size samples [16].

The ion irradiation experiment will be performed in the materials research terminal of the Heavy Ion Research Facility (HIRFL) in Lanzhou using a ^{20}Ne ion beam with energy of >50 MeV/u and intensity of >500 nA. The irradiated material will be CLF-1 steel of miniature size samples for mechanical properties testing and microstructural observation. The target irradiation temperatures are 300°C and 500°C, respectively, which are the inlet and outlet temperatures of the CH HCSB TBM. The expected displacement damage level is 1, 5 and 15 dpa at each irradiation temperature, which was determined by the increasing ion fluences, and the energy required to achieve this was estimated by means of SRIM code. After irradiation, the samples will be investigated by TEM observation, nano-indentation measurements and mechanical property test.

6. CONCLUSIONS

A neutron irradiation campaign of RAFM steel has been started by SWIP in China using different size samples for mechanical property testing and microstructural observation of RAFM steel CLF-1. Samples will be irradiated by neutrons in HFETR at 300°C up to 1 dpa by 2012. The planned neutron irradiation study in HFETR is expected to provide more supportive data for CLF-1 steel, which can be a candidate for the structural materials of TBM. For the preparation of studying the irradiation effects, SSTTs are ongoing in order to establish a standard of the sample size, the process of specimen preparation and test method. Several mechanical testing machines for small specimens have been developed at SWIP. In addition, along with the neutron irradiation, the ion irradiation experiment will be performed in the materials research terminal of HIRFL using a ^{20}Ne ion beam for irradiation hardening mechanism and helium effects studies.

REFERENCES

[1] KIMURA, A., et al., Recent progress in US-Japan collaborative research on ferritic steels R&D, Journal of Nuclear Materials **367–370** (2007) 60–67.

[2] VAN DER SCHAAF, B., et al., Structural materials development and database, Fusion Engineering and Design **81** (2006) 893–900.

[3] FENG, K.M., et al., Preliminary design for a China ITER test blanket module, Fusion Engineering and Design **81**(2006) 1219–1224.

[4] LUCON, E., et al., The European effort towards the development of a demo structural material: Irradiation behavior of the European reference RAFM steel EUROFER, Fusion Engineering and Design **81** (2006) 917–923.

[5] GAGANIDZE, E., et al., Mechanical properties and TEM examination of RAFM steels irradiated up to 70 dpa in BOR-60, Journal of Nuclear Materials **417** 1–3 (2011) 93–98.

[6] WANG, P.H., et al., Research and development of reduced activation ferritic/martensitic steel CLF-1 at SWIP, 23rd IAEA Fusion Energy Conference, Daejeon, 2010.
[7] GARIN, P., Start of the engineering validation and design phase of IFMIF, Journal of Nuclear Materials **386–388** (2009) 944–948.
[8] LEICHTLE, D., et al., Design optimization and experimental testing of the High Flux Test Module of IFMIF, Journal of Nuclear Materials **386–388** (2009) 954–957.
[9] WAKAI, E., KOGAWARA, T., KIKUCHI, T., Design status of post irradiation examination facilities in IFMIF/EVEDA, J. Plasma Fusion Res. Series **9** (2010) 242–247.
[10] FENG, P., Irradiation Ability of Research and Test Reactors, Nuclear Power Engineering, **25** (2004) 91–96 (in Chinese).
[11] WAKAI, E., et al., Mechanical properties of small size specimens of F82H steel, Fusion Engineering and Design **81** (2006) 1077–1084.
[12] HIROSE, T., et al., Effect of specimen size on fatigue properties of reduced activation ferritic/martensitic steel, Journal of Nuclear Materials **283–287** (2000) 1018–1022.
[13] KOHNO, Y., et al., Specimen size effects on the tensile properties of JPCA and JFMS, Journal of Nuclear Materials **283–287** (2000) 1014–1017.
[14] WAKAI, E., Status of SSTT Development, IEA Working Group on Irradiation Facilities and Testing, Rostock, 2008.
[15] ZHANG, C.H., et al., Void swelling in a 9Cr ferritic/martensitic steel irradiated with energetic Ne-ions at elevated temperatures, Journal of Nuclear Materials **375** (2009) 185–191.
[16] ZHIGUANG, W., Simulation of radiation effects in structural materials of reactors using high energy heavy ion radiations, Nuclear Physics Review **23** (2006) 155–160 (in Chinese).

ABBREVIATIONS

ASTRID	Advanced Sodium Technical Reactor for Industrial Demonstration
BESTH	Beryllium thermal sample
BWR	Boiling water reactor
CARR	China Advanced Research Reactor
CEFR	China Experimental Fast Reactor
CLAM	China low activation martensitic steel
CLF-1	China low activation ferritic steel
DBS	Doppler broadening spectroscopy
DBTT	Ductile to brittle transition temperature
EBSD	Electron backscatter diffraction
EFDA	European Fusion Development Agreement
F4E	Fusion for Energy
FWQM	First wall qualification mock-up
GFR	Gas cooled fast reactor
HCLL	Helium cooled lead lithium blanket
HCPB	Helium cooled pebble bed blanket
HEU	Highly enriched uranium
HFETR	High Flux Engineering Test Reactor
HFIR	High Flux Isotope Reactor
HFR	High Flux Reactor
HFTM	High flux test module
HTHL	High temperature helium loop
IFMIF	International Fusion Materials Irradiation Facility
INPRO	International Project on Innovative Power Reactors and Fuel Cycles

ITER	International Thermonuclear Experimental Reactor
JANNuS	Joint Accelerators for Nano-science and Nuclear Simulation
JHR	Jules Horowitz Reactor
JMTR	Japan Material Test Reactor
LAFM	Low activation ferritic–martensitic steel
LECI	Laboratory for Studies on Irradiated Fuel
LEU	Low enriched uranium
LFR	Lead cooled fast reactor
MBIR	Multipurpose Fast Neutron Research Reactor
MBN	Magnetic Barkhausen noise
MLT	Mean lifetime
MSR	Molten salt cooled fast reactor
MTR	Material test reactor
NRT	Norbert, Robinson, Torrens standard
ODS	Oxide dispersion strengthened (steel)
ORR	Oak Ridge Research Reactor
PALS	Positron annihilation lifetime spectroscopy
PAS	Positron annihilation spectroscopy
PFBR	Prototype Fast Breeder Reactor
PFW	Primary first wall
PKA	Primary knock-on atom
RAFM	Reduced activation ferritic–martensitic steel
RMS	Root mean squared
SANS	Small angle neutron scattering
SCWL	Subcritical water loop

SCWR	Subcritical water reactor
SEM	Scanning electron microscopy
SFR	Sodium cooled fast reactor
SIA	Self-interstitial atom
SMoRE	Accelerator Simulation and Theoretical Modelling of Radiation Effects
TBB	Tritium breeding blanket
TEM	Transmission electron microscopy
VHTR	Very high temperature reactor
XADS	Experimental accelerator driven system

CONTRIBUTORS TO DRAFTING AND REVIEW

Boutard, J.-L.	Atomic Energy and Alternative Energies Commission (CEA), France
Di Pietro, P.	Australian Nuclear Science and Technology Organisation (ANSTO)
González de Vicente, S.M.	European Fusion Development Agreement Close Support Unit, Germany
Henry, J.	Atomic Energy and Alternative Energies Commission (CEA), France
Horváth, Á.	KFKI Atomic Energy Research Institute, Hungary
Ibarra, A.	Research Centre for Energy, Environment and Technology (CIEMAT), Spain
Laha, K.	Indira Ghandi Centre for Atomic Research, India
Long, Y.	University of Science and Technology, China
Kamendje, R.	International Atomic Energy Agency
Koleska, M.	Research Centre Řež, Czech Republic
Krzysztoszek, G.	Institute of Atomic Energy POLATOM, Poland
Peld, N.	International Atomic Energy Agency
Ridikas, D.	International Atomic Energy Agency
Roux, P.	Atomic Energy and Alternative Energies Commission (CEA), France
Sandim, H.R.Z.	University of São Paolo, Brazil
Shikama, T.	Tohoku University, Japan
Slugeň, V.	Slovak University of Technology, Slovakia
Tazhibayeva, I.	Institute of Atomic Energy, National Nuclear Center of the Republic of Kazakhstan
Trkov, A.	Jožef Stefan Institute, Slovenia
Van der Laan, J.G.	Nuclear Research and Consultancy Group (NRG), Netherlands
Wan, F.	University of Science and Technology, China
Wang, P.	Southwestern Institute of Physics, China
Xu, Z.	Southwestern Institute of Physics, China

IAEA
International Atomic Energy Agency

No. 23

ORDERING LOCALLY

In the following countries, IAEA priced publications may be purchased from the sources listed below, or from major local booksellers.

Orders for unpriced publications should be made directly to the IAEA. The contact details are given at the end of this list.

AUSTRALIA
DA Information Services
648 Whitehorse Road, Mitcham, VIC 3132, AUSTRALIA
Telephone: +61 3 9210 7777 • Fax: +61 3 9210 7788
Email: books@dadirect.com.au • Web site: http://www.dadirect.com.au

BELGIUM
Jean de Lannoy
Avenue du Roi 202, 1190 Brussels, BELGIUM
Telephone: +32 2 5384 308 • Fax: +61 2 5380 841
Email: jean.de.lannoy@euronet.be • Web site: http://www.jean-de-lannoy.be

CANADA
Renouf Publishing Co. Ltd.
Telephone: +1 613 745 2665 • Fax: +1 643 745 7660
5369 Canotek Road, Ottawa, ON K1J 9J3, CANADA
Email: order@renoufbooks.com • Web site: http://www.renoufbooks.com

Bernan Associates
4501 Forbes Blvd., Suite 200, Lanham, MD 20706-4391, USA
Telephone: +1 800 865 3457 • Fax: +1 800 865 3450
Email: orders@bernan.com • Web site: http://www.bernan.com

CZECH REPUBLIC
Suweco CZ, spol. S.r.o.
Klecakova 347, 180 21 Prague 9, CZECH REPUBLIC
Telephone: +420 242 459 202 • Fax: +420 242 459 203
Email: nakup@suweco.cz • Web site: http://www.suweco.cz

FINLAND
Akateeminen Kirjakauppa
PO Box 128 (Keskuskatu 1), 00101 Helsinki, FINLAND
Telephone: +358 9 121 41 • Fax: +358 9 121 4450
Email: akatilaus@akateeminen.com • Web site: http://www.akateeminen.com

FRANCE
Form-Edit
5, rue Janssen, PO Box 25, 75921 Paris CEDEX, FRANCE
Telephone: +33 1 42 01 49 49 • Fax: +33 1 42 01 90 90
Email: fabien.boucard@formedit.fr • Web site: http://www.formedit.fr

Lavoisier SAS
14, rue de Provigny, 94236 Cachan CEDEX, FRANCE
Telephone: +33 1 47 40 67 00 • Fax: +33 1 47 40 67 02
Email: livres@lavoisier.fr • Web site: http://www.lavoisier.fr

L'Appel du livre
99, rue de Charonne, 75011 Paris, FRANCE
Telephone: +33 1 43 07 50 80 • Fax: +33 1 43 07 50 80
Email: livres@appeldulivre.fr • Web site: http://www.appeldulivre.fr

GERMANY
Goethe Buchhandlung Teubig GmbH
Schweitzer Fachinformationen
Willstaetterstrasse 15, 40549 Duesseldorf, GERMANY
Telephone: +49 (0) 211 49 8740 • Fax: +49 (0) 211 49
Email: s.dehaan@schweitzer-online.de • Web site: http://www. http://www.goethebuch.de/

HUNGARY
Librotade Ltd., Book Import
PF 126, 1656 Budapest, HUNGARY
Telephone: +36 1 257 7777 • Fax: +36 1 257 7472
Email: books@librotade.hu • Web site: http://www.librotade.hu

INDIA
Allied Publishers
1st Floor, Dubash House, 15, J.N. Heredi Marg
Ballard Estate, Mumbai 400001, INDIA
Telephone: +91 22 2261 7926/27 • Fax: +91 22 2261 7928
Email: alliedpl@vsnl.com • Web site: http://www.alliedpublishers.com

Bookwell
3/79 Nirankari, Dehli 110009, INDIA
Tel.: +91 11 2760 1283 • +91 11 27604536
Email: bkwell@nde.vsnl.net.in • Web site: http://www.bookwellindia.com/

ITALY
Libreria Scientifica "AEIOU"
Via Vincenzo Maria Coronelli 6, 20146 Milan, ITALY
Tel.: +39 02 48 95 45 52 • Fax: +39 02 48 95 45 48
Email: info@libreriaaeiou.eu • Web site: http://www.libreriaaeiou.eu/

JAPAN
Maruzen Co., Ltd.
1-9-18 Kaigan, Minato-ku, Tokyo 105-0022, JAPAN
Tel.: +81 3 6367 6047 • Fax: +81 3 6367 6160
Email: journal@maruzen.co.jp • Web site: http://maruzen.co.jp

NETHERLANDS
Martinus Nijhoff International
Koraalrood 50, Postbus 1853, 2700 CZ Zoetermeer, NETHERLANDS
Tel.: +31 793 684 400 • Fax: +31 793 615 698
Email: info@nijhoff.nl • Web site: http://www.nijhoff.nl

Swets
PO Box 26, 2300 AA Leiden
Dellaertweg 9b, 2316 WZ Leiden, NETHERLANDS
Telephone: +31 88 4679 263 • Fax: +31 88 4679 388
Email: tbeysens@nl.swets.com • Web site: www.swets.com

SLOVENIA
Cankarjeva Zalozba dd
Kopitarjeva 2, 1515 Ljubljana, SLOVENIA
Tel.: +386 1 432 31 44 • Fax: +386 1 230 14 35
Email: import.books@cankarjeva-z.si • Web site: http://www.mladinska.com/cankarjeva_zalozba

SPAIN
Diaz de Santos, S.A.
Librerias Bookshop • Departamento de pedidos
Calle Albasanz 2, esquina Hermanos Garcia Noblejas 21, 28037 Madrid, SPAIN
Telephone: +34 917 43 48 90
Email: compras@diazdesantos.es • Web site: http://www.diazdesantos.es/

UNITED KINGDOM
The Stationery Office Ltd. (TSO)
PO Box 29, Norwich, Norfolk, NR3 1PD, UNITED KINGDOM
Telephone: +44 870 600 5552
Email (orders): books.orders@tso.co.uk • (enquiries): book.enquiries@tso.co.uk • Web site: http://www.tso.co.uk

On-line orders:
DELTA International Ltd.
39, Alexandra Road, Addlestone, Surrey, KT15 2PQ, UNITED KINGDOM
Email: info@profbooks.com • Web site: http://www.profbooks.com

United Nations (UN)
300 East 42nd Street, IN-919J, New York, NY 1001, USA
Telephone: +1 212 963 8302 • Fax: 1 212 963 3489
Email: publications@un.org • Web site: http://www.unp.un.org

UNITED STATES OF AMERICA
Bernan Associates
4501 Forbes Blvd., Suite 200, Lanham, MD 20706-4391, USA
Tel.: +1 800 865 3457 • Fax: +1 800 865 3450
Email: orders@bernan.com • Web site: http://www.bernan.com

Renouf Publishing Co. Ltd.
812 Proctor Avenue, Ogdensburg, NY 13669, USA
Tel.: +800 551 7470 (toll free) • +800 568 8546 (toll free)
Email: orders@renoufbooks.com • Web site: http://www.renoufbooks.com

Orders for both priced and unpriced publications may be addressed directly to:

IAEA Publishing Section, Marketing and Sales Unit, International Atomic Energy Agency
Vienna International Centre, PO Box 100, 1400 Vienna, Austria
Telephone: +43 1 2600 22529 or 22488 • Fax: +43 1 2600 29302
Email: sales.publications@iaea.org • Web site: http://www.iaea.org/books

13-41911

International Atomic Energy Agency
Vienna
ISBN 978–92–0–113713–5
ISSN 1011–4289